DI Andreas Frank Martitsch, BSc

Modeling of Plasma Rotation in Tokamaks

DOCTORAL THESIS

to achieve the university degree of

Doktor der technischen Wissenschaften

submitted to

Graz University of Technology

Supervisor

Ao.Univ.-Prof. Dipl.-Ing. Dr.phil. Martin Heyn

Institute of Theoretical and Computational Physics

Co-Supervisor
Ass.Prof. Dipl.-Ing. Dr.techn. Winfried Kernbichler

Graz, June 2016

AFFIDAVIT

I declare that I have authored this thesis independently, that I have not used other than the declared sources/resources, and that I have explicitly indicated all material which has been quoted either literally or by content from the sources used. The text document uploaded to TUGRAZonline is identical to the present doctoral thesis.

Date

Signature

Kurzfassung

Störungen der axialen Symmetrie des Magnetfeldes in einem Tokamak führen zu neoklassischen radialen Plasmaströmen, die wiederum Drehmomente erzeugen und damit die Plasmarotation beeinflussen können. Da diese Drehmomente oft in Form einer Viskosität beschrieben werden, wird dieses Phänomen auch als neoklassische toroidale Viskosität (NTV) bezeichnet. Zur Berechnung der NTV Drehmomente werden derzeit analytische, semi-analytische und numerische Modelle verwendet, die Vereinfachungen bezüglich der Geometrie, Stoßoperatoren und Transportregime machen, welche eine Verringerung der Dimensionalität des ursprünglichen 4D Problems ermöglichen. In dieser Arbeit wurde eine numerische Methode entwickelt, die die Dimension des Standardansatzes zur Lösung des neoklassischen Transportproblems um eins reduziert und dabei auf die oben genannten Vereinfachungen verzichtet. Die einzige Annahme dieser Methode ist, dass die Störungen des Magnetfeldes hinreichend klein sind und damit die Teilchenbewegung innerhalb der gestörten Flussfläche kaum durch das Störfeld beeinflusst wird (quasilinearer Ansatz). Dennoch decken quasilineare Transportregime einen großen Parameterbereich moderner Tokamak-Experimente ab. Basierend auf diesem quasilinearen Ansatz wurde eine Version des Codes NEO-2 entwickelt und mit verschiedenen analytischen und semi-analytischen Modellen, sowie mit dem nichtlinearen Code DKES verglichen. Für eine reale Tokamak-Geometrie wird ein Verfahren zur Auswertung der NTV Drehmomente besprochen, das aus der quasilinearen NEO-2 Version und dem Code NEMEC zur Berechnung der Magnetfeldgleichgewichte besteht. Mit Hilfe dieser Prozedur wird das NTV Drehmoment für ein ASDEX Upgrade Gleichgewicht und ein Einteilchen-Plasma berechnet. Die erhaltenen Resultate werden mit Ergebnissen von SFINCS, einem nichtlinearen Code zur Lösung der drift-kinetischen Gleichung, sowie mit semi-analytischen Modellen verglichen. Weiters wurde das bisher in NEO-2 implementierte Stoßmodell (der gesamte linearisierte Stoßoperator) von einem simplen Plasma (Elektronen und eine Ionensorte) auf ein beliebiges Plasma mit mehreren Ionensorten erweitert. Dies erlaubt in Zukunft die Berechnung der NTV Drehmomente in Plasmen mit einem signifikanten Anteil von Verunreinigungen.

Abstract

Plasma rotation in tokamaks can be significantly influenced by the torque arising from neoclassical radial plasma currents due to 3D magnetic perturbations, e.g., the toroidal field (TF) coil ripple, error fields, coils for edge localized modes (ELM) mitigation purposes. Since this torque is often expressed through a viscous force, the phenomenon is termed as neoclassical toroidal plasma viscosity (NTV). For the evaluation of the NTV torque several analytical, semi-analytical and numerical approaches are presently used, which make simplifying assumptions concerning geometry, collision operators and transport regimes, which, in particular, help to reduce the dimension of the original 4D problem. In this thesis a numerical approach has been developed, which reduces the dimension of the standard neoclassical transport problem by one without such simplifications of the linearized drift kinetic equation. The only assumption is that the perturbations are small enough such that the particle motion within the perturbed flux surface is only weakly affected by the perturbation field (quasilinear approach). Nevertheless, these quasilinear regimes cover a significant range of the parameter domain of modern tokamak experiments. Based on this quasilinear approach, a version of the code NEO-2 has been developed and benchmarked against various analytical and semi-analytical models, as well as the nonlinear code DKES. For a real tokamak geometry a procedure for the evaluation of the NTV torque, which consists of the upgraded version of NEO-2 and the code NEMEC for the computation of the magnetic field equilibria, is discussed. Using this procedure, the NTV torque is evaluated numerically for an ASDEX Upgrade equilibrium and a single-species plasma. The obtained results are compared to computations of the nonlinear drift kinetic equation solver SFINCS, as well as to semi-analytical models. Furthermore, the collision model (full linearized collision operator), which has been implemented so far in NEO-2 for a simple plasma (electrons and one sort of ions), has been generalized here for the general case of a multi-species plasma. This would allow computations of the torque for plasmas with significant impurity contents including the computations of the additional impurity transport caused in tokamaks by the violation of the toroidal magnetic field symmetry.

Acknowledgments

Since a lot of people are involved in this thesis in its present form, it would be impossible to thank all of them. Any person involved played an important role in the course of this work and the thesis might not look like this or would even not exists if one of them would miss.

At first, I want to express my gratitude to my supervisor *Prof. Dr. Martin Heyn* and to my co-supervisor *Prof. Dr. Winfried Kernbichler* for guiding me through this thesis. They were always available for clarifying discussions and provided a lot of ideas concerning the basic concepts as well as the computational implementation. At this place I also would like to thank *Dr. Sergei Kasilov* for supporting me at every stage of this work and for all the knowledge he shared with me. Without him it would not have been possible to address this range of topics presented here.

I also appreciate having had the chance to work in the plasma physics group at the Institute of Theoretical and Computational Physics with *Klaus Allmaier*, *Peter Leitner*, *Gernot Kapper* and *Christopher Albert*. I am very grateful to my office mate *Gernot Kapper*, who was also a part of the NEO-2 code development team, for sharing his experience with me and for the good time during the last years. Especially, the multi-species version of NEO-2 would not exist without him. I also want to thank *Christopher Albert* who joined our "NTV group" two years ago and since then contributed a lot to the progress of this thesis.

I am very grateful to our IT administrator *Andreas Hirczy* for all the help related to computer issues and for the many useful discussions within the last years. For guiding me through the administrative matters I want to thank *Brigitte Schwarz*. In remembrance of the good time during the study period, I thank *Iris Hehn*, *Martin Nuss* and *Matthias Hasewend*.

For providing benchmarking results from the DKES code and several useful discussions I am very grateful to *Dr. Henning Maassberg* and to *Dr. Craig Beidler* from the IPP Greifswald. I also want to thank *Dr. Sina Fietz* from the IPP Garching for her interest in my work and for giving me insights into the experimental setup. I am very grateful to *Dr. Erika Strumberger*

(IPP Garching) for providing the NEMEC calculations of the magnetic field equilibria which are the basis of all studies related to ASDEX Upgrade discharges. For providing results from the SFINCS code I want to express my gratitude to *Dr. Håkan Smith* (IPP Greifswald).

Finally, I want to thank my mother *Marion* and my fiancee *Anna* for their love, support and encouragement.

I gratefully acknowledge financial support from the "Friedrich Schiedel Stiftung für Energietechnik" during the initial phase of this work which made all these studies possible. I also gratefully acknowledge funding from the KKKÖ at ÖAW for a project for the continuation of the PhD thesis.

This work has been carried out within the framework of the EUROfusion Consortium and has received funding from the Euratom research and training programme 2014-2018 under grant agreement No 633053. The views and opinions expressed herein do not necessarily reflect those of the European Commission.

Contents

Chapter 1

Introduction

The two most advanced concepts for magnetic confinement fusion devices are the tokamak and the stellarator. Examples of a tokamak and a stellarator configuration are shown in Figure 1.1 and Figure 1.2, respectively. In Figure 1.1 an insight into the cryostat vessel of the tokamak ITER is given, which is currently being built in Cadarache (France). The advanced stellarator experiment Wendelstein 7-X, see Figure 1.2, is located in Greifswald (Germany) and went into operation in December 2015. Both concepts have in common that they generate strong magnetic fields to confine the plasma particles which travel along the magnetic field lines belonging to toroidal magnetic surfaces. Typically, the tokamak is assumed to be a perfectly axisymmetric device, whereas the stellarator has a much more complex magnetic field geometry and, therefore, is considered as non-axisymmetric. In a real tokamak experiment this axial symmetry is often violated due to, e.g., the toroidal field (TF) coil ripple, error fields and resonant magnetic perturbation (RMP) coils used for the mitigation of edge localized modes (ELMs). Thus, a strict separation into axisymmetric and non-axisymmetric fusion devices is not possible anymore. The perturbations of the axial symmetry in a tokamak are of importance since they cause non-ambipolar radial particle fluxes. These non-ambipolar particle fluxes can modify the toroidal plasma rotation which, in turn, affects the stability and transport in tokamak plasmas.

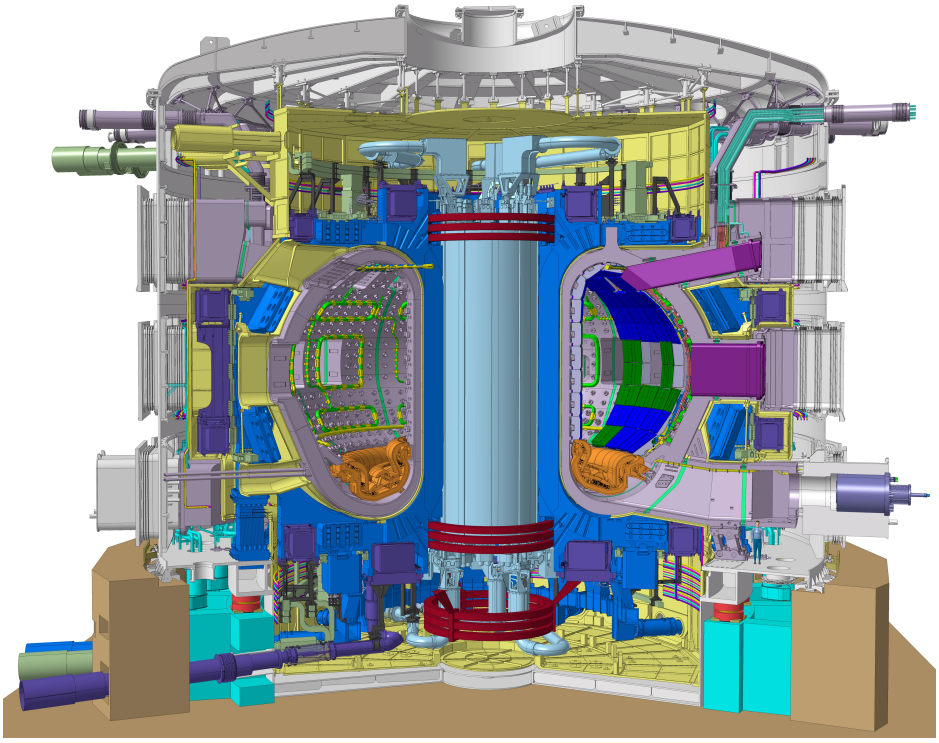

Figure 1.1: In-cryostat overview of the tokamak ITER. ©ITER Organization Source: https://www.iter.org/doc/all/content/com/gallery/media/7%20-%20technical/in-cryostat%20overview%20130116.jpg

The purpose of this thesis has been to provide a contribution to the better understanding of the plasma rotation in tokamaks, which influences the plasma confinement and, thus, the performance of future power plants based on nuclear fusion. As a result of this endeavor a tool for the numerical evaluation of the neoclassical toroidal viscosity (NTV), which is produced by non-resonant magnetic perturbations in a tokamak, has been developed. This numerical tool, an upgraded version of the code NEO-2 [1, 2], allows for an efficient evaluation of non-ambipolar particle fluxes due to non-axisymmetric electromagnetic field perturbations, which in turn produce a toroidal torque affecting the plasma rotation. This is accomplished without making simplifying assumptions for all quasilinear regimes. In this context quasilinear regimes mean parameter domains where the particle motion within a magnetic flux surface is not influenced by the perturbation field itself. Since the

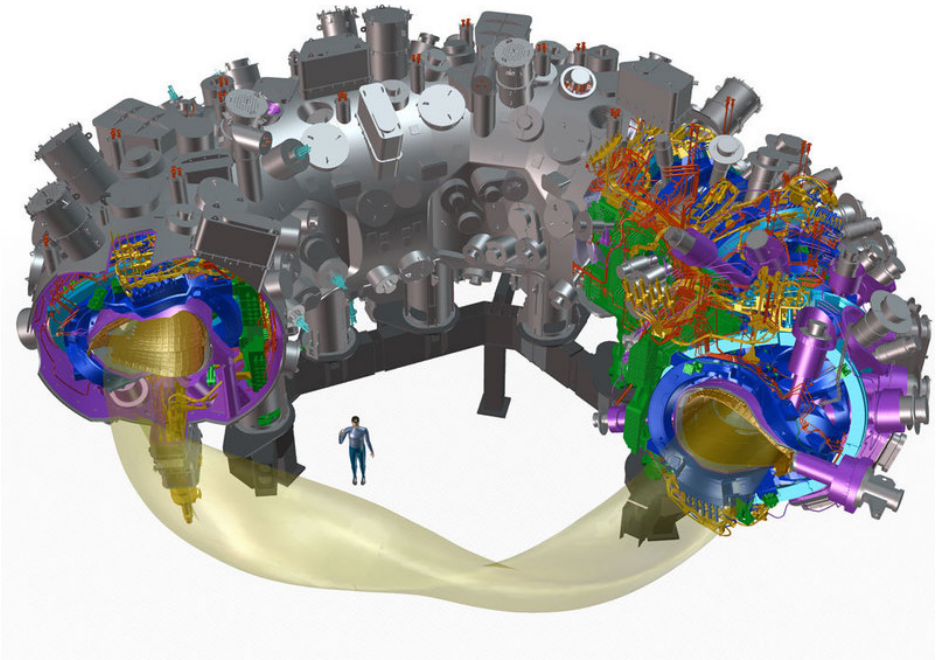

Figure 1.2: Technical drawing of the advanced stellarator Wendelstein 7-X. ©Max-Planck-Institut für Plasmaphysik, Source: http://www.ipp.mpg.de/2498182/zoom.jpg

relative magnitude of electromagnetic field perturbations with respect to the total magnetic field is small, quasilinear regimes cover a large domain of parameters including the reactor scale plasmas. Before this upgraded version of the code NEO-2 there existed various analytical and semi-analytical models for the computation of NTV [3, 4, 5], which have in common that they make simplifications such as the restriction to certain transport regimes, simplified device geometry or Coulomb collision model. Well-established codes for the evaluation of particle fluxes in stellarators as the DKES code [6] make often also use of certain simplifications of the underlying drift kinetic equation. For example, DKES uses a Lorentz collision model and neglects the contribution from magnetic drifts to the poloidal and toroidal rotation velocity. With respect to Monte-Carlo methods [7, 8, 9], which provide also a universal approach for the evaluation of NTV, the numerical approach realized within the upgraded version of the code NEO-2 is more efficient and,

thus, would allow for the use of NEO-2 within a 1D transport code. The upgraded version of NEO-2 has been validated and benchmarked against various analytical and semi-analytical models, as well as the nonlinear codes DKES [6] and NEO [10]. The derivations of the theoretical framework for the upgraded code NEO-2 and the results of the extensive benchmarking phase have been published in Ref. [2]. In Ref. [2], aside from the developed theoretical formalism, also a re-derivation of the exact toroidal momentum conservation equation and its approximate form including all leading order terms in Larmor radius and perturbation amplitude is presented. Furthermore, the flux-force relation has been generalized there for the case of fast plasma rotation.

After the benchmarking phase, the quasilinear version of the code NEO-2 has been extended to the case of general tokamak geometry. The procedure for the evaluation of non-ambipolar particle fluxes in a real tokamak device consists of two steps, the calculation of the equilibrium including the non-axisymmetric magnetic perturbations using the code NEMEC [11] and a subsequent computation of the non-ambipolar particle fluxes with NEO-2. Based on this procedure, a study of the NTV torque for a few ASDEX Upgrade equilibria has been carried out. These equilibria include perturbations from the TF ripple and from ELM mitigation coils with different distribution of current values resulting in different perturbation field spectra in the ASDEX Upgrade shot #30835. Since RMPs are strongly shielded by plasma response currents in ASDEX Upgrade [12], magnetic fields computed within ideal MHD theory, where RMPs are shielded perfectly, provide a good approximation in a major part of the plasma volume except for narrow resonant layers around resonant rational flux surfaces. For this set of equilibria the NEO-2 results for the ion NTV torque have been compared to results obtained by the code SFINCS [13], which solves the nonlinear problem pertinent to neoclassical stellarator transport and, therefore, is not limited to small values of the perturbation amplitude. Computationally, this is a much more demanding task than solving the quasilinear problem. In contrast to the DKES code, which solves the reduced monoenergetic problem, SFINCS as NEO-2 uses the full linearized Coulomb collision operator.

The structure of this thesis is as follows. In Chapter 2 the quasilinear approach used for the evaluation of the torque produced by non-resonant non-axisymmetric magnetic perturbations is derived, as well as a discussion of the toroidal momentum conservation in a plasma is given. The benchmarking results for a simplified tokamak geometry with circular flux surfaces are shown in Chapter 3, and in Chapter 4 an application of the quasilinear version of the code NEO-2 to an ASDEX Upgrade discharge is presented. In Chapter 5 the numerical approach implemented in NEO-2 is generalized for the case of a multi-species plasma, and in Chapter 6 the results of this thesis are summarized. In Appendices A, B and C analytical approaches for the evaluation of non-ambipolar particle fluxes in the $1/\nu$ regime, a method for the transformation from Boozer [14] to Hamada [15] coordinates, and details regarding the derivation of the quasilinear approach are given, respectively.

Publications associated with this thesis

Peer-reviewed journal articles

- S. V. Kasilov, W. Kernbichler, A. F. Martitsch, H. Maassberg, and M. F. Heyn. Evaluation of the toroidal torque driven by external non-resonant non-axisymmetric magnetic field perturbations in a tokamak. *Phys. Plasmas*, 21(9):092506, 2014.

- W. Kernbichler, S. V. Kasilov, G. Kapper, A. F. Martitsch, V .V. Nemov, C. G. Albert, and M. F. Heyn. Solution of drift kinetic equation in stellarators and tokamaks with broken symmetry using the code NEO-2. *Plasma Phys. Contr. Fusion*, submitted, 2016.

- A. F. Martitsch, S. V. Kasilov, W. Kernbichler, G. Kapper, C. G. Albert, M. F. Heyn, H. M. Smith, E. Strumberger, S. Fietz, W. Suttrop, M. Landreman, the ASDEX Upgrade Team and the EUROfusion MST1 Team. Effect of 3D magnetic perturbations on the plasma rotation in ASDEX Upgrade. *Plasma Phys. Contr. Fusion*, 58(7):074007, 2016.

Conference proceedings

- A. F. Martitsch, S. V. Kasilov, W. Kernbichler, and H. Maassberg. Evaluation of non-ambipolar particle fluxes driven by external non-resonant magnetic perturbations in a tokamak. In *41st EPS Conference on Plasma Physics*, volume 38F, page P1.049, Berlin, Deutschland, 2014. European Physical Society.

- A. F. Martitsch, S. V. Kasilov, W. Kernbichler, M. F. Heyn, E. Strumberger, S. Fietz, W. Suttrop, A. Kirk, the ASDEX Upgrade Team and the EUROfusion MST1 Team. Evaluation of the neoclassical toroidal viscous torque in ASDEX Upgrade. In *42nd EPS Conference on Plasma Physics*, volume 39E, page P1.146, Lisbon, Portugal, 2015. European Physical Society.

Poster presentations

- S. V. Kasilov, W. Kernbichler, and A. F. Martitsch. Evaluation of non-ambipolar particle fluxes driven by non-resonant magnetic perturbations in a tokamak. *Joint 19th ISHW and 16th RFP workshop*, Padova, Italy, 2013.

- A. F. Martitsch, W. Kernbichler, S. V. Kasilov, M. F. Heyn, and H. Maassberg. Evaluation of the toroidal torque driven by external non-resonant non-axisymmetric magnetic field perturbations in a tokamak. *19th Joint EU-US Transport Task Force Meeting*, Culham, UK, 2014.

- A. F. Martitsch, S. V. Kasilov, W. Kernbichler, G. Kapper, C. G. Albert, M. F. Heyn, E. Strumberger, S. Fietz, W. Suttrop, the ASDEX Upgrade Team and the EUROfusion MST1 Team. Effect of 3D magnetic perturbations on the plasma rotation in tokamaks. *20th International Stellarator-Heliotron Workshop*, Greifswald, Germany, 2015.

Chapter 2

Methods

In this chapter a method for the evaluation of the torque produced by non-resonant non-axisymmetric magnetic field perturbations is presented, which has been developed in the course of this thesis together with Sergei V. Kasilov and my supervisors. It has to be noted that the methods described in Sections 2.2 and 2.3 have been published in the following journal article [2] and conference proceeding [16]:

- S. V. Kasilov, W. Kernbichler, A. F. Martitsch, H. Maassberg, and M. F. Heyn. Evaluation of the toroidal torque driven by external non-resonant non-axisymmetric magnetic field perturbations in a tokamak. *Phys. Plasmas*, 21(9):092506, 2014.

- A. F. Martitsch, S. V. Kasilov, W. Kernbichler, and H. Maassberg. Evaluation of non-ambipolar particle fluxes driven by external non-resonant magnetic perturbations in a tokamak. In *41st EPS Conference on Plasma Physics*, volume 38F, page P1.049, Berlin, Deutschland, 2014. European Physical Society.

The developed numerical approach has been implemented in an upgraded version of the code NEO-2 [1, 2], which is benchmarked against various analytical [3, 17, 18] and semi-analytical models [19], as well as the DKES code [6] and SFINCS [13]. The benchmarking results are summarized in Chapter 3 and an application of the code NEO-2 to ASDEX Upgrade equilibria is shown in Chapter 4. The structure of this chapter is as follows.

In Section 2.1 basic definitions are given, in particular, a relation between plasma rotation and radial electric field is established and the drift kinetic equation equation is introduced. The toroidal momentum conservation in a plasma and the neoclassical toroidal viscous (NTV) torque are discussed in Section 2.2. The derivation of the quasilinear approach implemented in the upgraded version of the code NEO-2 is given in Section 2.3, and in Section 2.4 analytical models used for benchmarking are described.

2.1 Definitions

2.1.1 Coordinates and geometry

Modeling of plasma transport in toroidal confinement devices requires the knowledge of the magnetic field $\mathbf{B}$ in a complex geometry. Thus a proper choice of the coordinate system can tremendously simplify the algebra pertinent to the physical problem. There exists a large variety of so-called toroidal flux coordinate systems, which have been extensively studied since the middle of the last century. In this section basic features of specific sets of toroidal flux coordinate systems, where the magnetic field lines become straight, are listed and fundamental quantities are defined. A more detailed discussion of straight field line flux coordinate systems can be found in in the book of W.D.D'haeseleer *et al* [20].

Let $\mathbf{x} = (x^1, x^2, x^3) = (r, \vartheta, \varphi)$ denote straight field line flux coordinates, i.e. $B^r = 0$ and $B^\varphi = qB^\vartheta$, where the toroidal angle φ is a symmetry variable and $q = q(r)$ denotes the safety factor. The magnetic field can be presented either in a co-variant form,

$$\mathbf{B} = B_r \nabla r + B_\vartheta \nabla \vartheta + B_\varphi \nabla \varphi, \tag{2.1}$$

or in a contra-variant form,

$$\mathbf{B} = B^\vartheta e_\vartheta + B^\varphi e_\varphi = B^\vartheta \sqrt{g}\,(\nabla\varphi \times \nabla r) + B^\varphi \sqrt{g}\,(\nabla r \times \nabla \vartheta) \tag{2.2}$$

where the components of the magnetic field are given by [20, p. 77],

$$B^{\vartheta} = \frac{1}{2\pi\sqrt{g}}\frac{\partial\Psi^{\mathrm{r}}_{\mathrm{pol}}}{\partial r}, \qquad B^{\varphi} = \frac{1}{2\pi\sqrt{g}}\frac{\partial\Psi_{\mathrm{tor}}}{\partial r}, \tag{2.3a}$$

$$B_r = -\frac{4\pi}{c}\tilde{\eta} + \frac{\partial\tilde{\Phi}_{\mathrm{m}}}{\partial r}, \quad B_{\vartheta} = \frac{2}{c}I_{\mathrm{tor}} + \frac{\partial\tilde{\Phi}_{\mathrm{m}}}{\partial\vartheta}, \quad B_{\varphi} = \frac{2}{c}I^{\mathrm{d}}_{\mathrm{pol}} + \frac{\partial\tilde{\Phi}_{\mathrm{m}}}{\partial\varphi}. \tag{2.3b}$$

In (2.3a) and (2.3b) $\Psi_{\mathrm{tor}}(r)$, $\Psi^{\mathrm{r}}_{\mathrm{pol}}(r)$, c, $I_{\mathrm{tor}}(r)$, $I^{\mathrm{d}}_{\mathrm{pol}}(r)$, $\tilde{\eta}(r,\vartheta,\varphi)$ and $\tilde{\Phi}_{\mathrm{m}}(r,\vartheta,\varphi)$ are toroidal magnetic flux, poloidal-ribbon magnetic flux, speed of light, toroidal current, poloidal-disk current, current stream function and scalar magnetic potential, respectively (see [20, p. 77]), and $\sqrt{g}$ denotes the metric determinant,

$$\sqrt{g} = \frac{\partial\mathbf{r}}{\partial r} \times \frac{\partial\mathbf{r}}{\partial\vartheta} \cdot \frac{\partial\mathbf{r}}{\partial\varphi}. \tag{2.4}$$

The current stream function and the scalar magnetic potential are periodic functions in the angles, see [20, pp. 129–142]. For the axisymmetric, unperturbed tokamak magnetic field the derivative of the scalar magnetic potential along φ is zero and, therefore, the co-variant toroidal **B**-field component is constant on a flux surface, i.e. $B_{\varphi} = B_{\varphi}(r)$. Here, the effective radius r [10] is used to label flux surfaces, which is defined by the condition

$$\langle|\nabla r|\rangle = 1, \tag{2.5}$$

where

$$\langle a\rangle \equiv \frac{1}{\delta V}\int\limits_{\delta V} \mathrm{d}^3 r\; a(\mathbf{r}) = \left(\int\limits_0^{2\pi}\mathrm{d}\vartheta\int\limits_0^{2\pi}\mathrm{d}\varphi\;\sqrt{g}\right)^{-1}\left(\int\limits_0^{2\pi}\mathrm{d}\vartheta\int\limits_0^{2\pi}\mathrm{d}\varphi\;\sqrt{g}a(\mathbf{x})\right) \tag{2.6}$$

denotes the neoclassical flux surface average [20, 2]. The neoclassical flux surface average of a quantity a means volume averaging of a over an infinitesimally small shell with volume δV lying between two neighboring flux surfaces [20, p. 85]. Using this definition, the flux surface area S can be

expressed through the neoclassical surface average (2.6) as

$$S(r) = \int_0^{2\pi} \mathrm{d}\vartheta \int_0^{2\pi} \mathrm{d}\varphi \, \frac{\partial \mathbf{r}}{\partial \vartheta} \times \frac{\partial \mathbf{r}}{\partial \varphi} \cdot \frac{\nabla r}{|\nabla r|} = \int_0^{2\pi} \mathrm{d}\vartheta \int_0^{2\pi} \mathrm{d}\varphi \, \sqrt{g} |\nabla r| = \int_0^{2\pi} \mathrm{d}\vartheta \int_0^{2\pi} \mathrm{d}\varphi \, \sqrt{g}. \tag{2.7}$$

The flux surface average of the contra-variant component of the particle flux density corresponds to the flux density averaged over the flux surface area,

$$\langle n_\alpha V_\alpha^r \rangle = \langle n_\alpha \mathbf{V}_\alpha \cdot \nabla r \rangle = \frac{1}{S} \int_0^{2\pi} \mathrm{d}\vartheta \int_0^{2\pi} \mathrm{d}\varphi \, \frac{\partial \mathbf{r}}{\partial \vartheta} \times \frac{\partial \mathbf{r}}{\partial \varphi} \cdot \mathbf{V}_\alpha n_\alpha = \frac{1}{S} \oint \mathrm{d}\mathbf{S} \cdot \mathbf{V}_\alpha n_\alpha = \Gamma_\alpha, \tag{2.8}$$

where n_α is the density and $\mathbf{V}_\alpha$ is the fluid velocity of species α.

The straight field line flux coordinate system introduced above is based on a particular choice for the angles, which is well-suited for the mathematical description of axisymmetric devices. This degree of freedom can be used to design coordinate systems with certain features. One straight field line flux coordinate system (r,ϑ_f,φ_f) is related to another (r,ϑ_F,φ_F) by following set of transformation equations,

$$\vartheta_\mathrm{F} = \vartheta_\mathrm{f} + \frac{\partial \Psi_\mathrm{pol}^\mathrm{r}}{\partial r} G_\mathrm{F}(r, \vartheta_\mathrm{f}, \varphi_\mathrm{f}), \tag{2.9a}$$

$$\varphi_\mathrm{F} = \varphi_\mathrm{f} + \frac{\partial \Psi_\mathrm{tor}}{\partial r} G_\mathrm{F}(r, \vartheta_\mathrm{f}, \varphi_\mathrm{f}), \tag{2.9b}$$

where $G_\mathrm{F}(r, \vartheta_\mathrm{f}, \varphi_\mathrm{f})$ is an arbitrary periodic function which fulfills the subsequent magnetic differential equation,

$$2\pi \mathbf{B} \cdot \nabla G_\mathrm{F} = \frac{1}{\sqrt{g_\mathrm{F}}} - \frac{1}{\sqrt{g_\mathrm{f}}}. \tag{2.10}$$

For example, Hamada coordinates (r,ϑ_H,φ_H) [15] are obtained by deforming the angles in such a way that aside from magnetic field lines also current density lines appear to be straight. This results in a Jacobian which is

constant on a flux surface,

$$\sqrt{g_{\rm H}} = \frac{\partial V}{\partial r}\left(\frac{\partial \mathbf{r}}{\partial V}\times\frac{\partial \mathbf{r}}{\partial \vartheta_{\rm H}}\cdot\frac{\partial \mathbf{r}}{\partial \varphi_{\rm H}}\right) = \frac{\partial V}{\partial r}\left(\sqrt{g}\right)_{\rm H} = \frac{\partial V}{\partial r}\frac{1}{4\pi^2} = \frac{S(r)}{4\pi^2}. \quad (2.11)$$

In Boozer coordinates (r,$\vartheta_{\rm B}$,$\varphi_{\rm B}$) [14] this free parameter is used to make the periodic magnetic scalar potential vanish, which yields very simple expressions for the co-variant poloidal and toroidal $\mathbf{B}$-field components,

$$B_{\vartheta_{\rm B}} = \frac{2}{c}I_{\rm tor}, \qquad B_{\varphi_{\rm B}} = \frac{2}{c}I^{\rm d}_{\rm pol}. \quad (2.12)$$

The Jacobian for Boozer coordinates with r as a flux surface label is given by

$$\begin{aligned}\sqrt{g_{\rm B}} &= \frac{\partial \Psi_{\rm tor}}{\partial r}\left(\frac{\partial \mathbf{r}}{\partial \Psi_{\rm tor}}\times\frac{\partial \mathbf{r}}{\partial \vartheta_{\rm B}}\cdot\frac{\partial \mathbf{r}}{\partial \varphi_{\rm B}}\right) = \frac{\partial \Psi_{\rm tor}}{\partial r}\left(\sqrt{g}\right)_{\rm B} = \frac{\partial \Psi_{\rm tor}}{\partial r}\frac{\iota I_{\rm tor} + I^{\rm d}_{\rm pol}}{\pi c B^2} \\ &= \frac{\partial \Psi_{\rm tor}}{\partial r}\frac{\iota B_{\vartheta_{\rm B}} + B_{\varphi_{\rm B}}}{2\pi B^2} = \frac{\partial \psi_{\rm tor}}{\partial r}\frac{\iota B_{\vartheta_{\rm B}} + B_{\varphi_{\rm B}}}{B^2} = \frac{\partial \psi^{\rm r}_{\rm pol}}{\partial r}\frac{B_{\vartheta_{\rm B}} + q B_{\varphi_{\rm B}}}{B^2}, \quad (2.13)\end{aligned}$$

where $\psi_{\rm tor} = \Psi_{\rm tor}/(2\pi)$ and $\psi^{\rm r}_{\rm pol} = \Psi^{\rm r}_{\rm pol}/(2\pi)$.

2.1.2 Plasma rotation and radial electric field

The equilibrium electric field $\mathbf{E} = -\nabla\Phi$ is linked with the plasma ion fluid velocity $\mathbf{V}$ via the ideal MHD momentum conservation equation neglecting inertia and viscosity [21, 2],

$$\nabla p_i = e_i n_i\left(\mathbf{E} + \frac{1}{c}\mathbf{V}\times\mathbf{B}\right), \quad (2.14)$$

where p_i, e_i and n_i are ion pressure, charge and density, respectively. In the following relations between the radial electric field and the contra-variant poloidal and toroidal components of the plasma rotation velocity are established using standard neoclassical theory. At first the perpendicular component of the fluid velocity $\mathbf{V}_\perp$ is obtained from the cross-product of (2.14)

with $\mathbf{B}$,

$$\mathbf{V}_\perp = \mathbf{V} - \mathbf{hh}\cdot\mathbf{V} = \frac{c}{B}\mathbf{h}\times\left(\frac{\nabla p_i}{e_i n_i} - \mathbf{E}\right), \tag{2.15}$$

where $\mathbf{h} = \mathbf{B}/B$ is the unit vector along the magnetic field. The contravariant components of $\mathbf{V}_\perp$ are then,

$$V_\perp^r = \mathbf{V}_\perp\cdot\nabla r = 0, \tag{2.16}$$

$$V_\perp^\vartheta = \mathbf{V}_\perp\cdot\nabla\vartheta = \frac{cB_\varphi}{\sqrt{g}B^2}\left(\frac{p_i'}{e_i n_i} - E_r\right) = \frac{cT_iB_\varphi}{e_i\sqrt{g}B^2}\left(\frac{p_i'}{p_i} + \frac{e_i\Phi'}{T_i}\right), \tag{2.17}$$

$$V_\perp^\varphi = \mathbf{V}_\perp\cdot\nabla\varphi = -\frac{cB_\vartheta}{\sqrt{g}B^2}\left(\frac{p_i'}{e_i n_i} - E_r\right) = -\frac{cT_iB_\vartheta}{e_i\sqrt{g}B^2}\left(\frac{p_i'}{p_i} + \frac{e_i\Phi'}{T_i}\right), \tag{2.18}$$

where $T_i = p_i n_i^{-1}$ is the ion temperature and primed quantities denote partial radial derivatives of the respective quantities, e.g., $p_i' = \partial p_i/\partial r$. Here, pressure, density, temperature and radial electric field are assumed to be flux surface functions (constant on a flux surface), i.e. poloidal and toroidal variations of these quantities are not considered. The parallel component of the fluid velocity, $\mathbf{V}_\parallel = V_\parallel\mathbf{h}$, is determined by the condition of divergence free rotation,

$$\begin{aligned}\nabla\cdot\mathbf{V} = \nabla\cdot\left(\mathbf{V}_\perp + \mathbf{V}_\parallel\right) &= \frac{1}{\sqrt{g}}\frac{\partial}{\partial x_i}\sqrt{g}\left(V_\perp^i + V_\parallel^i\right)\\ &= \frac{1}{\sqrt{g}}\frac{\partial}{\partial\vartheta}\sqrt{g}\left(V_\perp^\vartheta + V_\parallel^\vartheta\right) = 0,\end{aligned} \tag{2.19}$$

which is valid for subsonic incompressible flows. This condition immediately follows from the continuity equation if the quantities considered in the transport ordering have a weak time dependence [21, p. 156]. The term with the derivative over φ in (2.19) vanishes in the unperturbed tokamak field because of axisymmetry. It should be noted that $\mathbf{V}_\perp$ itself is not divergence free, which results in the existence of a parallel fluid velocity that eventually

balances the divergence. Upon inserting (2.17) into (2.19),

$$\begin{aligned} 0 &= \frac{\partial}{\partial\vartheta}\sqrt{g}\left(\frac{cT_iB_\varphi}{e_i\sqrt{g}B^2}\left(\frac{p_i'}{p_i}+\frac{e_i\Phi'}{T_i}\right)+\frac{B^\vartheta}{B}V_\parallel\right) \\ &= \sqrt{g}B^\vartheta\frac{\partial}{\partial\vartheta}\left(\frac{cT_iB_\varphi}{e_i\sqrt{g}B^\vartheta B^2}\left(\frac{p_i'}{p_i}+\frac{e_i\Phi'}{T_i}\right)+\frac{V_\parallel}{B}\right), \end{aligned} \tag{2.20}$$

one can solve for $V_\parallel$ which is determined up to an arbitrary flux surface function $K(r)$ times B,

$$V_\parallel = -\frac{cT_iB_\varphi}{e_i\sqrt{g}B^\vartheta B}\left(\frac{p_i'}{p_i}+\frac{e_i\Phi'}{T_i}\right)+K(r)B. \tag{2.21}$$

In order to retain the generic form of $V_\parallel$ given by (5) in [2], $K(r)$ is cast in terms of Onsager symmetric transport coefficients D_{ij} ($D_{ij} = D_{ji}$), which link the thermodynamic forces A_j defined by

$$A_1 = \frac{1}{n_\alpha}\frac{\partial n_\alpha}{\partial r}-\frac{e_\alpha E_r}{T_\alpha}-\frac{3}{2T_\alpha}\frac{\partial T_\alpha}{\partial r},\quad A_2=\frac{1}{T_\alpha}\frac{\partial T_\alpha}{\partial r},\quad A_3=\frac{e_\alpha}{T_\alpha}\frac{\langle E_\parallel B\rangle}{\langle B^2\rangle}, \tag{2.22}$$

where $E_\parallel$ is the inductive electric field, with the thermodynamic fluxes I_i defined as

$$I_1=\Gamma_\alpha,\qquad I_2=\frac{Q_\alpha}{T_\alpha},\qquad I_3=n_\alpha\langle V_\parallel B\rangle, \tag{2.23}$$

where Q_α is the flux surface averaged heat flux density, via the relations

$$I_i=-n_\alpha\sum_{j=1}^{3}D_{ij}A_j. \tag{2.24}$$

After multiplying (2.21) with B and flux surface averaging, the subsequent expression for the parallel flow is obtained,

$$\begin{aligned} \langle BV_\parallel\rangle &= -\frac{cT_iB_\varphi}{e_i\sqrt{g}B^\vartheta}\left(\frac{p_i'}{p_i}+\frac{e_i\Phi'}{T_i}\right)+K(r)\langle B^2\rangle \\ &= -\left(D_{31}\left(\frac{p_i'}{p_i}+\frac{e_i\Phi'}{T_i}\right)+\left(D_{32}-\frac{5}{2}D_{31}\right)\frac{T_i'}{T_i}\right). \end{aligned} \tag{2.25}$$

The arbitrary integration constant $K(r)$ is fixed by (2.25) as

$$K(r) = \frac{D_{31}}{\langle B^2 \rangle} \left(\frac{5}{2} - \frac{D_{32}}{D_{31}} \right) \frac{T_i'}{T_i} = \frac{ckB_\varphi}{e_i \sqrt{g} B^\vartheta \langle B^2 \rangle} \frac{\partial T_i}{\partial r}, \quad D_{31} = \frac{cT_i B_\varphi}{e_i \sqrt{g} B^\vartheta}, \quad (2.26)$$

where the coefficient $k(r) = 2.5 - D_{32}/D_{31}$ depending on plasma collisionality changes for a tokamak with infinite aspect ratio between -2.1 and 1.17, see [22, 23, 24, 25, 2]. In case of a tokamak with unit aspect ratio the plasma cannot rotate poloidally and, therefore, k has to vanish because all particles are trapped in such a configuration, which in turn results in an infinite neoclassical parallel viscosity (see, e.g., Ref. [21, p. 198]). This coefficient k is computed by the original version of the code NEO-2 [1], which is used to evaluate the distribution function and the transport coefficients for toroidal confinement devices in regimes where the effect of electric field on the transport coefficients is negligible. Using (2.26), the expression for the parallel velocity becomes

$$V_\parallel = -\frac{cT_i B_\varphi}{e_i \sqrt{g} B^\vartheta B} \left(\frac{p_i'}{p_i} + \frac{e_i \Phi'}{T_i} \right) + \frac{ckBB_\varphi}{e_i \sqrt{g} B^\vartheta \langle B^2 \rangle} \frac{\partial T_i}{\partial r}. \quad (2.27)$$

For the divergence free poloidal and toroidal components of the fluid velocity (angular frequencies) one obtains

$$V^\vartheta = \frac{ckB_\varphi}{e_i \sqrt{g} \langle B^2 \rangle} \frac{\partial T_i}{\partial r}, \qquad V^\varphi = qV^\vartheta - \frac{cT_i}{e_i \sqrt{g} B^\vartheta} \left(\frac{p_i'}{p_i} + \frac{e_i \Phi'}{T_i} \right). \quad (2.28)$$

2.1.3 Guiding center motion of a charged particle in a electromagnetic field

A description of transport processes within kinetic theory requires the knowledge of the charged particle trajectories in an electromagnetic field. The associated equations of guiding center motion are well-known and have been extensively discussed in the review of Morozov and Solov'ev [26]. The derivation of the equations of motion, which is presented in this section, follows the variational principle introduced by R. G. Littlejohn [27]. In this approach an adiabatic ordering parameter ϵ, which physically represents the smallness of

Larmor radius ρ_L to the macroscopic scale length L, is naturally included. The ordering parameter will be kept in the final expressions to illustrate the transport ordering used upon deriving the drift kinetic equation in Section 2.1.4. A very detailed re-derivation of the guiding center Lagrangian and the corresponding set of equations of motion is given in the thesis of P. Leitner [28] for the case of static electromagnetic fields. In this section also slow variations in time, $\tau = \epsilon t$, of the electromagnetic fields are taken into account.

The guiding center Lagrangian $L_{\mathrm{gc}} = L_{\mathrm{gc}}(\mathbf{z}, \dot{\mathbf{z}})$ expanded up to the first order in ϵ for phase space variables $\mathbf{z} = (\mathbf{r}_{\mathrm{g}}, J_\perp, \phi, w)$ is given by (see also Eq. (29) in Ref. [27]),

$$L_{\mathrm{gc}} = \frac{e_\alpha}{c\epsilon}\mathbf{A}(\mathbf{r}_{\mathrm{g}}, \tau) \cdot \dot{\mathbf{r}}_{\mathrm{g}} + m_\alpha v_\parallel \mathbf{h}(\mathbf{r}_{\mathrm{g}}, \tau) \cdot \dot{\mathbf{r}}_{\mathrm{g}} - w - \epsilon J_\perp \dot{\phi}, \tag{2.29}$$

where m_α is species α mass, $\mathbf{r}_{\mathrm{g}}$ is the position of the guiding center, ϕ is the gyrophase,

$$J_\perp \approx \frac{m_\alpha v_\perp^2}{2\omega_{\mathrm{c},\alpha}} \tag{2.30}$$

is the perpendicular adiabatic invariant and w is the total energy

$$w = \frac{m_\alpha v^2}{2} + e_\alpha \Phi(\mathbf{r}_{\mathrm{g}}, \tau). \tag{2.31}$$

Here, $\mathbf{A}$, $\omega_{\mathrm{c},\alpha} = e_\alpha B (m_\alpha c)^{-1}$, $v_\parallel = \sigma\sqrt{2m_\alpha^{-1}(w - e_\alpha \Phi(\mathbf{r}_{\mathrm{g}}, \tau) - J_\perp \omega_{\mathrm{c},\alpha})}$ and $\sigma = \pm 1$ are the magnetic vector potential, cyclotron frequency, parallel velocity and velocity sign, respectively. Dotted quantities denote the total time derivative of the respective quantity. The equations of motion are obtained from the Euler-Lagrange equations,

$$\frac{\mathrm{d}}{\mathrm{d}t}\frac{\partial L_{\mathrm{gc}}}{\partial \dot{\mathbf{z}}} - \frac{\partial L_{\mathrm{gc}}}{\partial \mathbf{z}} = 0. \tag{2.32}$$

For the velocity space variables $J_\perp$, ϕ and w subsequent set of relations is

found,

$$\dot{\phi} = -\frac{\omega_{\mathrm{c},\alpha}}{\epsilon}, \qquad \dot{J}_\perp = 0, \qquad v_\parallel = \mathbf{h}\cdot\dot{\mathbf{r}}_\mathrm{g}. \tag{2.33}$$

From the cross-product of the Euler-Lagrange equation for $\mathbf{r}_\mathrm{g}$,

$$\begin{aligned} 0 &= \frac{\mathrm{d}}{\mathrm{d}t}\frac{\partial L_\mathrm{gc}}{\partial \dot{\mathbf{r}}_\mathrm{g}} - \frac{\partial L_\mathrm{gc}}{\partial \mathbf{r}_\mathrm{g}} \\ &= m_\alpha \dot{v}_\parallel \mathbf{h} - \frac{e_\alpha}{c\epsilon}\dot{\mathbf{r}}_\mathrm{g}\times\mathbf{B}^* + \frac{e_\alpha}{c}\frac{\partial \mathbf{A}}{\partial \tau} + \epsilon m_\alpha v_\parallel \frac{\partial \mathbf{h}}{\partial \tau} + \frac{\mathbf{h}}{v_\parallel}\left(\dot{\mathbf{r}}_\mathrm{g}\cdot\nabla\right)\left[e_\alpha\Phi + J_\perp\omega_{\mathrm{c},\alpha}\right], \end{aligned} \tag{2.34}$$

with $\mathbf{h}$, the guiding center velocity $\mathbf{v}_\mathrm{g} = \dot{\mathbf{r}}_\mathrm{g}$ can be determined

$$\begin{aligned} \mathbf{v}_\mathrm{g} = \dot{\mathbf{r}}_\mathrm{g} &= v_\parallel \frac{\mathbf{B}^*}{B^*_\parallel} + \frac{\epsilon}{B^*_\parallel}\mathbf{h}\times\frac{\partial \mathbf{A}}{\partial \tau} = v_\parallel \frac{\mathbf{B}}{B^*_\parallel} + \mathbf{v}_\mathrm{gd} \\ &= v_\parallel \frac{\mathbf{B}}{B^*_\parallel} + \frac{\epsilon}{B^*_\parallel}\left(\frac{v_\parallel^2}{\omega_{\mathrm{c},\alpha}}\nabla\times\mathbf{B} + \frac{v_\perp^2 + 2v_\parallel^2}{2\omega_{\mathrm{c},\alpha}}\mathbf{h}\times\nabla B - c\mathbf{h}\times\mathbf{E}\right), \end{aligned} \tag{2.35}$$

where $\mathbf{B}^* = \nabla\times\mathbf{A}^*$, $B^*_\parallel = \mathbf{B}^*\cdot\mathbf{h}$ and $\mathbf{A}^*$ is the modified vector potential [26],

$$\mathbf{A}^* = \mathbf{A} + \epsilon\frac{m_\alpha c}{e_\alpha} v_\parallel \mathbf{h}. \tag{2.36}$$

The scalar product of (2.34) with $\dot{\mathbf{r}}_\mathrm{g}$ gives the relation for the change of energy with time,

$$\dot{w} = e_\alpha \dot{\mathbf{r}}_\mathrm{g}\cdot\mathbf{E}^{(A)}, \tag{2.37}$$

whereby only leading order terms in ϵ are retained and $\mathbf{E}^{(A)}$ denotes here the inductive electric field,

$$\mathbf{E}^{(A)} = -\frac{1}{c}\frac{\partial \mathbf{A}}{\partial \tau}. \tag{2.38}$$

The complete set of equations of motion for the phase space variables $\mathbf{z} = (\mathbf{r}_\mathrm{g}, J_\perp, \phi, w)$ are given by,

$$\dot{\mathbf{r}}_\mathrm{g} = \mathbf{v}_\mathrm{g}, \qquad \dot{J}_\perp = 0, \qquad \dot{\phi} = -\frac{\omega_{\mathrm{c},\alpha}}{\epsilon}, \qquad \dot{w} = e_\alpha \dot{\mathbf{r}}_\mathrm{g}\cdot\mathbf{E}^{(A)}. \tag{2.39}$$

The Jacobian of these variables is

$$J_{\text{inv}} = \frac{\partial(\mathbf{r}, \mathbf{p})}{\partial(\mathbf{r}_g, J_\perp, \phi, w)} = \frac{eB_\parallel^*}{c\left|v_\parallel\right|}. \tag{2.40}$$

2.1.4 Drift kinetic equation

The kinetic equation is the basis for all transport studies on a microscopic level. Due to the very different time and length scales involved in plasma transport the kinetic equation is a stiff integro-differential equation in a six-dimensional phase space. A numerical solution of the kinetic equation without model simplifications is therefore not possible. Here, the linearized drift kinetic equation (LDKE) is derived using the standard neoclassical transport ordering, which reduces the problem dimension by two. The four-dimensional LDKE is the starting point for the evaluation of non-ambipolar fluxes due to non-axisymmetric magnetic fields.

The kinetic equation expressed in terms of phase space variables $\mathbf{z} = (\mathbf{r}_\mathrm{g}, J_\perp, \phi, w)$ is given by

$$\frac{\partial f}{\partial t} + \mathbf{v}_\mathrm{g} \cdot \frac{\partial f}{\partial \mathbf{r}_\mathrm{g}} + \dot{w}\frac{\partial f}{\partial w} + \dot{\phi}\frac{\partial f}{\partial \phi} = \hat{L}_\mathrm{c} f, \tag{2.41}$$

where $\hat{L}_\mathrm{c}$ is the Landau collision integral [29]. Note that the species index α is omitted here and in the following expressions in order not to overload the notation. The collision integral can also be presented in a standard Fokker-Planck form

$$\hat{L}_\mathrm{c} f = \frac{\partial}{\partial \mathbf{v}} \cdot \left[\overleftrightarrow{\mathbf{D}} \cdot \frac{\partial f}{\partial \mathbf{v}} - \frac{\mathbf{F}}{m} f, \right] \tag{2.42}$$

where $\overleftrightarrow{\mathbf{D}}$ is the velocity space diffusion tensor and $\mathbf{F}$ the drag force [30]. The gyro-motion of the charged particle, which is described by the last term on the left-hand side of (2.41), represents the shortest time scale of all processes investigated here and, especially, is much faster than transport processes. Therefore, it is useful to average (2.41) over the gyrophase, which yields the

gyrokinetic equation,

$$\frac{\partial f}{\partial t} + \mathbf{v}_\mathrm{g} \cdot \frac{\partial f}{\partial \mathbf{r}_\mathrm{g}} + \langle \dot{w} \rangle_\phi \frac{\partial f}{\partial w} = \left\langle \hat{L}_\mathrm{c} f \right\rangle_\phi , \tag{2.43}$$

where f is considered to be independent of gyrophase from now on and $\langle \ldots \rangle_\phi$ denotes the gyro-average. Formally, the gyro-average of the collision integral can be obtained when velocity space diffusion coefficients and drag force components evaluated at the actual particle position are replaced with the respective quantities evaluated at the guiding center position.

In the standard neoclassical transport ansatz the Larmor radius ρ_L is assumed to be small in comparison to the macroscopic scale length L of radial gradients (of density, temperature, magnetic field,...) [21],

$$\epsilon \equiv \rho_\mathrm{L}/L \ll 1, \tag{2.44}$$

where $\rho_\mathrm{L} = v_T/\omega_\mathrm{c}$ and $v_T = \sqrt{2T/m}$ is the thermal velocity. The radial transport considered here is purely diffusive which results in time derivatives of the order of [21]

$$\frac{\partial}{\partial t} \sim \frac{D}{L^2} \sim \epsilon^2 \nu \sim \epsilon^2 \frac{v_T}{L}, \tag{2.45}$$

where ν is the collision frequency and $D \sim \nu\epsilon^2$ is the diffusion coefficient. Furthermore, plasmas shall be strongly magnetized,

$$\Delta \equiv \nu/\omega_\mathrm{c} \ll 1, \tag{2.46}$$

and flow velocities are regarded to be subsonic, i.e. smaller than the thermal speed,

$$V \sim \epsilon v_T. \tag{2.47}$$

Using the neoclassical transport ordering (2.44)–(2.47), the drift kinetic equation in the lowest order with respect to ϵ is obtained from the gyrokinetic equation (2.43) as

$$v_\parallel \mathbf{h} \cdot \nabla f_0 = \hat{L}_c f_0. \tag{2.48}$$

In order to show that the solution to the lowest order in ϵ, f_0, corresponds to

a Maxwellian (see, e.g., Ref. [21] or Ref. [23]), equation (2.48) is multiplied by $\ln f_0$, integrated over velocity space and flux-surface averaged,

$$\left\langle \int \mathrm{d}^3v \, (\ln f_0) \, v_\parallel \mathbf{h} \cdot \nabla f_0 \right\rangle = \left\langle \int \mathrm{d}^3v \, (\ln f_0) \, \hat{L}_c f_0 \right\rangle . \tag{2.49}$$

The left-hand side of (2.49) becomes zero,

$$\begin{aligned} 0 &= \sum_{\sigma=\pm 1} \frac{2\pi e\sigma}{c} \left\langle \int_{e\Phi}^{\infty} \mathrm{d}w \int_0^{\frac{w-e\Phi}{\omega_c}} \mathrm{d}J_\perp \mathbf{B} \cdot \nabla f_0 \, (\ln f_0 - 1) \right\rangle \\ &= \left\langle \int \mathrm{d}^3v \, (\ln f_0) \, v_\parallel \mathbf{h} \cdot \nabla f_0 \right\rangle , \end{aligned} \tag{2.50}$$

because the flux-surface average annihilates the operator $\mathbf{B} \cdot \nabla g$ for any periodic function $g(r, \vartheta)$ (see Eq. (4.9.32) of Ref. [20]). Due to Boltzmann's H-theorem,

$$\int \mathrm{d}^3v \, (\ln f) \, \hat{L}_c f \leq 0, \tag{2.51}$$

where the equality holds if f is a Maxwellian f_M, equation (2.49) can be fulfilled only if $f_0 = f_\mathrm{M}$. This means that the distribution function to the lowest order in ϵ must be a Maxwellian,

$$f_0 = f_\mathrm{M}(r, w) = \frac{n}{\pi^{3/2} v_T^3} e^{-(w - e\Phi)/T}. \tag{2.52}$$

Therefore, one can expand the solution f in powers of ϵ with respect to a local Maxwellian,

$$f = f_\mathrm{M} + f_1 + \mathcal{O}(\epsilon^2), \tag{2.53}$$

whereby straight field line flux coordinates are introduced for the guiding center position $\mathbf{r}_\mathrm{g} = (r, \vartheta, \varphi)$. The first-order drift kinetic equation (4D LDKE) is then given by,

$$\hat{L} f_1 \equiv v_\mathrm{g}^\vartheta \frac{\partial f_1}{\partial \vartheta} + v_\mathrm{g}^\varphi \frac{\partial f_1}{\partial \varphi} - \hat{L}_\mathrm{cL} f_1 = -v_\mathrm{g}^r \frac{\partial f_\mathrm{M}}{\partial r} - e E_\parallel v_\parallel \frac{\partial f_\mathrm{M}}{\partial w} \equiv \dot{f}_\mathrm{M}, \tag{2.54}$$

where $E_\parallel = \mathbf{h} \cdot \mathbf{E}^{(A)}$ and $\hat{L}_\mathrm{cL}$ is the linearized collision operator. The full time

derivative of the Maxwellian can be expressed in terms of thermodynamic forces (2.22),

$$\dot{f}_{\mathrm{M}} = -f_{\mathrm{M}} \sum_{k=1}^{3} q_k A_k + \frac{e f_{\mathrm{M}}}{T} v_{\parallel} \mathbf{h} \cdot \nabla \delta\Phi, \tag{2.55}$$

where

$$q_1 = -v_{\mathrm{g}}^r, \qquad q_2 = -\frac{mv^2}{2T} v_{\mathrm{g}}^r, \qquad q_3 = v_{\parallel} B, \tag{2.56}$$

and $\delta\Phi$ is the solution to the magnetic differential equation,

$$\mathbf{h} \cdot \nabla \delta\Phi = B \frac{\langle E_{\parallel} B \rangle}{\langle B^2 \rangle} - E_{\parallel} \tag{2.57}$$

which also satisfies $\langle \delta\Phi \rangle = 0$ [6]. Since (2.54) is a linear integro-differential equation, in a simple plasma where the coupling between the perturbed distributions of different species (electrons and ions) can be ignored, the distribution function f_1 can be written as a superposition of solutions for the individual thermodynamic forces,

$$f_1 = f_{\mathrm{M}} \sum_{k=1}^{3} f_{1,k} A_k - \frac{e\delta\Phi}{T} f_{\mathrm{M}}, \tag{2.58}$$

where $f_{1,k}$ are solutions to

$$\hat{L} f_{\mathrm{M}} f_{1,k} = q_k f_{\mathrm{M}}. \tag{2.59}$$

The more general case, where the coupling between different particle species is treated accurately as required in the presence of a few sorts of ions, is discussed in Chapter 5.

2.2 Toroidal momentum conservation in a plasma and neoclassical toroidal viscous torque

2.2.1 General form of the toroidal momentum conservation equation in a plasma

The fluid momentum conservation equation for species α is obtained from the first moment of the kinetic equation [21],

$$\frac{\partial}{\partial t} m_\alpha n_\alpha \mathbf{V}_\alpha + \nabla \cdot \overleftrightarrow{\mathbf{\Pi}}_\alpha = e_\alpha n_\alpha \left(\mathbf{E} + \frac{1}{c} \mathbf{V} \times \mathbf{B} \right) + \mathbf{R}_\alpha, \tag{2.60}$$

where $\mathbf{R}_\alpha$ is the Coulomb friction force and $\overleftrightarrow{\mathbf{\Pi}}_\alpha$ is the stress tensor, which includes the inertial term, the scalar pressure p_α and the viscous stress tensor $\overleftrightarrow{\pi}_\alpha$,

$$\overleftrightarrow{\mathbf{\Pi}}_\alpha = m_\alpha \int \mathrm{d}^3 v \mathbf{v}\mathbf{v} f_\alpha = m_\alpha n_\alpha \mathbf{V}_\alpha \mathbf{V}_\alpha + p_\alpha \overleftrightarrow{\mathbf{I}} + \overleftrightarrow{\pi}_\alpha. \tag{2.61}$$

Summation of (2.60) over all species leads to the conservation law for the total momentum,

$$\frac{\partial}{\partial t} \sum_\alpha m_\alpha n_\alpha \mathbf{V}_\alpha + \sum_\alpha \nabla \cdot \overleftrightarrow{\mathbf{\Pi}}_\alpha = \rho \mathbf{E} + \frac{1}{c} \mathbf{j} \times \mathbf{B}, \tag{2.62}$$

ρ and $\mathbf{j}$ are the total plasma charge and current density, respectively. Due to third Newton's law the friction forces cancel each other and, therefore, no such term appears in (2.62). Using Maxwell's equations for the closure of ρ and $\mathbf{j}$,

$$\nabla \cdot \mathbf{E} = 4\pi\rho, \qquad \nabla \times \mathbf{B} = \frac{4\pi}{c} \mathbf{j} + \frac{1}{c} \frac{\partial \mathbf{E}}{\partial t}, \tag{2.63}$$

the Lorentz force density on the right-hand side of (2.62) can also be evaluated in terms of electromagnetic field quantities [31, 32, 33],

$$\rho \mathbf{E} + \frac{1}{c} \mathbf{j} \times \mathbf{B} = \nabla \cdot \overleftrightarrow{\boldsymbol{\sigma}} - \frac{1}{c^2} \frac{\partial \mathbf{S}}{\partial t}, \tag{2.64}$$

where $\overleftrightarrow{\boldsymbol{\sigma}}$ and $\mathbf{S}$ are Maxwell stress tensor and Pointing flux, respectively,

$$\overleftrightarrow{\boldsymbol{\sigma}} = \frac{1}{4\pi}\left(\mathbf{EE} - \frac{E^2}{2}\overleftrightarrow{\mathbf{I}} + \mathbf{BB} - \frac{B^2}{2}\overleftrightarrow{\mathbf{I}}\right), \qquad \mathbf{S} = \frac{c}{4\pi}\mathbf{E}\times\mathbf{B}. \tag{2.65}$$

With (2.64) it is possible to express the conservation law for the total momentum (2.62) in a conservative form [34, 2],

$$\frac{\partial \mathbf{P}}{\partial t} + \nabla\cdot\overleftrightarrow{\mathbf{\Pi}} = 0, \tag{2.66}$$

where the total momentum $\mathbf{P}$ and total stress tensor $\overleftrightarrow{\mathbf{\Pi}}$ of plasma and electromagnetic field are given by,

$$\mathbf{P} = \sum_\alpha m_\alpha n_\alpha \mathbf{V}_\alpha + \frac{1}{c^2}\frac{\partial \mathbf{S}}{\partial t}, \qquad \overleftrightarrow{\mathbf{\Pi}} = \sum_\alpha \overleftrightarrow{\mathbf{\Pi}}_\alpha - \overleftrightarrow{\boldsymbol{\sigma}} \tag{2.67}$$

The toroidal momentum conservation equation follows from multiplication of (2.66) with the toroidal co-variant basis vector $\mathbf{e}_\varphi$,

$$\left(\frac{\partial P_\varphi}{\partial t}\right)_{\mathbf{x}} + \left(\frac{\partial x^i}{\partial t}\right)_{\mathbf{r}}\frac{\partial P_\varphi}{\partial x^i} + \frac{1}{\sqrt{g}}\frac{\partial}{\partial x^i}\sqrt{g}\;\Pi^i_\varphi = 0, \tag{2.68}$$

where the time derivative of P_φ at a fixed spatial point $\mathbf{r}$ is evaluated in the moving frame $\mathbf{x} = \mathbf{x}(\mathbf{r}, t)$,

$$\left(\frac{\partial P_\varphi}{\partial t}\right)_{\mathbf{r}} = \left(\frac{\partial P_\varphi}{\partial t}\right)_{\mathbf{x}} + \left(\frac{\partial x^i}{\partial t}\right)_{\mathbf{r}}\frac{\partial P_\varphi}{\partial x^i}. \tag{2.69}$$

Due to the symmetry of the stress tensor, $\Pi^{ij} = \Pi^{ji}$, and the rotational symmetry of the metric tensor g_{ij} no additional source term occurs in (2.68),

$$\begin{aligned}
\mathbf{e}_\varphi\cdot\nabla\cdot\overleftrightarrow{\mathbf{\Pi}} &= \frac{1}{\sqrt{g}}\frac{\partial}{\partial x^i}\sqrt{g}\;\Pi^{ij}\mathbf{e}_j\cdot\mathbf{e}_\varphi - \Pi^{ij}\mathbf{e}_j\cdot\frac{\partial}{\partial x^i}\mathbf{e}_\varphi \\
&= \frac{1}{\sqrt{g}}\frac{\partial}{\partial x^i}\sqrt{g}\;\Pi^i_\varphi - \Pi^{ij}\frac{\partial \mathbf{r}}{\partial x^j}\cdot\frac{\partial^2\mathbf{r}}{\partial\varphi\partial x^i} \\
&= \frac{1}{\sqrt{g}}\frac{\partial}{\partial x^i}\sqrt{g}\;\Pi^i_\varphi - \underbrace{\Pi^{ij}\Gamma_{j,\varphi i}}_{=0} = \frac{1}{\sqrt{g}}\frac{\partial}{\partial x^i}\sqrt{g}\;\Pi^i_\varphi,
\end{aligned} \tag{2.70}$$

where $\Gamma_{j,\varphi i}$ denotes the Christoffel symbol of first kind,

$$\Gamma_{j,\varphi i} = \frac{\partial \mathbf{r}}{\partial x^j} \cdot \frac{\partial^2 \mathbf{r}}{\partial \varphi \partial x^i} = \underbrace{\frac{\partial}{\partial \varphi}\left(\frac{\partial \mathbf{r}}{\partial x^j} \cdot \frac{\partial \mathbf{r}}{\partial x^i}\right)}_{\to \partial g_{ji}/\partial \varphi = 0} - \frac{\partial \mathbf{r}}{\partial x^i} \cdot \frac{\partial^2 \mathbf{r}}{\partial \varphi \partial x^j} = -\Gamma_{i,\varphi j}. \tag{2.71}$$

The change of coordinates in time considered here takes place on a longer time scale than the viscosity changes. This means also that temporal variations of the magnetic field equilibria have only a negligible small effect on the evaluation of viscosities. Averaging over the toroidal angle leads to the 2D toroidal momentum conservation equation,

$$\left(\frac{\partial \bar{P}_\varphi}{\partial t}\right)_{\mathbf{x}_p} + \left(\frac{\partial x_p^i}{\partial t}\right)_{\mathbf{r}} \frac{\partial \bar{P}_\varphi}{\partial x_p^i} + \frac{1}{\sqrt{g}} \frac{\partial}{\partial x_p^i} \sqrt{g}\ \bar{\Pi}_\varphi^i = 0, \tag{2.72}$$

where bar denotes averaging over the toroidal angle φ and x_p^i are the poloidal coordinates, e.g., R and Z for cylindrical coordinates $\mathbf{x} = (R, \varphi, Z)$ or r and ϑ for flux coordinates $\mathbf{x} = (r, \vartheta, \varphi)$. Using

$$\begin{aligned}
0 &= \left(\frac{\partial}{\partial t}\left(\sqrt{g}\right)^{-1}\right)_{\mathbf{r}} - \left(\frac{\partial}{\partial t}\left(\nabla x^1 \cdot \nabla x^2 \times \nabla x^3\right)\right)_{\mathbf{r}} \\
&= -\frac{1}{g}\left(\frac{\partial \sqrt{g}}{\partial t}\right)_{\mathbf{r}} - \left(\frac{\partial \nabla x^i}{\partial t}\right)_{\mathbf{r}} \frac{1}{\sqrt{g}}\left(\frac{\partial \mathbf{r}}{\partial x^i}\right)_t \\
&= -\frac{1}{g}\left[\left(\frac{\partial \sqrt{g}}{\partial t}\right)_{\mathbf{r}} + \sqrt{g}\left(\frac{\partial \mathbf{r}}{\partial x^i}\right)_t \left(\nabla x^j\right)_t \frac{\partial}{\partial x^j}\left(\frac{\partial x^i}{\partial t}\right)_{\mathbf{r}}\right] \\
&= -\frac{1}{g}\left[\left(\frac{\partial \sqrt{g}}{\partial t}\right)_{\mathbf{x}} + \left(\frac{\partial x^i}{\partial t}\right)_{\mathbf{r}} \frac{\partial \sqrt{g}}{\partial x^i} + \sqrt{g}\frac{\partial}{\partial x^i}\left(\frac{\partial x^i}{\partial t}\right)_{\mathbf{r}}\right] \\
&= -\frac{1}{g}\left[\left(\frac{\partial \sqrt{g}}{\partial t}\right)_{\mathbf{x}} + \frac{\partial}{\partial x^i}\sqrt{g}\left(\frac{\partial x^i}{\partial t}\right)_{\mathbf{r}}\right],
\end{aligned} \tag{2.73}$$

one can re-write (2.72) in the form of a 4D divergence,

$$\frac{1}{\sqrt{g}}\frac{\partial}{\partial t}\sqrt{g}\bar{P}_\varphi + \frac{1}{\sqrt{g}}\frac{\partial}{\partial x_p^i}\sqrt{g}\left(\left(\frac{\partial x_p^i}{\partial t}\right)_{\mathbf{r}} \bar{P}_\varphi + \bar{\Pi}_\varphi^i\right) = 0. \tag{2.74}$$

After averaging over unperturbed flux surfaces the term with the time derivative of coordinates in (2.72) vanishes and the 1D toroidal momentum conser-

vation equation is obtained,

$$
\begin{aligned}
0 &= \left\langle \frac{1}{\sqrt{g}}\frac{\partial}{\partial t}\sqrt{g}\bar{P}_\varphi + \frac{1}{\sqrt{g}}\frac{\partial}{\partial x_p^i}\sqrt{g}\left(\left(\frac{\partial x_p^i}{\partial t}\right)_{\mathbf{r}}\bar{P}_\varphi + \bar{\Pi}_\varphi^i\right)\right\rangle \\
&= \frac{1}{\delta V}\Bigg\{\frac{\partial}{\partial t}\underbrace{\int_{r_1(t)}^{r_2(t)} \mathrm{d}r}_{=\delta r \neq f(t)} \int_0^{2\pi}\mathrm{d}\vartheta \int_0^{2\pi}\mathrm{d}\varphi \sqrt{g}\bar{P}_\varphi - \int_0^{2\pi}\mathrm{d}\vartheta\int_0^{2\pi}\mathrm{d}\varphi\left[\sqrt{g}\bar{P}_\varphi\left(\frac{\partial r}{\partial t}\right)_{\mathbf{r}}\right]_{r_1(t)}^{r_2(t)} + \\
&\quad + \int_0^{2\pi}\mathrm{d}\vartheta\int_0^{2\pi}\mathrm{d}\varphi\Bigg[\sqrt{g}\left(\frac{\partial r}{\partial t}\right)_{\mathbf{r}}\bar{P}_\varphi + \underbrace{\sqrt{g}\,\bar{\Pi}_\varphi^r}_{\to \delta r \frac{\partial}{\partial r}\sqrt{g}\bar{\Pi}_\varphi^r}\Bigg]_{r_1(t)}^{r_2(t)}\Bigg\} \\
&= \frac{1}{S}\frac{\partial}{\partial t}S\left\langle P_\varphi\right\rangle + \frac{1}{S}\frac{\partial}{\partial r}S\left\langle \Pi_\varphi^r\right\rangle, \qquad (2.75)
\end{aligned}
$$

where the Leibniz integral rule has been used in the second step and S denotes here the surface area (2.7).

2.2.2 Toroidal rotation equation for small amplitude external perturbations

In this section a re-derivation of the toroidal rotation equation [3, 35] according to Ref. [2] is given in order to show the underlying approximations and to introduce a common notation. The approximations made upon the derivation use only the smallness of perturbation field amplitudes and of the Larmor radius. The toroidal torque density due to non-resonant non-axisymmetric magnetic perturbations, which enters the toroidal rotation equation as a source term, is typically cast in terms of a neoclassical toroidal viscosity [3, 4, 36] (NTV). This viscosity is evaluated via a flux-force relation [37] from the non-ambipolar particle fluxes. Such a simple relation holds only for Hamada coordinates, see Ref. [38], whereas for other flux coordinates the whole pressure tensor has to be considered. In Ref. [2] it has been found that not only the pressure tensor but also the inertial term drives the NTV torque, whereby the latter becomes important for fast plasma rotation. The remaining part of this subsection corresponds to the coauthored Section IIIB

of the publication by Kasilov *et al.* [2]. Equation and reference numbers have been modified accordingly.

The exact total momentum conservation equations (2.72) and (2.75) are rather demonstrative but not very useful for practical evaluation of the effects of external non-resonant ideal magnetic perturbations. Instead, an approximate equation retaining the leading order terms in Larmor radius and perturbation amplitude is used in practice. For a derivation of the approximate rotation equation straight field line flux coordinates (generally time dependent) associated with the perturbed magnetic field [3, 4] with vector potential in the form

$$\mathbf{A} = A_\vartheta(t,r)\nabla\vartheta + A_\varphi(t,r)\nabla\varphi \tag{2.76}$$

are a convenient choice. Summing up the toroidal co-variant components of Eq. (2.60) over species and averaging the result over perturbed flux surfaces gives

$$\frac{1}{S}\frac{\partial}{\partial t}S\left\langle\frac{\partial\mathbf{r}}{\partial\varphi}\cdot\sum_\alpha m_\alpha n_\alpha\mathbf{V}_\alpha\right\rangle+\left\langle\frac{\partial\mathbf{r}}{\partial\varphi}\cdot\sum_\alpha\nabla\cdot\mathbf{\Pi}_\alpha\right\rangle+$$
$$+\frac{1}{c}\left(\frac{\mathrm{d}A_\varphi}{\mathrm{d}t}\langle\rho\rangle-\sqrt{g}B^\vartheta\left\langle j^r\right\rangle\right)=\left\langle\frac{\partial^2\mathbf{r}}{\partial t\partial\varphi}\cdot\sum_\alpha m_\alpha n_\alpha\mathbf{V}_\alpha\right\rangle+\langle\rho E_\varphi\rangle+\frac{1}{c}\frac{\mathrm{d}A_\varphi}{\mathrm{d}t}\langle\rho\rangle. \tag{2.77}$$

So far this equation is exact. The purpose now is to retain in (2.77) only the leading order terms in the perturbation amplitude ε_M and in the Larmor radius ρ_L. Thus, first of all, one has to ignore the difference between the perturbed and unperturbed flux coordinates in the first term because this difference is a negligible next order correction in ε_M. For the same reason one has to ignore all right hand side terms, which result from the time dependence of the coordinates, because it is assumed that the ramp up of the toroidal current and of the perturbation field are singular events (the axisymmetric inductive field coming from variation of the poloidal flux $\psi = -A_\varphi$ is already separated to the left hand side while the toroidal flux A_ϑ can contribute only

due to the time dependence of flux coordinates).

The flux-force relation is obtained starting from the stationary kinetic equation where the dependence of the electromagnetic field on time is parametric due to different time scales involved, and the plasma is assumed to be strictly neutral. Thus, one obtains an analog of (2.77) where only the stress tensor and the term with radial current remain,

$$\left\langle \frac{\partial \mathbf{r}}{\partial \varphi} \cdot \sum_\alpha \nabla \cdot \mathbf{\Pi}_\alpha^{NA} \right\rangle = \frac{1}{c} \sqrt{g} B^\vartheta \sum_\alpha e_\alpha \Gamma_\alpha^{NA} \equiv -T_\varphi^{NA}. \tag{2.78}$$

Here T_φ^{NA} denotes the toroidal torque density from non-axisymmetric (NA) external magnetic perturbations. Particle flux densities Γ_α^{NA} are approximated in this relation by the leading order in ρ_L through the solution of the linearized drift-kinetic equation obtained with the standard neoclassical ansatz. Thus, one neglects classical transport (since it is ambipolar it does not affect the radial current), polarization drift, and radial transport of momentum (being of higher order in ρ_L). Note that at this point it is assumed that the poloidal rotation is at its equilibrium value and, therefore, the non-ambipolar flux densities in (2.78) can be expressed through the thermodynamic forces and transport coefficients D_{ij}^{NA} using (2.24). (In case of fast rotations, the poloidal flow is compressible in contrast to subsonic flows discussed in Section 2.1.2, and the toroidal rotation shear should be included in the set of thermodynamic forces, see, e.g., Ref. [21].) The product $\sqrt{g} B^\vartheta = -\partial A_\varphi / \partial r = \partial \psi_{\mathrm{pol}} / \partial r$ does not depend on the particular choice of the straight field line coordinate system. Within the leading order in ε_M, it should be computed for unperturbed coordinates.

Subtracting Eq. (2.78) from what remains of Eq. (2.77) and retaining only the leading order terms in ε_M and ρ_L one obtains an equation for the axisymmetric radial current,

$$\begin{aligned} &\frac{1}{S} \frac{\partial}{\partial t} S \left\langle \frac{\partial \mathbf{r}}{\partial \varphi} \cdot \sum_\alpha m_\alpha n_\alpha \mathbf{V}_\alpha \right\rangle + \frac{1}{S} \frac{\partial}{\partial r} S \left\langle \Pi_\varphi^r \right\rangle_{AX} + \frac{1}{c} \frac{\mathrm{d} A_\varphi}{\mathrm{d} t} \langle \rho \rangle = \\ &= \frac{1}{c} \sqrt{g} B^\vartheta \left\langle j^r \right\rangle + T_\varphi^{NA} \equiv \frac{1}{c} \sqrt{g} B^\vartheta \left\langle j^r \right\rangle_{\mathrm{AX}}. \end{aligned} \tag{2.79}$$

Here, the right hand side corresponds to the axisymmetric radial current, $\langle j^r \rangle_{AX} = \langle j^r \rangle - \sum_\alpha e_\alpha \Gamma_\alpha^{NA}$, which is driven by the axisymmetric momentum transport and by the time derivative of the toroidal momentum (polarization current). All terms on the left hand side correspond to unperturbed flux coordinates and $\left\langle \Pi_\varphi^r \right\rangle_{AX}$ is the axisymmetric stress (excluding the scalar pressure) responsible for the radial momentum transport [22, 39], which appears in the next order over ρ_L (i.e., this transport is absent in standard neoclassical theory). An essential point in obtaining Eq. (2.79) is to ignore the contribution of the polarization drift to the non-axisymmetric part of the stress tensor. This contribution would appear in Eq. (2.79) because Eq. (2.78) does not include this drift and Eq. (2.77) does. It has been ignored because it is a next order correction in ε_M to the non-axisymmetric stress tensor (which is already small in the leading order over ε_M) because the polarization drift driven by non-axisymmetric stress is respectively small over ε_M too.

Note that so far the radial electric field and its time derivative are not determined by Eq. (2.79) rather they are external parameters, which determine the radial current. The closure of the problem is achieved by expressing the total radial current in (2.79) via the time derivative of the radial electric field with help of flux surface averaged contra-variant radial component of Ampere's law [40, 3, 41],

$$\langle j^r \rangle = -\frac{1}{4\pi} \left\langle \frac{\partial \mathbf{E}}{\partial t} \cdot \nabla r \right\rangle, \tag{2.80}$$

which leads to the momentum conservation equation in a usual form,

$$\frac{1}{S}\frac{\partial}{\partial t} S \langle P_\varphi \rangle + \frac{1}{S}\frac{\partial}{\partial r} S \left\langle \Pi_\varphi^r \right\rangle = T_\varphi^{NA}. \tag{2.81}$$

Here only the axisymmetric Pointing flux S_φ and the Maxwell stress tensor component σ_φ^r,

$$S_\varphi = \frac{c}{4\pi}\sqrt{g} E^r B^\vartheta, \qquad \sigma_\varphi^r = \frac{1}{4\pi} E^r E_\varphi, \tag{2.82}$$

appear in the total quantities P_φ and Π_φ^r, respectively. To complete the set,

the contributions from turbulent fluctuations are included a-posteriori, thus re-defining the total axisymmetric toroidal momentum and its radial flux density in Eq. (2.81) as

$$\begin{aligned} \langle P_\varphi \rangle &= \left\langle \frac{\partial \mathbf{r}}{\partial \varphi} \cdot \sum_\alpha m_\alpha n_\alpha \mathbf{V}_\alpha \right\rangle + \frac{1}{4\pi c} \sqrt{g} \langle g^{rr} \rangle E_r B^\vartheta + \left\langle \overline{\Delta P_\varphi} \right\rangle , \\ \left\langle \Pi^r_\varphi \right\rangle &= \left\langle \Pi^r_\varphi \right\rangle_{AX} - \frac{1}{4\pi} \langle g^{rr} \rangle E_r E_\varphi + \left\langle \overline{\Delta \Pi^r_\varphi} \right\rangle , \end{aligned} \tag{2.83}$$

where $g^{rr} = |\nabla r|^2$ is the contra-variant radial component of the metric tensor. For computing $\left\langle \overline{\Delta P_\varphi} \right\rangle$ and $\left\langle \overline{\Delta \Pi^r_\varphi} \right\rangle$ one should take their values from the Eq. (2.75) in presence of turbulent fluctuations but in absence of the external perturbation magnetic field, subtract their axisymmetric values given by the terms shown explicitly in (2.83) and ensemble average the result (compare to Refs. [42, 43, 35]). Another, rather demonstrative form of the conservation law for the canonical angular momentum of the plasma (see also Ref. [34]) is obtained expressing in $\langle P_\varphi \rangle$ the poloidal field as $\sqrt{g} B^\vartheta = -\partial A_\varphi / \partial r$ and using $\nabla \cdot \mathbf{E} = 4\pi\rho$ and Eq. (2.80),

$$\begin{aligned} \langle P_\varphi \rangle &= \sum_\alpha \left\langle n_\alpha \left(m_\alpha \mathbf{V}_\alpha \cdot \frac{\partial \mathbf{r}}{\partial \varphi} + \frac{e_\alpha}{c} A_\varphi \right) \right\rangle + \left\langle \overline{\Delta P_\varphi} \right\rangle , \\ \left\langle \Pi^r_\varphi \right\rangle &= \left\langle \Pi^r_\varphi \right\rangle_{AX} + \frac{1}{c} \langle j^r \rangle A_\varphi + \left\langle \overline{\Delta \Pi^r_\varphi} \right\rangle . \end{aligned} \tag{2.84}$$

It can be seen from (2.78) that non-ambipolar fluxes are driven not only by toroidal viscosity and the pressure gradients within the flux surface but also by inertia. This part of stress can be ignored for subsonic rotations where the role of inertia is negligible. Actually, this is the case in stellarators where the violation of axial symmetry is strong. This is not necessarily the case in tokamaks. The original flux-force relation [37] has been derived for general type devices ignoring the case of fast toroidal rotation, which is not important if the non-axisymmetric field is strong. The omission of the inertial term, obviously, has no consequences for the evaluation of the toroidal torque via non-ambipolar particle fluxes, if these fluxes are directly computed from the solution of linearized drift-kinetic equation [3, 4, 5] (the standard

way). Moreover, In Refs. [44, 12] the torque in the form of non-ambipolar fluxes is computed also for the resonant small-amplitude perturbations in the framework of quasilinear theory (evaluation of the fluxes in this case is performed then in unperturbed flux coordinates). Note that the various parts of the non-axisymmetric plasma stress tensor appearing in the flux-force relation do not enter the toroidal rotation equation (2.81). They have only been used for terming the phenomenon as "neoclassical toroidal viscosity".

The presence of the inertial term in the torque does not contradict the result of Ref. [38] where the guiding center expression for the non-ambipolar flux has been directly related to the pressure tensor. Partly the inertial term can be recovered there by setting the parallel guiding center velocity to $v_\parallel = V_\parallel + v'_\parallel$ where $V_\parallel$ is the (small) parallel flow velocity and $v'_\parallel$ is the relative velocity contributing to the pressure tensor. Contributions of the perpendicular flow velocity (essentially the $\mathbf{E} \times \mathbf{B}$ velocity because the gradient drift velocity is always negligible in the guiding center ordering) is recovered if instead of the guiding center velocity for the usual (weak) electric field ordering used in Ref. [38] one uses the expression for the strong electric field.

Note that equation (2.81) is almost the same as Eq. (6) of Ref. [40]. If one ignores the anomalous terms or moves them to the external non-axisymmetric torque and expresses their sum in the form of the "non-Coulombic friction force", and then represents the second term in the expression (2.83) for P_φ as $\mathbf{E} \cdot \nabla\psi \, (4\pi c)^{-1}$, the only difference would be the second term in the momentum flux density $\left\langle \Pi^r_\varphi \right\rangle$, which has been ignored in Ref. [40] by assuming strict plasma neutrality when computing radial fluxes driven by the inductive field. The axisymmetric electromagnetic momentum retained in Ref. [40] is usually ignored [3, 41] because it is small compared to the plasma momentum as $v_A^2 c^{-2} B_{\mathrm{pol}}^2 B^{-2}$ where v_A is the Alfven speed and B_{pol} is the poloidal magnetic field (this estimate follows immediately if one assumes the toroidal rotation (2.28) being purely due to the electric field). The axisymmetric electromagnetic momentum flux scales to the axisymmetric neoclassical momentum flux by the same parameter times $(m_e/m_i)^{1/2} \beta_i^{-1} B_{\mathrm{pol}}^2 B^{-2} A^{1/2}$, where β_i is the normalized pressure and A is aspect ratio. Therefore, it is also ignored.

Ignoring also the electromagnetic momentum of the turbulent fluctuations, the evolution of the toroidal velocity (essentially of the radial electric field) is described by a simplified toroidal rotation equation in symmetry flux variables [20] (compare to Ref. [41]) neglecting contributions from NBI and other external sources except for the non-resonant magnetic perturbations,

$$\frac{1}{S}\frac{\partial}{\partial t}S\sum_{\alpha} m_\alpha \left\langle g_{\varphi\varphi} n_\alpha V_\alpha^\varphi \right\rangle + \frac{1}{S}\frac{\partial}{\partial r}S\left\langle \Pi_\varphi^r \right\rangle = T_\varphi^{NA}, \tag{2.85}$$

where $g_{\varphi\varphi} = R^2$ is the co-variant toroidal component of the metric tensor. Rather demonstrative is the "generic" form of the torque density [41],

$$T_\varphi^{NA} = -\nu_\mathrm{t} m_i n_i \left\langle g_{\varphi\varphi}\left(V^\varphi - V_\mathrm{in}^\varphi\right)\right\rangle, \tag{2.86}$$

which is obtained expressing the non-ambipolar flux densities in (2.78) through the thermodynamic forces and the transport coefficients D_{ij}^{NA} using (2.24) and replacing in forces A_1 the radial electric field with the ion toroidal rotation velocity V^φ via (2.28). The rotation relaxation rate ν_t (toroidal viscosity frequency) and the "intrinsic" ("offset") rotation velocity V_in^φ take a particular simple form if the electron particle flux is negligible. Then they are fully determined by ion transport coefficients as follows,

$$\nu_\mathrm{t} = \frac{e_i^2 g \left(B^\vartheta\right)^2 D_{11}^{NA}}{c^2 m_i T_i \left\langle g_{\varphi\varphi}\right\rangle} = \frac{D_{11}^{NA}}{\rho_\vartheta^2}, \qquad V_\mathrm{in}^\varphi = \frac{c\, k_{NA}}{e_i\sqrt{g}B^\vartheta}\frac{\mathrm{d}T_i}{\mathrm{d}r}, \tag{2.87}$$

where

$$k_{NA} = \frac{D_{12}^{NA}}{D_{11}^{NA}} - \frac{5}{2} + \frac{B_\varphi^2\, k}{\left\langle B^2\right\rangle \left\langle g_{\varphi\varphi}\right\rangle}, \tag{2.88}$$

and ρ_ϑ is the poloidal ion gyroradius. The generic form of the torque, which is valid for the bounce averaged drift kinetic equation, has been indicated in Ref. [36].

It should be noted that the assumption of negligible electron transport is generally not valid [36, 45] and is made here to allow for a simple expression for the offset rotation velocity. It is needed below for an illustration of numerical results for single component transport coefficients. In a general

case, this offset velocity contains additional contributions proportional to the density gradient and electron temperature gradient.

2.3 Quasilinear approach for the evaluation of non-ambipolar particle fluxes

Due to violations of the axial symmetry in a tokamak, the linearized drift kinetic equation (2.54) becomes a four-dimensional integro-differential equation, which is a rather difficult task for a direct numerical evaluation. This problem is well-known in stellarator theory because the magnetic fields are there 3D by construction. Therefore, it seems to be natural to adapt methods developed for stellarators to tokamaks with small amplitude magnetic field perturbations. A possibility to reduce the problem dimension by one is to use a mono-energetic approach [6, 46], which provides a rather good approximation for transport coefficients in most transport regimes of importance. In the mono-energetic approach Eq. (2.54) is solved using a Lorentz collision model. Based on this mono-energetic result, a solution to the full kinetic equation can be approximated using a truncated momentum preserving collision operator [47]. The standard version of NEO-2 [1] solves Eq. (2.54) with the full linearized collision operator but only in regimes where the effect of the cross-field rotation frequency on the transport is negligible small. In case of sufficiently small magnetic perturbation field amplitudes this limitation can be removed using a quasilinear approach. Based on this quasilinear approach, a modified version of the code NEO-2 [2] has been developed for the treatment of quasilinear transport regimes where the effect of the perturbation field on the particle motion within flux surfaces is small. The perturbed distribution function is then linear in the perturbation field and, thus, the problem dimension can be reduced by one using a Fourier analysis with respect to the toroidal angle. The quasilinear approach requires small enough perturbation amplitudes ε_M (relative amplitude of the non-axisymmetric perturbation of the magnetic field module) such that, in particular, the effect of locally trapped (blocked by the perturbation field) particles can be ignored.

This can be done if at least one of the two conditions (see Eq. (41) of Ref. [2])

$$\varepsilon_M < \frac{\varepsilon_t}{\left(k_\parallel qR\right)^2} \sim \frac{\varepsilon_t}{q^2 n^2}, \qquad \varepsilon_M < \left(\frac{\nu}{k_\parallel v_T}\right)^{2/3} \sim \left(\frac{\nu R}{n v_T}\right)^{2/3} \tag{2.89}$$

is satisfied, i.e., blocked particles are either completely absent or rapidly detrapped by collisions. Here $\varepsilon_t = 1/A$ is the toroidicity parameter (inverse aspect ratio), ν is the collision (deflection) frequency, $v_T = \sqrt{2T_\alpha/m_\alpha}$ is the thermal velocity, $k_\parallel$ is a characteristic parallel wave number estimated for the toroidal field ripple as n/R where n is the toroidal harmonic index (number of ripples) and R is the major radius. The retrapping-detrapping and the superbanana regime, which are described by the bounce averaged drift kinetic equation, are not covered by the quasilinear approximation. These bounce averaged transport regimes can be ignored if (see Eq. (42) of Ref. [2])

$$\varepsilon_M < \left(\frac{\varepsilon_t \nu}{\omega_E}\right)^{1/2}, \qquad \varepsilon_M < \frac{\varepsilon_t}{(nq)^{1/6}} \left(\frac{\nu \varepsilon_t^2 R^2}{D_B}\right)^{2/3}, \tag{2.90}$$

where $\omega_E = n\Omega_{tE}$ is the electric drift frequency and D_B is the Bohm diffusion coefficient. The first condition in (2.90) means that the relative change of the trapping parameter by collisions during an electric drift period $\sim \omega_E^{-1}$ is larger than the perturbation field amplitude so that trapping of transient particles by the perturbations is impossible. The second condition means that the collisional decorrelation time of the resonance between electric and magnetic drifts is smaller than the period of the banana orbit oscillation within the superbanana. In case $n \sim q \sim 1$ these conditions are the same with the respective conditions of Ref. [3].

2.3.1 Neoclassical transport ansatz

The linearized drift kinetic equation, see Eq. (2.54), is given by

$$v_g^\vartheta \frac{\partial f_1}{\partial \vartheta} + v_g^\varphi \frac{\partial f_1}{\partial \varphi} - \hat{L}_{\mathrm{cL}} f_1 = -v_{gd}^r \frac{\partial f_M}{\partial r}. \tag{2.91}$$

The term with the parallel electric field responsible for the Ware pinch in (2.54) has been omitted here for simplicity. In typical experimental conditions, the Ware pinch has a small effect as compared to the gradient driven terms retained here. This term will be recovered in the final expressions without derivation since the account of this term is similar to the account of gradient drive. The derivative of a Maxwellian should be expressed through the thermodynamic forces (2.22),

$$\frac{\partial f_M}{\partial r} = \left(A_1 + \frac{mv^2}{2T} A_2 \right) f_M. \tag{2.92}$$

Although in the following a different set of variables will be used in the velocity space, expression (2.92) is assumed everywhere below for this derivative. The particle flux is determined then solely by the first order distribution function f_1,

$$\begin{aligned} \Gamma \;=\; & \left(\int_0^{2\pi} \mathrm{d}\vartheta \int_0^{2\pi} \mathrm{d}\varphi \sqrt{g} |\nabla r| \right)^{-1} 2\pi \sum_{\sigma=\pm 1} \int_0^{2\pi} \mathrm{d}\vartheta \int_0^{2\pi} \mathrm{d}\varphi \times \\ & \times \int_{e\Phi}^{\infty} \mathrm{d}w \int_0^{(w-e\Phi)/\omega_c} \mathrm{d}J_\perp \sqrt{g} J_{\mathrm{inv}} v^r_{gd} f_1, \end{aligned} \tag{2.93}$$

because the contribution of the Maxwellian is zero. It should be noted that polarization effects connected with the time derivative of the electrostatic potential have been ignored here setting Φ to be a constant of time. These effects are of higher order in Larmor radius and definitely should be ignored in the computation of f_1. In contrast to the drifts retained here, the contribution of polarization effects to the flux of the bulk Maxwellian particles is non-zero and of the same order as the non-ambipolar flux computed below. Polarization flux, however, is only weakly influenced by the small non-axisymmetric field which can therefore be ignored in computations of this flux.

For the subsequent computations flux coordinates are fixed to Boozer coordinates. In Boozer coordinates co-variant angular components of the

magnetic field are constant on the flux surface, $B_\vartheta = B_\vartheta(r)$, $B_\varphi = B_\varphi(r)$. Respectively, the dependence on angles of the contra-variant components is determined by the square of the magnetic field module, i.e. quantities $B^\vartheta B^{-2}$ and $B^\varphi B^{-2}$ are constant on a flux surface. This holds for any coordinate system with straight field lines where the following relations are valid,

$$B^\varphi = qB^\vartheta, \qquad B^\vartheta = \frac{B^2}{B_\vartheta + qB_\varphi}, \tag{2.94}$$

The dependence of the metric determinant on angles is also fully determined by the magnetic field module,

$$\sqrt{g} = \frac{C_g}{B^2} \tag{2.95}$$

where $C_g = C_g(r)$ is constant on a flux surface. In a more explicit form, components of the guiding center velocity in Boozer coordinates are given by

$$\begin{aligned}
v^r_{gd} &= \frac{v_\perp^2 + 2v_\parallel^2}{2\sqrt{g}B^*_\parallel\omega_c}\left(\frac{B_\vartheta}{B}\frac{\partial B}{\partial\varphi} - \frac{B_\varphi}{B}\frac{\partial B}{\partial\vartheta}\right), \\
v^\vartheta_{gd} &= \frac{v_\perp^2 + 2v_\parallel^2}{2\sqrt{g}B^*_\parallel\omega_c}\left(\frac{B_\varphi}{B}\frac{\partial B}{\partial r} - \frac{B_r}{B}\frac{\partial B}{\partial\varphi}\right) + \\
&\quad + \frac{v_\parallel^2}{\sqrt{g}B^*_\parallel\omega_c}\left(\frac{\partial B_r}{\partial\varphi} - \frac{\partial B_\varphi}{\partial r}\right) + \frac{cB_\varphi}{\sqrt{g}B^*_\parallel B}\frac{\partial\Phi}{\partial r}, \\
v^\varphi_{gd} &= \frac{v_\perp^2 + 2v_\parallel^2}{2\sqrt{g}B^*_\parallel\omega_c}\left(\frac{B_r}{B}\frac{\partial B}{\partial\vartheta} - \frac{B_\vartheta}{B}\frac{\partial B}{\partial r}\right) + \\
&\quad + \frac{v_\parallel^2}{\sqrt{g}B^*_\parallel\omega_c}\left(\frac{\partial B_\vartheta}{\partial r} - \frac{\partial B_r}{\partial\vartheta}\right) - \frac{cB_\vartheta}{\sqrt{g}B^*_\parallel B}\frac{\partial\Phi}{\partial r},
\end{aligned} \tag{2.96}$$

where the perpendicular and parallel velocity components have been introduced according to

$$v_\perp = \sqrt{\frac{2J_\perp\omega_c}{m}}, \qquad v_\parallel = \sigma\sqrt{\frac{2}{m}(\omega - e\Phi - J_\perp\omega_c)}. \tag{2.97}$$

Equation (2.91) still contains Larmor radius corrections which can be

ignored for simplicity. In order to do this one can switch from coordinates θ, φ on the flux surface to coordinates θ, φ_0 where

$$\varphi_0 = \varphi - q\vartheta \tag{2.98}$$

labels the field lines. Due to $B^\varphi = qB^\vartheta$, this variable is not changed by parallel motion,

$$v_g^{\varphi_0} = v_g^\vartheta \frac{\partial \varphi_0}{\partial \vartheta} + v_g^\varphi \frac{\partial \varphi_0}{\partial \varphi} = v_{gd}^\varphi - q v_{gd}^\vartheta. \tag{2.99}$$

Parallel motion is contained solely in ϑ variable. Since this is the leading order term one can ignore the cross field drift over ϑ. In addition the Larmor radius correction in guiding center velocity (2.35) and (2.96) and in the Jacobian of the guiding center variables (2.40) are ignored by replacing $B_\parallel^*$ with B. If this is done simultaneously, the property that a Maxwellian gives zero flux is retained. Thus, equation (2.91) takes the form

$$v_\parallel \frac{B^\vartheta}{B} \frac{\partial f_1}{\partial \vartheta} + v_g^{\varphi_0} \frac{\partial f_1}{\partial \varphi_0} - \hat{L}_{cL} f_1 = -v_{gd}^r \frac{\partial f_M}{\partial r}. \tag{2.100}$$

In the following it is convenient to change velocity space variables from invariants of motion w and $J_\perp$ to perpendicular and parallel velocities defined by (2.97). Equations of motion for these quantities are obtained by differentiating them along the zero order orbits with constant w and $J_\perp$,

$$\begin{aligned} \dot{v}_\perp &= v_\parallel \frac{B^\vartheta}{B} \frac{\partial v_\perp}{\partial \vartheta} + v_g^{\varphi_0} \frac{\partial v_\perp}{\partial \varphi_0} = \frac{v_\perp v_\parallel}{2B} \left(\frac{B^\vartheta}{B} \frac{\partial B}{\partial \vartheta} + \frac{v_g^{\varphi_0}}{v_\parallel} \frac{\partial B}{\partial \varphi_0} \right), \\ \dot{v}_\parallel &= v_\parallel \frac{B^\vartheta}{B} \frac{\partial v_\parallel}{\partial \vartheta} + v_g^{\varphi_0} \frac{\partial v_\parallel}{\partial \varphi_0} = -\frac{v_\perp^2}{2B} \left(\frac{B^\vartheta}{B} \frac{\partial B}{\partial \vartheta} + \frac{v_g^{\varphi_0}}{v_\parallel} \frac{\partial B}{\partial \varphi_0} \right). \end{aligned} \tag{2.101}$$

Actually these equations of motion are correct only up to the leading order because second order terms (linear corrections over the Larmor radius) do not include radial drift. These correction terms, which additionally are singular due to such a truncation, are kept here only for estimates. Below it will be shown that they provide a next order correction which is of the same order

as the term $v_{gd}^r \partial f_1/\partial r$ ignored during the linearization. Thus, the linearized kinetic equation (2.100) is transformed to

$$-v_{gd}^r \frac{\partial f_M}{\partial r} = v_\parallel \frac{B^\vartheta}{B}\frac{\partial f_1}{\partial \vartheta} + v_g^{\varphi_0}\frac{\partial f_1}{\partial \varphi_0} + \frac{v_\perp}{2B}\left(\frac{B^\vartheta}{B}\frac{\partial B}{\partial \vartheta} + \frac{v_g^{\varphi_0}}{v_\parallel}\frac{\partial B}{\partial \varphi_0}\right) \times \\ \times \left(v_\parallel \frac{\partial f_1}{\partial v_\perp} - v_\perp \frac{\partial f_1}{\partial v_\parallel}\right) - \hat{L}_{cL} f_1, \tag{2.102}$$

and the particle flux (2.93) is transformed to

$$\Gamma = \left(\int_0^{2\pi} \mathrm{d}\vartheta \int_0^{2\pi} \mathrm{d}\varphi_0 \frac{|\nabla r|}{B^2}\right)^{-1} 2\pi \int_0^{2\pi} \mathrm{d}\vartheta \int_0^{2\pi} \mathrm{d}\varphi_0 \int_0^{\infty} \mathrm{d}v_\perp \int_{-\infty}^{\infty} \mathrm{d}v_\parallel \frac{v_\perp}{B^2} v_{gd}^r f_1. \tag{2.103}$$

2.3.2 Perturbation theory

In the following a slightly perturbed axisymmetric magnetic field is considered. In Boozer coordinates the only quantities which contain an angular dependence are the magnetic field module B and the co-variant radial component of the magnetic field B_r. Thus, only these quantities contain the non-axisymmetric magnetic perturbation. At first it is checked that the transport for the axisymmetric field is ambipolar. In this case nothing depends on φ_0 and equation (2.102) is of the form

$$v_\parallel \frac{B^\vartheta}{B}\frac{\partial f_1}{\partial \vartheta} + \frac{v_\perp B^\vartheta}{2B^2}\frac{\partial B}{\partial \vartheta}\left(v_\parallel \frac{\partial f_1}{\partial v_\perp} - v_\perp \frac{\partial f_1}{\partial v_\parallel}\right) - \hat{L}_{cL} f_1 = \frac{v_\perp^2 + 2v_\parallel^2}{2C_g \omega_c} B_\varphi \frac{\partial B}{\partial \vartheta}\frac{\partial f_M}{\partial r}, \tag{2.104}$$

while (2.103) takes the form

$$\Gamma = \left(\int_0^{2\pi} \mathrm{d}\vartheta \frac{|\nabla r|}{B^2}\right)^{-1} \frac{\pi B B_\varphi}{2C_g \omega_c} \int_0^{2\pi} \mathrm{d}\vartheta \int_0^{\infty} \mathrm{d}v_\perp \int_{-\infty}^{\infty} \mathrm{d}v_\parallel v_\perp \left(v_\perp^2 + 2v_\parallel^2\right) f_1 \frac{\partial}{\partial \vartheta}\frac{1}{B^2}. \tag{2.105}$$

One can multiply now (2.104) with $v_\perp v_\parallel B^{-3}$ and integrate it over velocity space components and poloidal angle. The right hand side gives zero for two reasons: firstly because it is symmetric over $v_\parallel$ and, secondly, because it is a

full derivative over ϑ. From the left hand side one gets

$$0 = \frac{B^\vartheta}{4B^2}\int_0^{2\pi}\mathrm{d}\vartheta\int_0^\infty \mathrm{d}v_\perp \int_{-\infty}^{\infty}\mathrm{d}v_\parallel v_\perp\left(v_\perp^2+2v_\parallel^2\right) f_1\frac{\partial}{\partial\vartheta}\frac{1}{B^2} + \\ + \int_0^{2\pi}\mathrm{d}\vartheta\int_0^\infty \mathrm{d}v_\perp \int_{-\infty}^{\infty}\mathrm{d}v_\parallel \frac{v_\perp v_\parallel}{B^3}\hat{L}_{cL}f_1, \tag{2.106}$$

where derivatives of the distribution function have been removed using integration by parts. Substituting (2.105) in the first term of Eq. (2.106) yields a force-flux relation for the axisymmetric tokamak,

$$\frac{e}{c}\Gamma B^\vartheta\sqrt{g} + \frac{1}{\langle|\nabla r|\rangle}\left\langle\frac{B_\varphi}{B}\int \mathrm{d}^3v m v_\parallel \hat{L}_{cL}f_1\right\rangle = 0. \tag{2.107}$$

Namely, particle flux is produced by the flux surface averaged toroidal moment of the parallel friction force between ions and electrons. Due to third Newton's law fluxes of electrons and ions are ambipolar, $e_i\Gamma_i + e_e\Gamma_e = 0$.

For the perturbed system the solution is looked in the form of a series expansion over the perturbation amplitude,

$$f_1 = f_{10} + f_{11} + f_{12} + O(\delta B^3). \tag{2.108}$$

Coefficients of the kinetic equation (2.102) are split into a (quasi-) axisymmetric part and a non-axisymmetric perturbation by multiplying it with B^{-3} and separating the averages of the coefficients over the toroidal angle φ_0,

$$\overline{\hat{L}}f_1 + \delta\hat{L}f_1 = -\left(\overline{\left(\frac{v_{gd}^r}{B^3}\right)} + \delta\left(\frac{v_{gd}^r}{B^3}\right)\right)\frac{\partial f_M}{\partial r}, \tag{2.109}$$

whereby it is convenient to split the averaged operator into two parts as follows,

$$\overline{\hat{L}} = \overline{\hat{L}}_{QA} + \overline{\hat{L}}_{NQ}, \tag{2.110}$$

with

$$\overline{\hat{L}}_{QA} = \frac{B^\vartheta}{B^2}\left[v_\parallel \overline{\left(\frac{1}{B^2}\right)}\frac{\partial}{\partial\vartheta} + \frac{v_\perp}{4}\overline{\left(\frac{\partial}{\partial\vartheta}\frac{1}{B^2}\right)}\left(v_\perp\frac{\partial}{\partial v_\parallel} - v_\parallel\frac{\partial}{\partial v_\perp}\right)\right] - - \overline{\left(\frac{1}{B^3}\right)}\hat{L}_{cL} + \overline{\left(\frac{v_g^{\varphi_0}}{B^3}\right)}\frac{\partial}{\partial\varphi_0}, \quad (2.111)$$

$$\overline{\hat{L}}_{NQ} = \frac{v_\perp}{2v_\parallel}\overline{\left(\frac{v_g^{\varphi_0}}{B^4}\frac{\partial B}{\partial\varphi_0}\right)}\left(v_\parallel\frac{\partial}{\partial v_\perp} - v_\perp\frac{\partial}{\partial v_\parallel}\right). \quad (2.112)$$

Similarly one can split the perturbation operator,

$$\delta\hat{L} = \delta\hat{L}_\parallel + \delta\hat{L}_\perp, \quad (2.113)$$

where

$$\delta\hat{L}_\parallel = \frac{B^\vartheta}{B^2}\left[v_\parallel\delta\left(\frac{1}{B^2}\right)\frac{\partial}{\partial\vartheta} + \frac{v_\perp}{4}\delta\left(\frac{\partial}{\partial\vartheta}\frac{1}{B^2}\right)\times \times\left(v_\perp\frac{\partial}{\partial v_\parallel} - v_\parallel\frac{\partial}{\partial v_\perp}\right)\right] - \delta\left(\frac{1}{B^3}\right)\hat{L}_{cL}, \quad (2.114)$$

$$\delta\hat{L}_\perp = \delta\left(\frac{v_g^{\varphi_0}}{B^3}\right)\frac{\partial}{\partial\varphi_0} + \frac{v_\perp}{2v_\parallel}\delta\left(\frac{v_g^{\varphi_0}}{B^4}\frac{\partial B}{\partial\varphi_0}\right)\left(v_\parallel\frac{\partial}{\partial v_\perp} - v_\perp\frac{\partial}{\partial v_\parallel}\right). \quad (2.115)$$

Here the notation is as follows,

$$\overline{(a)} = \frac{1}{2\pi}\int_0^{2\pi} \mathrm{d}\varphi_0\, a, \qquad \delta(a) = a - \overline{(a)}. \quad (2.116)$$

The operators are splitted in order to estimate the roles of principal, first parts and correction, second parts which are assumed to be negligible small. In the fluxes terms up to the second order in perturbation amplitude and in Larmor radius are retained. All δ-quantities are at least of the first order in perturbation amplitude and can also contain second or higher order terms. Using the smallness of the $\delta\hat{L}$ operator and substituting f_1 in the series

form (2.108) into (2.109) a chain of equations is obtained,

$$\overline{\hat{L}} f_{10} = -\overline{\left(\frac{v_{gd}^r}{B^3}\right)} \frac{\partial f_M}{\partial r}, \tag{2.117}$$

$$\overline{\hat{L}} f_{11} = -\delta \left(\frac{v_{gd}^r}{B^3}\right) \frac{\partial f_M}{\partial r} - \delta \hat{L} f_{10}, \tag{2.118}$$

$$\overline{\hat{L}} f_{12} = -\delta \hat{L} f_{11}. \tag{2.119}$$

Firstly the role of the operator $\overline{\hat{L}}_{NQ}$ is estimated. This operator is of second order in perturbation amplitude. Therefore it can be immediately ignored in (2.118) and (2.119) because it provides there corrections of third and fourth order to f_{11} and f_{12}, respectively. This operator is also of first order in Larmor radius. Therefore it provides a second order in Larmor radius correction to f_{10} which respectively corrects the particle flux by a term of third order in Larmor radius. Thus, the operator $\overline{\hat{L}}_{NQ}$ can be completely ignored everywhere.

It should be noted that the operator $\delta L_\perp$ is of first order in Larmor radius. Since f_{10} is of first order in Larmor radius too, this operator gives a quadratic in Larmor radius contribution in the right hand side of (2.118). This contribution is one order higher than the linear order term with the Maxwellian. Similarly, it provides a quadratic correction in Larmor radius to the right hand side of (2.119) which would result in a negligible, third order correction to the flux. Thus, the operator $\delta L_\perp$ can be ignored everywhere too.

Moreover, one can see that f_{12} is of second order in perturbation amplitude. The non-axisymmetric part of this function gives a third order in perturbation amplitude correction to the flux because the zero order term in the product of radial drift velocity and metric determinant (factor $1/B^2$) in (2.103) is axisymmetric. With these approximations, the chain of equa-

tions takes the final form

$$\overline{\hat{L}}_{QA} f_{10} = -\overline{\left(\frac{v_{gd}^r}{B^3}\right)} \frac{\partial f_M}{\partial r}, \tag{2.120}$$

$$\overline{\hat{L}}_{QA} f_{11} = -\delta \left(\frac{v_{gd}^r}{B^3}\right) \frac{\partial f_M}{\partial r} - \delta \hat{L}_{\parallel} f_{10}, \tag{2.121}$$

$$\overline{\hat{L}}_{QA} f_{12} = -\overline{\delta \hat{L}_{\parallel} f_{11}}. \tag{2.122}$$

In fact, one can notice that the non-axisymmetric part of the covariant radial component of the magnetic field, B_r, is not needed in this approach because B_r enters only the toroidal rotation velocity $v_g^{\varphi_0}$ which is evaluated in the lowest (zero) order over the perturbation amplitude.

It should be mentioned that the operator $\overline{\hat{L}}_{QA}$, which is termed below quasi-axisymmetric operator, has a property similar to the kinetic operator in a real axisymmetric magnetic field. Namely, the particle flux (2.103) computed for the quasi-axisymmetric distribution function f_{10} given by (2.120) is ambipolar. This can be seen if one multiplies (2.120) with $v_{\parallel}$ and integrates it over velocity space and poloidal angle. However, it is more useful to compute the flux driven by the axisymmetric function f_{12}. Substituting this function in (2.103) one obtains

$$\begin{aligned}
\Gamma_{12} &= \frac{4\pi^2}{\int_0^{2\pi} \mathrm{d}\vartheta \int_0^{2\pi} \mathrm{d}\varphi_0 \frac{|\nabla r|}{B^2}} \int_0^{2\pi} \mathrm{d}\vartheta \int_0^{\infty} \mathrm{d}v_{\perp} \int_{-\infty}^{\infty} \mathrm{d}v_{\parallel} v_{\perp} f_{12} \overline{\left(\frac{v_{gd}^r}{B^2}\right)} \\
&= \left(\int_0^{2\pi} \mathrm{d}\vartheta \int_0^{2\pi} \mathrm{d}\varphi_0 \frac{|\nabla r|}{B^2}\right)^{-1} \frac{\pi^2 mcB_{\varphi}}{eC_g} \int_0^{2\pi} \mathrm{d}\vartheta \int_0^{\infty} \mathrm{d}v_{\perp} \int_{-\infty}^{\infty} \mathrm{d}v_{\parallel} \times \\
&\quad \times v_{\perp} \left(v_{\perp}^2 + 2v_{\parallel}^2\right) f_{12} \frac{\partial}{\partial \vartheta} \overline{\left(\frac{1}{B^2}\right)},
\end{aligned} \tag{2.123}$$

where following expression has been used

$$\begin{aligned}\overline{\left(\frac{v_{gd}^r}{B^2}\right)} &= \overline{\frac{v_\perp^2+2v_\parallel^2}{2C_gB^2\omega_c}\left(\left(B_\vartheta+qB_\varphi\right)\frac{\partial B}{\partial\varphi_0}-B_\varphi\frac{\partial B}{\partial\vartheta}\right)}\\ &= \frac{mcB_\varphi}{4eC_g}\left(v_\perp^2+2v_\parallel^2\right)\frac{\partial}{\partial\vartheta}\overline{\left(\frac{1}{B^2}\right)}. \end{aligned} \tag{2.124}$$

In a further step equation (2.122) is multiplied with $v_\perp v_\parallel$ and integrated over velocity components and over the poloidal angle,

$$\begin{aligned} 0 &= \int_0^{2\pi}\mathrm{d}\vartheta\int_0^\infty\mathrm{d}v_\perp\int_{-\infty}^\infty\mathrm{d}v_\parallel v_\perp v_\parallel\left(\overline{\hat{L}}_{QA}f_{12}+\overline{\delta\hat{L}_\parallel f_{11}}\right)\\ &= -\frac{B^\vartheta}{4B^2}\int_0^{2\pi}\mathrm{d}\vartheta\int_0^\infty\mathrm{d}v_\perp\int_{-\infty}^\infty\mathrm{d}v_\parallel\overline{\left(\frac{\partial}{\partial\vartheta}\frac{1}{B^2}\right)}v_\perp\left(v_\perp^2+2v_\parallel^2\right)f_{12}-\\ &- \int_0^{2\pi}\mathrm{d}\vartheta\overline{\left(\frac{1}{B^3}\right)}\int_0^\infty\mathrm{d}v_\perp\int_{-\infty}^\infty\mathrm{d}v_\parallel v_\perp v_\parallel\hat{L}_{cL}f_{12}+\int_0^{2\pi}\mathrm{d}\vartheta\int_0^\infty\mathrm{d}v_\perp\int_{-\infty}^\infty\mathrm{d}v_\parallel v_\perp v_\parallel\overline{\delta\hat{L}_\parallel f_{11}}. \end{aligned} \tag{2.125}$$

As for the axisymmetric case, the flux driven by f_{12} is obtained by comparing (2.125) to (2.123)

$$\begin{aligned}\Gamma_{12} = &-\frac{c}{e\sqrt{g}B^\vartheta}\frac{1}{\langle|\nabla r|\rangle}\left\langle\frac{B_\varphi}{B}\int\mathrm{d}^3v m v_\parallel\hat{L}_{cL}f_{12}\right\rangle+\\ &+\frac{mcB_\varphi}{e\sqrt{g}B^\vartheta}\frac{1}{\langle|\nabla r|\rangle}\left\langle B^2\int\mathrm{d}^3v v_\parallel\delta\hat{L}_\parallel f_{11}\right\rangle. \end{aligned} \tag{2.126}$$

It is very easy now to evaluate flux from f_{10}

$$\Gamma_{10} = -\frac{c}{e\sqrt{g}B^\vartheta}\frac{1}{\langle|\nabla r|\rangle}\left\langle\frac{B_\varphi}{B}\int\mathrm{d}^3v m v_\parallel\hat{L}_{cL}f_{10}\right\rangle, \tag{2.127}$$

where the source term does not contribute because it is symmetric over $v_\parallel$. One can see that this flux is completely ambipolar. The first term in (2.126) is also of no interest here because it is ambipolar too. Substituting now

into the second term the explicit form of the operator $\delta\hat{L}_{\parallel}$, Eq. (2.114), and removing the derivatives with help of integration by parts one gets

$$\Gamma_{12} = -\left(\left\langle \frac{B_\varphi}{B}\int \mathrm{d}^3v m v_\parallel \hat{L}_{cL} f_{12} + B_\varphi B^2 \delta\left(\frac{1}{B^3}\right)\int \mathrm{d}^3v m v_\parallel \hat{L}_{cL} f_{11}\right\rangle + \right.$$
$$\left. + \frac{m}{4}\left\langle B_\varphi B^\vartheta \delta\left(\frac{\partial}{\partial\vartheta}\frac{1}{B^2}\right)\int \mathrm{d}^3v \left(v_\perp^2 + 2v_\parallel^2\right) f_{11}\right\rangle\right)\frac{c}{e\sqrt{g}B^\vartheta}\frac{1}{\langle|\nabla r|\rangle}. \tag{2.128}$$

There appears an additional ambipolar term in (2.128) whereas the non-ambipolar contribution is described by the last term. Thus, the non-ambipolar flux is a sum of the last term in (2.128) and of the contribution from f_{11} which is evaluated by substituting this function into the expression for the particle flux (2.103),

$$\begin{aligned}
\Gamma_{11} &= \frac{1}{\langle|\nabla r|\rangle}\left\langle \int \mathrm{d}^3v v_{gd}^r f_{11}\right\rangle \\
&= \frac{mc}{2e\sqrt{g}B^\vartheta}\frac{1}{\langle|\nabla r|\rangle}\left\langle \frac{B^\vartheta}{B^3}\left(\left(B_\vartheta + qB_\varphi\right)\frac{\partial B}{\partial\varphi_0} - B_\varphi\frac{\partial B}{\partial\vartheta}\right)\int \mathrm{d}^3v \left(v_\perp^2 + 2v_\parallel^2\right) f_{11}\right\rangle \\
&= \frac{mc}{2e\sqrt{g}B^\vartheta}\frac{1}{\langle|\nabla r|\rangle}\left\langle \left(\frac{1}{B}\frac{\partial B}{\partial\varphi_0} - \frac{B^\vartheta B_\varphi}{B^3}\frac{\partial B}{\partial\vartheta}\right)\int \mathrm{d}^3v \left(v_\perp^2 + 2v_\parallel^2\right) f_{11}\right\rangle \\
&= \frac{mc}{4e\sqrt{g}B^\vartheta}\frac{1}{\langle|\nabla r|\rangle}\left\langle B^2\int \mathrm{d}^3v \left(v_\perp^2 + 2v_\parallel^2\right) f_{11}\left(\frac{B^\vartheta B_\varphi}{B^2}\frac{\partial}{\partial\vartheta}\frac{1}{B^2} - \frac{\partial}{\partial\varphi_0}\frac{1}{B^2}\right)\right\rangle.
\end{aligned} \tag{2.129}$$

The sum of both fluxes gives

$$\Gamma_{11} + \Gamma_{12}^{NA} = \frac{mc}{4e\sqrt{g}B^\vartheta}\frac{1}{\langle|\nabla r|\rangle}\left\langle B^2\int \mathrm{d}^3v \left(v_\perp^2 + 2v_\parallel^2\right) f_{11} \times \right.$$
$$\left. \times \left(\frac{B^\vartheta B_\varphi}{B^2}\overline{\left(\frac{\partial}{\partial\vartheta}\frac{1}{B^2}\right)} - \frac{\partial}{\partial\varphi_0}\frac{1}{B^2}\right)\right\rangle. \tag{2.130}$$

Next the contribution of the first term within the round brackets to the the total non-ambipolar particle flux is checked. Multiplication of Eq. (2.121) with $v_\parallel$ and subsequent integration over velocity space and over both angles

yields

$$\frac{1}{4}\left\langle B^{\vartheta}\overline{\left(\frac{\partial}{\partial\vartheta}\frac{1}{B^2}\right)}\int \mathrm{d}^3v\left(v_\perp^2+2v_\parallel^2\right)f_{11}\right\rangle = \\ =\left\langle B^2\int \mathrm{d}^3vv_\parallel\frac{\partial f_M}{\partial r}\delta\left(\frac{v_{gd}^r}{B^3}\right)\right\rangle+\left\langle B^2\int \mathrm{d}^3vv_\parallel\delta\hat{L}_\parallel f_{10}\right\rangle- \\ -\left\langle B^2\overline{\left(\frac{1}{B^3}\right)}\int \mathrm{d}^3vv_\parallel\hat{L}_{cL}f_{11}\right\rangle+\left\langle B^2\int \mathrm{d}^3vv_\parallel\overline{\left(\frac{v_{gd}^{\varphi_0}}{B^3}\right)}\frac{\partial f_{11}}{\partial\varphi_0}\right\rangle. \quad (2.131)$$

The first term on the right hand side of (2.131) is zero because the integrand is an odd function of $v_\parallel$. The second term gives only an ambipolar contribution to the particle flux. Third and fourth terms are zero because of averaging over the toroidal angle φ_0. Thus, the first term in the parentheses in (2.130) provides no contribution to the non-ambipolar flux which is obtained as follows

$$\Gamma^{NA}=-\frac{mc}{4e\sqrt{g}B^{\vartheta}}\frac{1}{\langle|\nabla r|\rangle}\left\langle B^2\int \mathrm{d}^3v\left(v_\perp^2+2v_\parallel^2\right)f_{11}\frac{\partial}{\partial\varphi_0}\frac{1}{B^2}\right\rangle. \quad (2.132)$$

The expression for the non-ambipolar particle flux can be further simplified because it contains not only leading order terms but also terms of higher order which should be ignored. It should be noted that f_{11} and the derivative over φ_0 are of first order in perturbation amplitude. Therefore, it makes no sense to take into account the non-axisymmetric magnetic field elsewhere. Splitting the magnetic field module into an unperturbed, axisymmetric part and a non-axisymmetric perturbation,

$$B=B_0+\delta B, \quad (2.133)$$

the expression for the flux (2.132) simplifies to

$$\Gamma^{NA}=\frac{mc}{2e\sqrt{g_0}B_0^{\vartheta}}\left(\int_0^{2\pi}\mathrm{d}\vartheta\frac{|\nabla r_0|}{B_0^2}\right)^{-1}\int_0^{2\pi}\frac{\mathrm{d}\vartheta}{B_0^3}\int \mathrm{d}^3v\left(v_\perp^2+2v_\parallel^2\right)\overline{f_{11}\frac{\partial\delta B}{\partial\varphi_0}}, \quad (2.134)$$

where r_0, g_0 and B_0^{ϑ} are the respective axisymmetric quantities. For the same

reason the operators $\overline{\hat{L}}_{QA}$, Eq. (2.111), and $\delta\hat{L}_{\parallel}$, Eq. (2.114), are replaced with

$$\hat{L}_{AX} \approx B_0^3 \overline{\hat{L}}_{QA}, \qquad \delta\hat{L}_A \approx B_0^3 \delta\hat{L}_{\parallel}, \tag{2.135}$$

so that

$$\begin{aligned}\hat{L}_{AX} = &\frac{B_0^\vartheta}{B_0}\left[v_\parallel \frac{\partial}{\partial\vartheta} + \frac{v_\perp}{2B_0}\frac{\partial B_0}{\partial\vartheta}\left(v_\parallel\frac{\partial}{\partial v_\perp} - v_\perp\frac{\partial}{\partial v_\parallel}\right)\right] - \\ &- \hat{L}_{cL} + v_{g0}^{\varphi_0}\frac{\partial}{\partial\varphi_0},\end{aligned} \tag{2.136}$$

$$\begin{aligned}\delta\hat{L}_A = &\frac{B_0^\vartheta}{B_0}\left[-2v_\parallel\frac{\delta B}{B_0}\frac{\partial}{\partial\vartheta} + \frac{v_\perp}{2B_0}\left(\frac{\partial\delta B}{\partial\vartheta} - \frac{3\delta B}{B_0}\frac{\partial B_0}{\partial\vartheta}\right)\times\right. \\ &\left.\times\left(v_\parallel\frac{\partial}{\partial v_\perp} - v_\perp\frac{\partial}{\partial v_\parallel}\right)\right] + \frac{3\delta B}{B_0}\hat{L}_{cL}.\end{aligned} \tag{2.137}$$

Then the simplified equation (2.120) takes a more explicit form,

$$\hat{L}_{AX} f_{10} = \frac{mcB_\varphi}{2e\sqrt{g_0}B_0^3}\left(v_\perp^2 + 2v_\parallel^2\right)\frac{\partial B_0}{\partial\vartheta}\frac{\partial f_M}{\partial r}. \tag{2.138}$$

Respectively, Eq. (2.121) becomes

$$\begin{aligned}\hat{L}_{AX} f_{11} = &\frac{mcB_\varphi}{2e\sqrt{g_0}B_0^3}\left(v_\perp^2 + 2v_\parallel^2\right)\left(\frac{\partial\delta B}{\partial\vartheta} - \frac{B_0^2}{B_0^\vartheta B_\varphi}\frac{\partial\delta B}{\partial\varphi_0} - \right. \\ &\left. - \frac{4\delta B}{B_0}\frac{\partial B_0}{\partial\vartheta}\right)\frac{\partial f_M}{\partial r} - \delta\hat{L}_A f_{10}.\end{aligned} \tag{2.139}$$

The operator (2.137) appearing in the last term on the right hand side of Eq. (2.139) leads to a derivative of f_{10} over ϑ, which can be eliminated with help of (2.136) and (2.138),

$$\begin{aligned}\delta\hat{L}_A f_{10} = &-\frac{mcB_\varphi}{2e\sqrt{g_0}B_0^3}\left(v_\perp^2 + 2v_\parallel^2\right)\frac{2\delta B}{B_0}\frac{\partial B_0}{\partial\vartheta}\frac{\partial f_M}{\partial r} - \frac{v_\perp B_0^\vartheta}{2B_0^2}\times \\ &\times\left(\frac{\delta B}{B_0}\frac{\partial B_0}{\partial\vartheta} - \frac{\partial\delta B}{\partial\vartheta}\right)\left(v_\parallel\frac{\partial f_{10}}{\partial v_\perp} - v_\perp\frac{\partial f_{10}}{\partial v_\parallel}\right) + \frac{\delta B}{B_0}\hat{L}_{cL} f_{10}.\end{aligned} \tag{2.140}$$

Substituting (2.140) into equation (2.139) yields

$$\hat{L}_{AX} f_{11} = \frac{mcB_\varphi}{2e\sqrt{g_0}B_0^3}\left(v_\perp^2 + 2v_\parallel^2\right)\left(\frac{\partial \delta B}{\partial \vartheta} - \frac{B_0^2}{B_0^\vartheta B_\varphi}\frac{\partial \delta B}{\partial \varphi_0} - \frac{2\delta B}{B_0}\frac{\partial B_0}{\partial \vartheta}\right)\frac{\partial f_M}{\partial r} + \\ + \frac{v_\perp B_0^\vartheta}{2B_0^2}\left(\frac{\delta B}{B_0}\frac{\partial B_0}{\partial \vartheta} - \frac{\partial \delta B}{\partial \vartheta}\right)\left(v_\parallel \frac{\partial f_{10}}{\partial v_\perp} - v_\perp \frac{\partial f_{10}}{\partial v_\parallel}\right) - \frac{\delta B}{B_0}\hat{L}_{cL} f_{10}. \tag{2.141}$$

Thus, the computation of non-axisymmetric particle fluxes is reduced to the solution of two problems: an axisymmetric and a non-axisymmetric problem described by Eq. (2.138) and Eq. (2.141), respectively. It is possible and desirable to transform the obtained expressions back to invariants of motion but now of the unperturbed motion. Since the potential is constant on a flux surface it is convenient to use the velocity module v as one such invariant (instead of the total energy (2.31)) and the normalized perpendicular invariant

$$\eta = \frac{v_\perp^2 B_{\mathrm{ref}}}{v^2 B_0}, \tag{2.142}$$

where B_{ref} is some reference magnetic field value. For the moment B_{ref} is set to 1 and the actual value is restored in the numerical section. As a result of this change of variables, the mirroring term disappears in (2.136) which is then of the form

$$\hat{L}_{AX} = v_\parallel \frac{B_0^\vartheta}{B_0}\frac{\partial}{\partial \vartheta} - \hat{L}_{cL} + v_{g0}^{\varphi_0}\frac{\partial}{\partial \varphi_0}. \tag{2.143}$$

The equation for the non-axisymmetric perturbation (2.141) changes to

$$\begin{aligned} \hat{L}_{AX} f_{11} &= \frac{mcB_\varphi v^2\left(2 - \eta B_0\right)}{2e\sqrt{g_0}B_0^3}\left(\frac{\partial \delta B}{\partial \vartheta} - \frac{B_0^2}{B_0^\vartheta B_\varphi}\frac{\partial \delta B}{\partial \varphi_0} - \frac{2\delta B}{B_0}\frac{\partial B_0}{\partial \vartheta}\right)\frac{\partial f_M}{\partial r} \\ &+ v_\parallel \frac{B_0^\vartheta}{B_0^2}\left(\frac{\delta B}{B_0}\frac{\partial B_0}{\partial \vartheta} - \frac{\partial \delta B}{\partial \vartheta}\right)\eta\frac{\partial f_{10}}{\partial \eta} - \frac{\delta B}{B_0}\hat{L}_{cL} f_{10}. \end{aligned} \tag{2.144}$$

Note that in both equations the parallel velocity is given by

$$v_\parallel = \sigma v\sqrt{1 - \eta B_0}. \tag{2.145}$$

It is convenient to split the toroidal rotation velocity appearing in (2.143)

into an electric and a magnetic rotation velocity,

$$v_{g0}^{\varphi_0} = \Omega_{tE} + \Omega_{tB}, \tag{2.146}$$

which are obtained by substituting (2.96) into (2.99)

$$\Omega_{tE} = -\frac{c}{\sqrt{g_0}B_0^{\vartheta}}\frac{\partial\Phi}{\partial r}, \tag{2.147}$$

$$\begin{aligned}\Omega_{tB} &= \frac{v_\perp^2 + 2v_\parallel^2}{2\sqrt{g_0}B_0\omega_{c0}}\left(\frac{B_r}{B_0}\frac{\partial B_0}{\partial\vartheta} - \frac{B_0}{B_0^{\vartheta}}\frac{\partial B_0}{\partial r}\right) + \frac{v_\parallel^2}{\sqrt{g_0}B_0\omega_{c0}}\left(\frac{\partial B_\vartheta}{\partial r} + q\frac{\partial B_\varphi}{\partial r} - \frac{\partial B_r}{\partial\vartheta}\right) \\ &= \frac{v^2\left(2-\eta B_0\right)}{2\sqrt{g_0}B_0\omega_{c0}}\left(\frac{B_r}{B_0}\frac{\partial B_0}{\partial\vartheta} - \frac{B_0}{B_0^{\vartheta}}\frac{\partial B_0}{\partial r}\right) + \frac{v^2\left(1-\eta B_0\right)}{\sqrt{g_0}B_0\omega_{c0}}\left(\frac{\partial B_\vartheta}{\partial r} + q\frac{\partial B_\varphi}{\partial r} - \frac{\partial B_r}{\partial\vartheta}\right).\end{aligned} \tag{2.148}$$

Finally, the expression for the non-ambipolar flux (2.134) in terms of invariants of motion is

$$\begin{aligned}\Gamma^{NA} = \frac{\pi mc}{2e\sqrt{g_0}B_0^{\vartheta}}\left(\int_0^{2\pi}\frac{\mathrm{d}\vartheta}{B_0^2}|\nabla r_0|\right)^{-1}\int_0^{2\pi}\frac{\mathrm{d}\vartheta}{B_0^2}\int_0^{\infty}\mathrm{d}v v^4\int_0^{1/B_0}\mathrm{d}\eta\frac{2-\eta B_0}{\sqrt{1-\eta B_0}}\times \\ \times\sum_{\sigma=\pm1}\overline{f_{11}\frac{\partial\delta B}{\partial\varphi_0}}.\end{aligned} \tag{2.149}$$

An obvious advantage of the quasilinear limit is that the dimension of the problem (2.144) can be reduced by one. Presenting the perturbation field δB and the linear perturbation of the distribution function f_{11} in the form of a Fourier series,

$$\delta B(\vartheta,\varphi_0) = \mathrm{Re}\sum_{n=1}^{\infty}B_n(\vartheta)\mathrm{e}^{in\varphi_0}, \qquad f_{11}(\vartheta,\varphi_0) = \mathrm{Re}\sum_{n=1}^{\infty}f_n(\vartheta)\mathrm{e}^{in\varphi_0}, \tag{2.150}$$

the kinetic equation (2.144) is reduced to an equation for the Fourier ampli-

tudes,

$$v_\parallel \frac{B_0^\vartheta}{B_0}\frac{\partial f_n}{\partial \vartheta} - \hat{L}_{cL} f_n + inv_{g0}^{\varphi_0} f_n = \frac{mcB_\varphi v^2\,(2-\eta B_0)}{2e\sqrt{g_0}B_0^3}\left(\frac{\partial B_n}{\partial \vartheta} - \frac{inB_0^2 B_n}{B_0^\vartheta B_\varphi} - \right.$$
$$\left. - \frac{2B_n}{B_0}\frac{\partial B_0}{\partial \vartheta}\right)\frac{\partial f_M}{\partial r} + v_\parallel \frac{B_0^\vartheta}{B_0^2}\left(\frac{B_n}{B_0}\frac{\partial B_0}{\partial \vartheta} - \frac{\partial B_n}{\partial \vartheta}\right)\eta\frac{\partial f_{10}}{\partial \eta} - \frac{B_n}{B_0}\hat{L}_{cL} f_{10}, \quad (2.151)$$

where f_n (as well as B_n) satisfies the periodicity condition

$$f_n(\vartheta + 2\pi) = f_n(\vartheta)\mathrm{e}^{2\pi i n q}. \quad (2.152)$$

In addition, toroidal harmonics of the perturbation field contribute independently to the flux (2.149),

$$\Gamma^{NA} = \sum_{n=1}^{\infty}\frac{\pi mc}{4e\sqrt{g_0}B_0^\vartheta}\left(\int_0^{2\pi}\frac{\mathrm{d}\vartheta}{B_0^2}|\nabla r_0|\right)^{-1}\int_0^{2\pi}\frac{\mathrm{d}\vartheta}{B_0^2}\int_0^{\infty}\mathrm{d}v v^4\int_0^{1/B_0}\mathrm{d}\eta\frac{2-\eta B_0}{\sqrt{1-\eta B_0}}\times$$
$$\times\sum_{\sigma=\pm 1} n\,\mathrm{Im} f_n B_n^*. \quad (2.153)$$

Account of the parallel electric field leads to additional terms in the right hand side of (2.138) and (2.151), which are given by

$$+\sigma v\sqrt{1-\eta B_0}B_0 f_M A_3, \qquad -2\sigma v\sqrt{1-\eta B_0}B_n f_M A_3, \quad (2.154)$$

respectively.

2.3.3 Simplified cases for the long mean free path limit

In this section cases are investigated where a numerical solution of the axisymmetric problem can be avoided. In absence of a density gradient the axisymmetric equation for ions is satisfied in all collisionality regimes by the following distribution function [21]

$$f_M + f_{10} = f_M(r_\varphi, w), \quad (2.155)$$

where f_M is a local Maxwellian distribution function and r_φ is a function of the generalized toroidal momentum P_φ, Eq (2.67). This function is implicitly defined by

$$\frac{e}{c}A_\varphi(r_\varphi) = P_\varphi, \tag{2.156}$$

where the co-variant toroidal component of the vector potential A_φ is the same in all flux coordinate systems (and in cylindrical too) if the axisymmetric field is independent of the toroidal angle in these variables. The solution (2.155) includes also the gyro-motion (classical transport), but for the following considerations it is sufficient to use the guiding center approximation described in Ref. [21] where within the linear order one can write

$$\frac{e}{c}A_\varphi(r_\varphi) = mv_\parallel\frac{B_\varphi}{B_0} + \frac{e}{c}A_\varphi(r) \approx P_\varphi. \tag{2.157}$$

In linear order over the Larmor radius Eq. (2.157) can be solved,

$$r_\varphi = r - \frac{mcv_\parallel B_\varphi}{e\sqrt{g_0}B_0^\vartheta B_0}, \tag{2.158}$$

so that the first correction to the distribution function is

$$f_{10} = -\frac{mcv_\parallel B_\varphi}{e\sqrt{g_0}B_0^\vartheta B_0}\frac{\partial f_M}{\partial r}. \tag{2.159}$$

One can see that the function (2.155) is a shifted Maxwellian up to linear order in Larmor radius. Therefore, the linearized collision operator in the right hand side of (2.141) gives zero for this function. Substituting the solution (2.159) in (2.141) one gets

$$\begin{aligned}\hat{L}_{AX}f_{11} = &-\frac{mc}{2e\sqrt{g_0}B_0^\vartheta}\left(v_\perp^2 + 2v_\parallel^2\right)\frac{1}{B_0}\frac{\partial\delta B}{\partial\varphi_0}\frac{\partial f_M}{\partial r} + \\ &+\frac{mcB_\varphi}{2e\sqrt{g_0}B_0^3}\left(2v_\parallel^2\frac{\partial\delta B}{\partial\vartheta} - \left(v_\perp^2 + 4v_\parallel^2\right)\frac{\delta B}{B_0}\frac{\partial B_0}{\partial\vartheta}\right)\frac{\partial f_M}{\partial r}.\end{aligned} \tag{2.160}$$

The solution (2.159) is valid for ions in absence of a temperature gradient in all collisionality regimes. However, it is not valid for electrons and for ions with radially varying temperature. Nevertheless, in the long mean free

path regime deviations from the solution (2.159) are small in the trapped particle domain, as the ratio of the poloidal connection length to the mean free path (see, e.g. Ref. [21]). Since in most low collisionality regimes the non-axisymmetric fluxes are produced by trapped particles, equation (2.160) is sufficient for those regimes. Due to the small collisionality it can be further simplified by bounce averaging. Using integrals of motion v and η the bounce average is defined for trapped particles as

$$\langle a\rangle_b = \left(\int\limits_{\vartheta_{\min}}^{\vartheta_{\max}} \frac{\mathrm{d}\vartheta B_0}{v_\parallel B_0^\vartheta}\right)^{-1} \int\limits_{\vartheta_{\min}}^{\vartheta_{\max}} \frac{\mathrm{d}\vartheta B_0}{v_\parallel B_0^\vartheta} a = \frac{1}{\tau_b}\int\limits_{\vartheta_{\min}}^{\vartheta_{\max}} \frac{\mathrm{d}\vartheta\ a}{B_0\sqrt{1-\eta B_0}}, \tag{2.161}$$

where $\vartheta_{\min}$ and $\vartheta_{\max}$ are the reflection points and

$$\tau_b = \int\limits_{\vartheta_{\min}}^{\vartheta_{\max}} \frac{\mathrm{d}\vartheta}{B_0\sqrt{1-\eta B_0}} \tag{2.162}$$

is the normalized bounce time. By applying this procedure to Eq. (2.160) and using (2.143), the bounce averaged equation is obtained

$$\left\langle v_{g0}^{\varphi_0}\right\rangle_b \frac{\partial f_{11}}{\partial\varphi_0} - \left\langle \hat{L}_{cL}\right\rangle_b f_{11} = -\frac{mcv^2}{2e\sqrt{g_0}B_0^\vartheta}\left\langle \frac{2-\eta B_0}{B_0}\frac{\partial\delta B}{\partial\varphi_0}\right\rangle_b \frac{\partial f_M}{\partial r}. \tag{2.163}$$

The last term on the right hand side of (2.160) does not contribute to bounce average because the factor depending on ϑ in this term can be presented as follows,

$$\frac{1}{B_0}\left(2v_\parallel^2\frac{\partial\delta B}{\partial\vartheta} - \left(v_\perp^2+4v_\parallel^2\right)\frac{\delta B}{B_0}\frac{\partial B_0}{\partial\vartheta}\right) = 2v_\parallel B_0\frac{\partial}{\partial\vartheta}\frac{v_\parallel\delta B}{B_0^2}, \tag{2.164}$$

where the derivative of $v_\parallel$ in the right hand side is taken keeping η and v constant. Since in the long mean free path regime f_{11} is independent of the parallel coordinate ϑ and on the parallel velocity sign σ, one can simplify the

expression for the flux (2.149) to

$$\Gamma^{NA} = \frac{\pi mc}{e\sqrt{g_0}B_0^\vartheta}\left(\int_0^{2\pi}\frac{\mathrm{d}\vartheta}{B_0^2}|\nabla r_0|\right)^{-1}\int_0^\infty \mathrm{d}v v^4 \int_{1/B_0^{\max}}^{1/B_0^{\min}} \mathrm{d}\eta\ \tau_b \overline{f_{11}\left\langle \frac{2-\eta B_0}{B_0}\frac{\partial \delta B}{\partial \varphi_0}\right\rangle_b}. \tag{2.165}$$

where $B_0^{\min}$ and $B_0^{\max}$ are minimum and maximum values of the magnetic field on the flux surface. The collisionless limit of the equation for the Fourier amplitudes (2.151) and of the flux density (2.153) are obtained as

$$in\left\langle v_{g0}^{\varphi_0}\right\rangle_b f_n - \left\langle \hat{L}_{cL}\right\rangle_b f_n = -in\frac{mcv^2}{2e\sqrt{g_0}B_0^\vartheta}\left\langle \frac{2-\eta B_0}{B_0}B_n\right\rangle_b \frac{\partial f_M}{\partial r}, \tag{2.166}$$

and

$$\Gamma^{NA} = \sum_{n=1}^\infty \frac{\pi mc}{2e\sqrt{g_0}B_0^\vartheta}\left(\int_0^{2\pi}\frac{\mathrm{d}\vartheta}{B_0^2}|\nabla r_0|\right)^{-1}\int_0^\infty \mathrm{d}v v^4 \int_{1/B_0^{\max}}^{1/B_0^{\min}} \mathrm{d}\eta\ \tau_b n\ \mathrm{Im} f_n \left\langle \frac{2-\eta B_0}{B_0}B_n^*\right\rangle_b, \tag{2.167}$$

respectively.

A useful limiting case is the $1/\nu$-regime where for the Lorentz collision model,

$$\hat{L}_{cL} = \frac{4\nu_d}{B_0}\sqrt{1-\eta B_0}\frac{\partial}{\partial \eta}\eta\sqrt{1-\eta B_0}\frac{\partial}{\partial \eta}, \tag{2.168}$$

the particle flux density can be expressed in terms of an effective ripple [10],

$$\Gamma^{NA} = -\frac{\sqrt{8}}{9\pi^{3/2}}\frac{n_\alpha v_T^2 \rho_L^2}{R^2}\epsilon_{\mathrm{eff}}^{3/2}\int_0^\infty \frac{\mathrm{d}z \mathrm{e}^{-z} z^{5/2}}{\nu_d}\left(A_1 + A_2 z\right). \tag{2.169}$$

Here, ν_d denotes the deflection frequency [48] (ν_D is the definition given in the book of *Helander and Sigmar* [21]),

$$\nu_{d,\alpha} = \frac{\nu_{D,\alpha}}{2} = \sum_\beta \hat{\nu}_{\alpha\beta}\frac{\phi(\sqrt{z_\beta}) - G(\sqrt{z_\beta})}{2z_\alpha^{3/2}}, \quad \hat{\nu}_{\alpha\beta} = \frac{4\pi n_\beta e_\alpha^2 e_\beta^2 \log\Lambda}{m_\alpha^2 v_{T,\alpha}^3}, \tag{2.170}$$

α and β are species indices, $\log\Lambda$ is the Coulomb logarithm, $\phi(x)$ is the error function, $G \equiv (\phi(x) - x\phi'(x))/(2x^2)$ is the Chandrasekhar function [21], the

integration variable

$$z = \frac{mv^2}{2T} \tag{2.171}$$

is the normalized kinetic energy, thermodynamic forces A_1 and A_2 are given by (2.22), $\rho_L = v_T \omega_{\rm cr}^{-1}$, and R and $\omega_{\rm cr}$ denote the reference radius and the cyclotron frequency for the reference magnetic field $B_{\rm ref}$ introduced above, respectively. The effective ripple is obtained in Appendix A.1 as

$$\epsilon_{\rm eff}^{3/2} = \frac{\pi q^2 R^2 B_{\rm ref}^2}{16\sqrt{2}} \int_0^{2\pi} \frac{{\rm d}\vartheta}{B_0^2} \left(\int_0^{2\pi} \frac{{\rm d}\vartheta}{B_0^2} |\nabla \psi_{\rm tor}| \right)^{-2} \sum_{n=1}^{\infty} \int_{1/B_0^{\rm max}}^{1/B_0^{\rm min}} {\rm d}\eta \, \frac{n^2 |H_n|^2}{\eta I}, \tag{2.172}$$

where quantities I and H_n are defined in Appendix A.1 by Eqs. (A.2) and (A.3), and $\psi_{\rm tor}$ is the toroidal magnetic flux normalized by 2π, see Eq. (2.13). This analytical limit is a useful check for the numerical procedure since f_{11} is evaluated there from the numerically computed f_{10}.

2.3.4 Numerical evaluation with the code NEO-2

The general problem described by equation (2.91) is four-dimensional and, therefore, rather difficult for a numerical evaluation. Aside from Monte Carlo methods (see, e.g., Ref. [8]) which are rather slow, a commonly used tool for the evaluation of transport coefficients in general type toroidal devices is the DKES code [6]. In this code, however, the problem dimensionality is reduced by using a model collision operator which allows for the computation of mono-energetic distribution functions. In turn, the code NEO-2 [1] uses the exact linearized collision operator but in its standard version is limited to the case of slow cross-field rotation. In this case it is also possible to reduce the dimensionality of the problem to 3D (two variables in velocity space and the coordinate along the field line). With help of the quasilinear approach described in the previous section this restriction is removed for small enough perturbation field amplitudes such that the effect on the particle motion within the flux surface is negligible small. The quasilinear approach reduces the general problem (2.91) to 3D and, thus, equation (2.138) is already in the

form solved by NEO-2. If the source term in this equation is replaced by the toroidal electric field (such a form is not considered here), it describes the generalized Spitzer function which has been studied for finite collisionalities in Ref. [49].

Here, a modification of the code NEO-2 is described which is based on the original velocity space discretization scheme [1]. The discretization scheme introduced in Ref. [1] uses an adaptive grid over the normalized perpendicular adiabatic invariant η while the dependence of the distribution function on v is discretized by an expansion over Sonine polynomials. Such a discretization scheme is sufficient for regimes without "collisionless" particle resonances such as the $1/\nu$ regime and the $\nu - \sqrt{\nu}$ regime. For a proper treatment of regimes with collisionless resonances such as the superbanana plateau regime or drift-orbit resonances, localized basis functions, e.g., hat functions, are used instead of Sonine polynomials for resolving the dependence of the distribution function on v. Due to the generalization of the original expansion method to arbitrary, non-orthogonal basis functions the analytically pre-computed matrix elements [1, 50] of the collision operator have been replaced by a fully numerical implementation in the present version of NEO-2.

Equations to be solved are the axisymmetric (2.138) and non-axisymmetric problem (2.151). Since the different Fourier modes are computed independently, the toroidal mode number is assumed to be a fixed parameter of the problem. In order not to overload the notation, it will be omitted in the following when indexing newly appearing quantities. For the same reason also the flux surface label r will be skipped as an argument of the distribution function.

The flux surface label is now specified as the normalized (divided by 2π) toroidal flux divided by its value at the edge,

$$r = s \equiv \frac{\psi_{\mathrm{tor}}}{\psi_{\mathrm{tor}}^{a}}, \tag{2.173}$$

where ψ_{tor}^{a} is the normalized toroidal flux at the edge (separatrix). Using this

definition of the flux surface label one gets

$$\sqrt{g_0}B_0^{\vartheta} = \frac{\mathrm{d}\psi_{\mathrm{pol}}}{\mathrm{d}r} = \iota\frac{\mathrm{d}\psi_{\mathrm{tor}}}{\mathrm{d}r} = \iota\psi_{\mathrm{tor}}^{a}, \tag{2.174}$$

where ψ_{pol} is the normalized poloidal flux and $\iota = 1/q$ is the rotational transform angle divided by 2π. Another useful formula is

$$\sqrt{g_0}B_0^2 = (\iota B_\vartheta + B_\varphi)\psi_{\mathrm{tor}}^{a}. \tag{2.175}$$

Historically, the variable measuring the distance along the field line in NEO-2 is not the poloidal angle ϑ but the toroidal angle which will be denoted below φ_s in order to distinguish it from φ and φ_0. It is linked with ϑ via the relation

$$\varphi_s = q\vartheta \tag{2.176}$$

and changes in the limits $0 < \varphi_s < 2\pi q$. Thus, the derivative along the field line in Eqs. (2.138) and (2.151) is transformed to

$$\frac{B_0^{\vartheta}}{B_0}\frac{\partial}{\partial\vartheta} = h^{\varphi}\frac{\partial}{\partial\varphi_s}, \tag{2.177}$$

where

$$h^{\varphi} = \frac{qB_0^{\vartheta}}{B_0} = \frac{B_0^{\varphi}}{B_0}. \tag{2.178}$$

The left hand side operator (2.143) in Eqs. (2.138) and (2.151) is transformed to

$$\hat{L}_{AX} = \sigma v\sqrt{1-\eta B_0}h^{\varphi}\frac{\partial}{\partial\varphi_s} - \hat{L}_{cL} + inv_{g0}^{\varphi_0}, \tag{2.179}$$

where $n = 0$ for the axisymmetric solution.

With help of formulas (2.174) and (2.175) one can transform the electric rotation frequency (2.147) as follows,

$$\Omega_{tE} = -\frac{c}{\iota}\frac{\mathrm{d}\Phi}{\mathrm{d}\psi_{\mathrm{tor}}} = -\frac{c}{\iota\psi_{\mathrm{tor}}^{a}}\frac{\mathrm{d}\Phi}{\mathrm{d}s}. \tag{2.180}$$

In a similar way the magnetic rotation frequency (2.148) is transformed to

$$\begin{aligned}\Omega_{tB} &= \Omega_{tB}^{\mathrm{ref}} z \left(\frac{2-\eta B_0}{\iota B_\vartheta + B_\varphi} \left(\frac{B_s}{B_0} \frac{\partial B_0}{\partial \vartheta} - \frac{\iota B_\vartheta + B_\varphi}{\iota B_0} \frac{\partial B_0}{\partial s} \right) + \right. \\ &\left. + \frac{2-2\eta B_0}{\iota B_\vartheta + B_\varphi} \left(\frac{\partial B_\vartheta}{\partial s} + \frac{1}{\iota} \frac{\partial B_\varphi}{\partial s} - \frac{\partial B_s}{\partial \vartheta} \right) \right), \end{aligned} \tag{2.181}$$

where z is the normalized energy (2.171) and the reference magnetic rotation frequency is

$$\Omega_{tB}^{\mathrm{ref}} = \frac{cT}{e\psi_{\mathrm{tor}}^a}. \tag{2.182}$$

The derivative of the Maxwellian in Eqs. (2.138) and (2.151) is expressed through thermodynamic forces (2.22) whereby the definition of these forces in terms of the effective radius fixed by the condition (2.5) is kept. Thus Eq. (2.138) takes the form

$$\begin{aligned}\hat{L}_{AX} f_{10} &= -\frac{\rho_L v_T}{\langle |\nabla s| \rangle} z(A_1 + zA_2) f_M \sqrt{1-\eta B_0} \frac{B_\varphi}{\iota B_\vartheta + B_\varphi} \frac{\partial B_0}{\partial \vartheta} \frac{B_{\mathrm{ref}}}{\psi_{\mathrm{tor}}^a} \times \\ &\times \frac{\partial}{\partial \eta} \frac{\sqrt{1-\eta B_0}}{B_0} \left(\frac{4}{3B_0} - \frac{\eta}{3} \right), \end{aligned} \tag{2.183}$$

where v_T and ρ_L are the thermal velocity and Larmor radius, respectively, and B_0 is now a normalized magnetic field (divided by B_{ref}). Introducing the geodesic curvature k_{G0} defined by

$$|\nabla s| k_{G0} = -\frac{B_\varphi}{\iota B_\vartheta + B_\varphi} \frac{\partial B_0}{\partial \vartheta} \frac{B_{\mathrm{ref}}}{\psi_{\mathrm{tor}}^a}, \tag{2.184}$$

one can bring this equation to the standard form implemented in NEO-2,

$$\hat{L}_{AX} f_{10} = \frac{\rho_L v_T}{\langle |\nabla s| \rangle} z(A_1 + zA_2) f_M \sqrt{1-\eta B_0} \frac{\partial}{\partial \eta} \frac{\sqrt{1-\eta B_0}}{B_0} \hat{V}_{G0}, \tag{2.185}$$

where V_{G0} (and other similar functions, which differ just by the definition of k_G) is linked to k_{G0} by

$$\hat{V}_G = \frac{1}{3} \left(\frac{4}{B_0} - \eta \right) |\nabla s| k_G. \tag{2.186}$$

Note that Gaussian units are used in NEO-2 which results in a conversion factor, $B_{\mathrm{ref}}/\psi^a_{\mathrm{tor}} = 10^{-4}B_{00}/\psi'$, where B_{00} and ψ' are the (0,0)-harmonic of Boozer field and the derivative of the toroidal flux over s, both in SI units, respectively.

The equation for the Fourier amplitudes of the perturbation of distribution function (2.151) is expressed then as follows,

$$\hat{L}_{AX} f_n = \frac{\rho_L v_T}{\langle|\nabla s|\rangle} z(A_1 + zA_2) f_M \sqrt{1-\eta B_0}\frac{\partial}{\partial\eta}\frac{\sqrt{1-\eta B_0}}{B_0}\hat{V}^{(f)}_{Gn} - \\ - v_T z^{1/2}\sigma\sqrt{1-\eta B_0}h^{\varphi}\left(\iota\frac{\partial}{\partial\vartheta}\frac{B_n}{B_0} + in\frac{B_n}{B_0}\right)\mathrm{e}^{in\varphi_s}\eta\frac{\partial f_{10}}{\partial\eta} - \frac{B_n}{B_0}\mathrm{e}^{in\varphi_s}\hat{L}_{cL}f_{10}, \tag{2.187}$$

where Fourier amplitudes B_n correspond now to a series over the toroidal angle φ of periodic Boozer coordinates, but not over φ_0 as in the previous section. It should be noted that all functions of ϑ are evaluated here at $\vartheta = \iota\varphi_s$. The quantity $\hat{V}^{(f)}_{Gn}$ is defined again by (2.186) when k_G is replaced there with $k^{(f)}_{Gn}$,

$$\begin{aligned} |\nabla s| k^{(f)}_{Gn} &= \left(inB_n - \frac{B_\varphi}{\iota B_\vartheta + B_\varphi}\left(\iota\frac{\partial B_n}{\partial\vartheta} + inB_n - \frac{2\iota B_n}{B_0}\frac{\partial B_0}{\partial\vartheta}\right)\right)\frac{B_{\mathrm{ref}}}{\iota\psi^a_{\mathrm{tor}}}\mathrm{e}^{in\varphi_s} \\ &= \left(in\frac{B_n}{B_0} - \frac{B_\varphi}{\iota B_\vartheta + B_\varphi}\left(\iota\frac{\partial}{\partial\vartheta}\frac{B_n}{B_0} + in\frac{B_n}{B_0} - \frac{\iota B_n}{B_0^2}\frac{\partial B_0}{\partial\vartheta}\right)\right)\frac{B_0 B_{\mathrm{ref}}}{\iota\psi^a_{\mathrm{tor}}}\mathrm{e}^{in\varphi_s}. \end{aligned} \tag{2.188}$$

The quantity $k^{(f)}_{Gn}$ has not the meaning of a geodesic curvature anymore because it includes also terms connected with the mirroring force. In the following also the quantity $k^{(b)}_{Gn}$ defined by

$$|\nabla s| k^{(b)}_{Gn} = inB_n\frac{B_{\mathrm{ref}}}{\iota\psi^a_{\mathrm{tor}}}\mathrm{e}^{in\varphi_s} = in\frac{B_n}{B_0}\frac{B_0 B_{\mathrm{ref}}}{\iota\psi^a_{\mathrm{tor}}}\mathrm{e}^{in\varphi_s}, \tag{2.189}$$

which is a linear perturbation of the geodesic curvature by the non-axisymmetric field, will be needed for the evaluation of particle fluxes. In (2.188) and (2.189) the ratio B_n/B_0 is introduced explicitly because the perturbation field B_n enters all equations through this combination only, which minimizes the in-

put.

Solutions to Eqs. (2.185) and (2.187) are looked for in the form of a series expansion over test functions $\phi_m(z)$,

$$f_{10} \approx \frac{\rho_L}{\langle|\nabla s|\rangle} f_M \sum_{m=0}^{M} \bar{f}_m^\sigma(\varphi_s,\eta)\phi_m(z), \qquad f_n \approx \frac{\rho_L}{\langle|\nabla s|\rangle} f_M \sum_{m=0}^{M} \tilde{f}_m^\sigma(\varphi_s,\eta)\phi_m(z), \tag{2.190}$$

where z is the normalized kinetic energy (2.171) and σ is the parallel velocity sign. For the following considerations normalized associated Laguerre polynomials of the order 3/2 (Sonine polynomials) are chosen as test functions, but with minor corrections it is possible to extend the resulting formulas to general basis functions. If nothing else is mentioned, this can be done by replacing $S_m(z)$ with $\phi_m(z)$. Corrections necessary for the generalization of the formulas are indicated below explicitly at the relevant places. Here, z is the normalized kinetic energy (2.171) and σ is the parallel velocity sign,

$$S_m(z) = \pi^{3/4}\sqrt{\frac{2\Gamma(m+1)}{\Gamma(m+5/2)}} L_m^{(3/2)}(z), \tag{2.191}$$

and $L_m^{(3/2)}(z)$ and $\Gamma(x)$ denote the associated Laguerre polynomials and the Gamma function, respectively. Functions f_m^σ satisfy the periodicity condition resulting from (2.152),

$$f_m^\sigma(\varphi_s + 2\pi q, \eta) = f_m^\sigma(\varphi_s,\eta)\mathrm{e}^{2\pi i n q}, \tag{2.192}$$

where f_m^σ is used as a common notation for $\bar{f}_m$ and $\tilde{f}_m$, and $n = 0$ for the axisymmetric solution $\bar{f}_m$. The set of coupled 2D equations solved by NEO-2,

$$\sum_{m'=0}^{M} \hat{L}_{mm'} f_{m'}^\sigma \equiv \sigma\frac{\partial f_m^\sigma}{\partial\varphi_s} - \frac{1}{h^\varphi}\sum_{m'=0}^{M} \hat{L}_{mm'}^c f_{m'}^\sigma + \sum_{m'=0}^{M} i\omega_{mm'} f_{m'}^\sigma = Q_m, \tag{2.193}$$

is obtained by substituting the unknowns in the form (2.190) into Eqs. (2.138) and (2.151) (note that the summation index is changed from m to m' there) and a subsequent integration of the resulting equations multiplied with the

factor $zS_m(z)v_T^2\langle|\nabla s|\rangle\left(2n_\alpha\rho_L h^\varphi\sqrt{1-\eta B_0}\right)^{-1}$ over z from 0 to infinity. In case of Sonine polynomials the term with the derivative along the field line is diagonal due to the orthogonality of basis functions S_m,

$$\frac{1}{2\pi^{3/2}}\int\limits_0^\infty \mathrm{d}z\ \mathrm{e}^{-z}z^{3/2}S_m(z)S_{m'}(z) = A_{mm'} = \delta_{mm'}, \tag{2.194}$$

where $\delta_{mm'}$ is the Kronecker symbol. For arbitrary basis functions the left hand side of equation (2.194) does not reduce to the unit tensor. Nevertheless, one can present the set (2.193) in the same form by multiplying the source term Q_m and the matrix elements of the collision operator $\hat{L}^c_{mm'}$ and of the dimensionless frequency matrix $\omega_{mm'}$ with the inverse $A^{-1}_{mm'}$. Up to the definition of the source term the set (2.193) describes both, axisymmetric and non-axisymmetric distribution functions. Note that the dimensionless frequency matrix is zero for the axisymmetric problem. Details regarding the computation of the matrix elements of the collision operator are presented in [1, 50]. New are the rotation frequency and the more general source term. Using (2.146) and (2.181) one obtains

$$\omega_{mm'} = \frac{n\Omega_{tE}}{v_T h^\varphi\sqrt{1-\eta B_0}}x^{(1)}_{mm'} + \frac{n\Omega^{\mathrm{ref}}_{tB}}{v_T h^\varphi\sqrt{1-\eta B_0}}x^{(2)}_{mm'}\left(\frac{2-\eta B_0}{\iota B_\vartheta + B_\varphi}\times\right.$$
$$\left.\times\left(\frac{B_s}{B_0}\frac{\partial B_0}{\partial\vartheta} - \frac{\iota B_\vartheta + B_\varphi}{\iota B_0}\frac{\partial B_0}{\partial s}\right) + \frac{2-2\eta B_0}{\iota B_\vartheta + B_\varphi}\left(\frac{\partial B_\vartheta}{\partial s} + \frac{1}{\iota}\frac{\partial B_\varphi}{\partial s} - \frac{\partial B_s}{\partial\vartheta}\right)\right), \tag{2.195}$$

where

$$x^{(k)}_{mm'} = \frac{1}{2\pi^{3/2}}\int\limits_0^\infty \mathrm{d}z\ \mathrm{e}^{-z}z^k S_m(z)S_{m'}(z). \tag{2.196}$$

For coding it is more convenient to re-write (2.195) in the form

$$\omega_{mm'} = \frac{n\kappa\bar{\Omega}_{tE}}{h^\varphi\sqrt{1-\eta B_0}}x^{(1)}_{mm'} + \frac{n\kappa\bar{\Omega}^{\mathrm{ref}}_{tB}}{h^\varphi\sqrt{1-\eta B_0}}\left(a^{(1)}_B + (1-\eta B_0)\,a^{(2)}_B\right)x^{(2)}_{mm'} \tag{2.197}$$

where

$$a_B^{(1)} = \frac{1}{\iota B_\vartheta + B_\varphi}\left(\frac{B_s}{B_0}\frac{\partial B_0}{\partial \vartheta} - \frac{\iota B_\vartheta + B_\varphi}{\iota B_0}\frac{\partial B_0}{\partial s}\right), \tag{2.198}$$

$$a_B^{(2)} = a_B^{(1)} + \frac{2}{\iota B_\vartheta + B_\varphi}\left(\frac{\partial B_\vartheta}{\partial s} + \frac{1}{\iota}\frac{\partial B_\varphi}{\partial s} - \frac{\partial B_s}{\partial \vartheta}\right). \tag{2.199}$$

The parameter κ is the inverse mean free path times 2,

$$\kappa = \frac{2}{l_c} = \frac{2}{v_T \tau_\alpha}, \tag{2.200}$$

where

$$\tau_\alpha = \frac{3m_\alpha^2 v_T^3}{16\sqrt{\pi} n_\alpha e_\alpha^4 \Lambda_\alpha}. \tag{2.201}$$

According to the definition of κ (2.200) dimensionless rotation frequencies are introduced as

$$\bar{\Omega}_{tE} = \frac{1}{2}\Omega_{tE}\tau_\alpha, \qquad \bar{\Omega}_{tB}^{\mathrm{ref}} = \frac{1}{2}\Omega_{tB}^{\mathrm{ref}}\tau_\alpha. \tag{2.202}$$

Since the problem (2.193) is linear,

$$f_m^\sigma = A_1 \tilde{f}_m^{\sigma(1)} + A_2 \tilde{f}_m^{\sigma(2)}, \tag{2.203}$$

solutions driven by different thermodynamic forces are computed separately. Thus, one can specify the sources Q_m for the axisymmetric problem,

$$\sum_{m'=0}^{M} \hat{L}_{mm'} \bar{f}_{m'}^{\sigma(k)} = a_m^{(k)} \frac{\partial}{\partial \eta}\frac{\sqrt{1-\eta B_0}}{B_0 h^\varphi}\hat{V}_{G0}, \tag{2.204}$$

and for the perturbed problem,

$$\begin{aligned}\sum_{m'=0}^{M} \hat{L}_{mm'} \tilde{f}_{m'}^{\sigma(k)} &= a_m^{(k)} \frac{\partial}{\partial \eta}\frac{\sqrt{1-\eta B_0}}{B_0 h^\varphi}\hat{V}_{Gn}^{(f)} - \sigma\left(\iota\frac{\partial}{\partial \vartheta}\frac{B_n}{B_0} + in\frac{B_n}{B_0}\right)\mathrm{e}^{in\varphi_s}\eta\frac{\partial \bar{f}_m^{\sigma(k)}}{\partial \eta} \\ &- \frac{B_n}{B_0}\mathrm{e}^{in\varphi_s}\frac{1}{h^\varphi}\sum_{m'=0}^{M}\hat{L}_{mm'}^c \bar{f}_{m'}^{\sigma(k)},\end{aligned} \tag{2.205}$$

where

$$a_m^{(k)} = \frac{1}{2\pi^{3/2}} \int_0^\infty \mathrm{d}z\ \mathrm{e}^{-z} z^{k+1} S_m(z), \qquad k = 1, 2. \tag{2.206}$$

Finally, the particle flux (2.153) is expressed as

$$\begin{aligned} \Gamma = & -v_T n_\alpha \left(\frac{\rho_L}{\langle |\nabla s| \rangle} \right)^2 \sum_m b_m^{(1)} \sum_{k=1}^{2} A_k \left\langle \frac{B_0}{2} \mathrm{Re} \sum_{\sigma=\pm 1} \sum_{n=0}^{\infty} \tilde{f}_m^{\sigma(k)} \times \right. \\ & \left. \times \frac{\partial}{\partial \eta} \frac{\sqrt{1-\eta B_0}}{B_0} \left(\hat{V}_{Gn}^{(b)} \right)^* \right\rangle, \end{aligned} \tag{2.207}$$

where the quantity $\hat{V}_{Gn}^{(b)}$ is defined by (2.186) and (2.189), and the constant $b_m^{(1)}$ is

$$b_m^{(1)} = \frac{1}{2\sqrt{\pi}} \int_0^\infty \mathrm{d}z\ \mathrm{e}^{-z} z^{3/2} S_m(z) = \frac{\sqrt{6\pi}}{4} \delta_{m0}. \tag{2.208}$$

With help of definitions (2.23) and (2.24) the particle flux density can be presented in terms of diffusion coefficients given in the form of Ref. [49],

$$D_{1k} = \frac{\rho_L^2}{\tau_\alpha} \gamma_{1k}, \qquad k = 1, 2, \tag{2.209}$$

where

$$\gamma_{1k} = \frac{l_c}{\langle |\nabla s| \rangle^2} \sum_m \sum_{\sigma=\pm 1} \sum_{n=0}^{\infty} b_m^{(1)} \left\langle \frac{B_0}{2} \mathrm{Re} \tilde{f}_m^{\sigma(k)} \frac{\partial}{\partial \eta} \frac{\sqrt{1-\eta B_0}}{B_0} \left(\hat{V}_{Gn}^{(b)} \right)^* \right\rangle. \tag{2.210}$$

Note that the flux surface average in (2.207) and (2.210) is performed over unperturbed flux surfaces, i.e.

$$\langle a \rangle = \left(\int_0^{2\pi q} \frac{\mathrm{d}\varphi_s}{B_0^2} \right)^{-1} \int_0^{2\pi q} \frac{\mathrm{d}\varphi_s}{B_0^2} a. \tag{2.211}$$

It can be seen that expressions for the coefficients γ_{1k} are the same as in Ref. [49] except for the re-definition of geodesic curvature and generalization to complex numbers.

2.4 Analytical models for the evaluation of non-ambipolar particle fluxes

2.4.1 Ripple plateau formula

For non-axisymmetric magnetic perturbations with a high toroidal mode number, such as the toroidal field ripple produced by the finite number of toroidal field coils in a tokamak, the non-ambipolar particle fluxes can be evaluated analytically [17]. In Ref. [17] the resulting formulas for the radial particle flux density and the ripple plateau diffusion coefficient have been evaluated for a model **B**-field with circular flux surfaces, see Eqs. (47) and (46) of Ref. [17]. In order to benchmark the quasilinear version of NEO-2 for a realistic tokamak geometry, the result of Boozer [17] is generalized to magnetic field spectra with a more complex poloidal mode number dependence in this section.

It is assumed that the magnetic field module B consists of an axisymmetric part B_0 and a non-axisymmetric perturbation δB with a single toroidal harmonic N,

$$\begin{aligned} B &= B_0 + \delta B, \\ B_0 &= \sum_{m=0}^{m0b} \left(b^c_{m0} \cos\left(m\vartheta\right) + b^s_{m0} \sin\left(m\vartheta\right) \right), \\ \delta B &= \sum_{m=-m0b}^{m0b} \left(b^c_{mN} \cos\left(m\vartheta + N\varphi\right) + b^s_{mN} \sin\left(m\vartheta + N\varphi\right) \right). \end{aligned} \tag{2.212}$$

The total particle flux across a magnetic surface is given by,

$$\Gamma^{\mathrm{tot}} = \int_\psi \mathrm{d}\mathbf{S} \cdot \int \mathrm{d}^3 v \; \mathbf{v}_\mathbf{r} f = \int_\psi \frac{\mathrm{d}\vartheta \mathrm{d}\varphi}{\mathbf{B} \cdot \nabla\vartheta} \int \mathrm{d}v \mathrm{d}\lambda \; 2\pi v^2 v_r^\psi f_E, \tag{2.213}$$

where in the notation of Boozer ψ denotes the poloidal magnetic flux. The generalized form of the radial drift velocity v_r^ψ and of the solution of the

ripple kinetic equation, Eq. (36) of Ref. [17], f_E are given by,

$$\begin{aligned} v_r^{\psi} &= \frac{m_\alpha c v^2}{2e_\alpha B_0}\frac{\partial B}{\partial \varphi} \\ &= \frac{m_\alpha c v^2}{2e_\alpha B_0}\sum_{m=-m0b}^{m0b}\left(-b_{mN}^c N\sin\left(m\vartheta+N\varphi\right)+b_{mN}^s N\cos\left(m\vartheta+N\varphi\right)\right) \\ &= \frac{m_\alpha c v^2}{2e_\alpha B_0}N\left(A_N(\vartheta)\cos\left(N\varphi\right)+B_N(\vartheta)\sin\left(N\varphi\right)\right), \qquad (2.214) \\ f_E &= -\frac{m_\alpha c}{2e_\alpha}\frac{v}{q}\frac{B}{\mathbf{B}\cdot\nabla\vartheta}\frac{\partial f_M}{\partial \psi}\frac{G(\lambda/\lambda_c)}{\lambda_c}\left(\frac{1}{B_0 N}\frac{\partial B}{\partial \varphi}\right), \qquad (2.215) \end{aligned}$$

where $G(\lambda/\lambda_c)$ is given by Eq. (40) of Ref. [17]. Inserting (2.214) and (2.215) into (2.213) yields the total particle flux,

$$\begin{aligned} \Gamma^{\mathrm{tot}} = &-\left(\frac{m_\alpha c}{e_\alpha}\right)^2\frac{\pi}{2}\frac{N}{q}\frac{\mathrm{d}r}{\mathrm{d}\psi}\int_\psi\frac{\mathrm{d}\vartheta\mathrm{d}\varphi}{\left(\mathbf{B}\cdot\nabla\vartheta\right)^2}B\left[\frac{1}{B_0 N}\frac{\partial B}{\partial\varphi}\right]^2\times \\ &\times\underbrace{\int_0^\infty \mathrm{d}v v^5\frac{\partial f_M}{\partial r}}_{=n_\alpha\left(\frac{2T_\alpha}{m_\alpha\pi}\right)^{3/2}(A_1+3A_2)}\underbrace{\int_{-1}^1\mathrm{d}\lambda\frac{G(\lambda/\lambda_c)}{\lambda_c}}_{\approx\pi} \\ \approx &-\sqrt{2\pi}\left(\frac{m_\alpha c}{e_\alpha}\right)^2\frac{N}{q}\frac{\mathrm{d}r}{\mathrm{d}\psi}\left(\frac{T_\alpha}{m_\alpha}\right)^{3/2}\left\{\int_\psi\frac{\mathrm{d}\vartheta\mathrm{d}\varphi}{\left(\mathbf{B}\cdot\nabla\vartheta\right)^2}B_0\left[\frac{1}{B_0 N}\frac{\partial B}{\partial\varphi}\right]^2\right\}\times \\ &\times\left[n_\alpha A_1+3n_\alpha A_2\right]. \qquad (2.216) \end{aligned}$$

Next the expression in the curly brackets is evaluated as follows,

$$\int_\psi\frac{\mathrm{d}\vartheta\mathrm{d}\varphi}{\left(\mathbf{B}\cdot\nabla\vartheta\right)^2}B_0\left[\frac{1}{B_0 N}\frac{\partial B}{\partial\varphi}\right]^2=\int_0^{2\pi}\mathrm{d}\vartheta\frac{\pi\left(B_\vartheta+qB_\varphi\right)^2}{B_0^3}\left[\left(\frac{A_N}{B_0}\right)^2+\left(\frac{B_N}{B_0}\right)^2\right]. \qquad (2.217)$$

In order to obtain a particle flux density Γ, one has to divide the total particle

flux (2.216) by the flux surface area S,

$$\Gamma = -\sqrt{\frac{\pi}{2}} n_\alpha \left(\frac{m_\alpha c}{e_\alpha}\right)^2 \frac{N}{q} \left(\frac{T_\alpha}{m_\alpha}\right)^{3/2} \frac{B_\vartheta + qB_\varphi}{\left(\frac{\mathrm{d}\psi}{\mathrm{d}r}\right)^2} \times \\ \times \int_0^{2\pi} \frac{\mathrm{d}\vartheta}{B_0^3} \left[\left(\frac{A_N}{B_0}\right)^2 + \left(\frac{B_N}{B_0}\right)^2\right] \left(\int_0^{2\pi} \frac{\mathrm{d}\vartheta}{B_0^2}\right)^{-1} [A_1 + 3A_2], \quad (2.218)$$

where the surface area has been substituted as

$$S = 2\pi \frac{\mathrm{d}\psi}{\mathrm{d}r} (B_\vartheta + qB_\varphi) \int_0^{2\pi} \frac{\mathrm{d}\vartheta}{B_0^2}. \quad (2.219)$$

2.4.2 Universal formula for quasilinear bounce-averaged transport regimes

For small and moderate values of the cross-field rotation frequency the non-ambipolar particle flux can be described by the bounce-averaged drift kinetic equation [3], since in this case contributions from drift-orbit resonances [51, 18] are small. The bounce-averaged approach [3] comprises the $1/\nu$, $\nu - \sqrt{\nu}$ and retrapping-detrapping regime for sufficiently small values of the magnetic rotation frequency, and the superbanana-plateau and superbanana regime for magnetic rotation frequencies comparable to or large than the $\mathbf{E} \times \mathbf{B}$ rotation frequency. Expressions for the particle fluxes presented in Ref. [3] have been derived for a model $\mathbf{B}$-field with circular flux surfaces and large aspect ratio. These restrictions can be removed in case of the $\nu - \sqrt{\nu}$ [52] and of the superbanana-plateau regime [53]. In this section only bounce-averaged transport regimes described by the quasilinear approach are considered, which is the case if the conditions given by (2.90) are fulfilled, i.e. the retrapping-detrapping regime and the superbanana regime are absent.

The different quasilinear bounce-averaged transport regimes can be connected smoothly using the joining procedure given in Appendix B of Ref. [3]. Here, a modification of the formula for the non-resonant particle flux (Eq. (B5) of Ref. [3]) is presented using the more general result of Ref. [54]. Neglecting the possibility of a superbanana-plateau regime, i.e. $x_{min} = \infty$, the universal

formula is given by Eq. (B7) of Ref. [3],

$$\Gamma_{\mathrm{non}} = -n_\alpha \frac{\varepsilon^{1/2}}{4\sqrt{2}\pi^{3/2}} \left(\frac{m_\alpha c}{e_\alpha \psi'_{\mathrm{pol}}}\right)^2 v_{T,\alpha}^4 \left[\lambda_1 \left(\frac{p'_\alpha}{p_\alpha} + \frac{e_\alpha \Phi'}{T_\alpha}\right) + \lambda_2 \frac{T'_\alpha}{T_\alpha}\right], \quad (2.220)$$

where magnetic field quantities are specified in Hamada coordinates, $\Gamma_{\mathrm{non}} = \langle n_\alpha \mathbf{V} \cdot \nabla V \rangle$ (see Eq. (A.15)), the flux surface label V is here the volume enclosed by the flux surface divided by $4\pi^2$, ϵ is the amplitude of $\cos\vartheta$ component of the axisymmetric magnetic field normalized by the magnetic field strength on the magnetic axis, and λ_j for $j = 1, 2$ is

$$\lambda_j = \frac{1}{2} \int_0^\infty \mathrm{d}x x^{5/2} e^{-x} \left(x - \frac{5}{2}\right)^{j-1} \sum_n \frac{1}{\frac{1}{k_{1/\nu,n}} + \frac{1}{k_{\sqrt{\nu},n}}}. \quad (2.221)$$

The kernel for the $1/\nu$ regime $k_{1/\nu,n}$ is given by Eq. (B1) of Ref. [3],

$$k_{1/\nu,n} = \frac{\varepsilon}{\nu_D} I_{1/\nu,n}. \quad (2.222)$$

The kernel $k_{\sqrt{\nu}}$ is determined by comparing the expression for the $\nu - \sqrt{\nu}$ particle flux given by Eq. (29) of Ref. [54],

$$\begin{aligned}\Gamma_{\sqrt{\nu}} = -n_\alpha \frac{\varepsilon^{-1/2}}{4\sqrt{2}\pi^{3/2}} \left(\frac{m_\alpha c}{e_\alpha \psi'_{\mathrm{pol}}}\right)^2 v_{T,\alpha}^4 \left(c\frac{\mathrm{d}\Phi}{\mathrm{d}\psi_{\mathrm{pol}}}\right)^{-2} \nu_t \Bigg[\left(\frac{p'_\alpha}{p_\alpha} + \frac{e_\alpha \Phi'}{T_\alpha}\right) \Bigg\{ \frac{1}{2} \int_0^\infty \mathrm{d}x \times \\ \times x^{5/2} e^{-x} \frac{\nu_D}{\nu_t} \int_0^1 \mathrm{d}\kappa^2 \left(E(\kappa) - (1-\kappa^2)K(\kappa)\right) \sum_n \left(\alpha_n^2 + \beta_n^2\right) \Bigg\} + \left(\frac{T'_\alpha}{T_\alpha}\right) \Bigg\{ \frac{1}{2} \int_0^\infty \mathrm{d}x \times \\ \times x^{5/2} e^{-x} \left(x - \frac{5}{2}\right) \frac{\nu_D}{\nu_t} \int_0^1 \mathrm{d}\kappa^2 \left(E(\kappa) - (1-\kappa^2)K(\kappa)\right) \sum_n \left(\alpha_n^2 + \beta_n^2\right) \Bigg\} \Bigg], \end{aligned} \quad (2.223)$$

to the $\nu - \sqrt{\nu}$ limit of the universal formula, i.e. $(k_{\sqrt{\nu},n})^{-1} \gg (k_{1/\nu,n})^{-1}$,

$$\Gamma_{\mathrm{non},\sqrt{\nu}} = -n_\alpha \frac{\varepsilon^{1/2}}{4\sqrt{2}\pi^{3/2}} \left(\frac{m_\alpha c}{e_\alpha \psi'_{\mathrm{pol}}}\right)^2 v_{T,\alpha}^4 \left[\left\{\frac{1}{2}\int_0^\infty \mathrm{d}x x^{5/2} e^{-x} \sum_n k_{\sqrt{\nu},n}\right\} \times \right.$$
$$\left. \times \left(\frac{p'_\alpha}{p_\alpha} + \frac{e_\alpha \Phi'}{T_\alpha}\right) + \left\{\frac{1}{2}\int_0^\infty \mathrm{d}x x^{5/2} e^{-x} \left(x - \frac{5}{2}\right) \sum_n k_{\sqrt{\nu},n}\right\} \frac{T'_\alpha}{T_\alpha}\right], \quad (2.224)$$

which yields

$$k_{\sqrt{\nu},n} = \frac{\nu_t}{\underbrace{\varepsilon \left(c \frac{\mathrm{d}\Phi}{\mathrm{d}\psi_{\mathrm{pol}}}\right)^2}_{=\Omega_{tE}^2}} \frac{\nu_D}{\nu_t} \int_0^1 \mathrm{d}\kappa^2 \left(E(\kappa) - (1-\kappa^2)K(\kappa)\right)\left(\alpha_n^2 + \beta_n^2\right). \quad (2.225)$$

Here, $E(\kappa)$ and $K(\kappa)$ denote the complete elliptic integrals of the second and the first kinds, respectively, and the coefficients α_n and β_n are specified by Eqs. (25) and (26) of Ref. [54]

In order to compare the results from the bounce-averaged approach to the NEO-2 results, the particle flux (2.220) is cast in terms of diffusion coefficients (2.24) and thermodynamic forces (2.22), and the flux surface label is changed from V to r,

$$\begin{aligned}\Gamma_{\mathrm{non}} = \langle n_\alpha \mathbf{V}\cdot\nabla V\rangle &= \Gamma^{\mathrm{NA}} \frac{\mathrm{d}V}{\mathrm{d}r} = \frac{\mathrm{d}V}{\mathrm{d}r}\left(-n_\alpha \sum_j D_{1j} A_j\right) \\ &= -n_\alpha \frac{\varepsilon^{1/2}}{4\sqrt{2}\pi^{3/2}} \left(\frac{m_\alpha c}{e_\alpha \frac{\mathrm{d}\psi_{\mathrm{pol}}}{\mathrm{d}r}}\right)^2 \frac{\mathrm{d}V}{\mathrm{d}r} v_{T,\alpha}^4 \left[\lambda_1 A_1 + \left(\lambda_2 + \frac{5}{2}\lambda_1\right) A_2\right].\end{aligned} \quad (2.226)$$

Then, the normalized diffusion coefficients are given by

$$\frac{D_{11}}{D_p} = \frac{4\sqrt{2}}{\pi^{5/2}} \frac{q}{R\varepsilon^{3/2}} \frac{\lambda_1}{\tau_\alpha} \kappa_\alpha^{-1}, \quad (2.227)$$

$$\frac{D_{12}}{D_p} = \frac{4\sqrt{2}}{\pi^{5/2}} \frac{q}{R\varepsilon^{3/2}} \left(\frac{\lambda_2}{\tau_\alpha} + 2.5\frac{\lambda_1}{\tau_\alpha}\right) \kappa_\alpha^{-1}, \quad (2.228)$$

where $D_p = \pi q v_{T,\alpha} \rho_{L,\alpha}^2 (16R)^{-1}$, $\rho_{L,\alpha} = v_{T,\alpha} \omega_{cr}^{-1}$, $\omega_{cr} = e_\alpha B_{\mathrm{ref}} (m_\alpha c)^{-1}$, $\kappa_\alpha = 2/(v_{T,\alpha}\tau_\alpha)$ is the collisionality parameter and τ_α is given by (2.201).

Chapter 3

Benchmarking results

In this chapter results from benchmarking the quasilinear version of the code NEO-2 [2] (see Section 2.3) against various analytical [3, 17, 18] and semi-analytical models [19], as well as the DKES code [6] and NEO [10], are shown. It should be noted that the numerical results described in Sections 3.2 and 3.3 have been published in the following journal articles [2, 55] and conference proceeding [16]:

- S. V. Kasilov, W. Kernbichler, A. F. Martitsch, H. Maassberg, and M. F. Heyn. Evaluation of the toroidal torque driven by external non-resonant non-axisymmetric magnetic field perturbations in a tokamak. *Phys. Plasmas*, 21(9):092506, 2014.

- W. Kernbichler, S. V. Kasilov, G. Kapper, A. F. Martitsch, V .V. Nemov, C. G. Albert, and M. F. Heyn. Solution of drift kinetic equation in stellarators and tokamaks with broken symmetry using the code NEO-2. *Plasma Phys. Control. Fusion*, submitted, 2016.

- A. F. Martitsch, S. V. Kasilov, W. Kernbichler, and H. Maassberg. Evaluation of non-ambipolar particle fluxes driven by external non-resonant magnetic perturbations in a tokamak. In *41st EPS Conference on Plasma Physics*, volume 38F, page P1.049, Berlin, Deutschland, 2014. European Physical Society.

For the $1/\nu$ regime it is possible to compare analytically the formula obtained by the quasilinear approach to the result of Nemov *et al* [10] and to the result of Shaing [3], see Section 3.1. In Section 3.2 results of the code NEO-2 are benchmarked against the DKES code [6] for a Lorentz collision model and against the universal formula connecting all quasilinear bounce-averaged transport regimes [3] in case of the full collision model. A summary of the numerical results shown in Section 3.2 including a comparison to results from the semi-analytical model [19] is given in Section 3.3.

3.1 Analytical comparison for the $1/\nu$ regime

In this section the expression for the non-ambipolar particle flux in the $1/\nu$ regime obtained from the quasilinear approach (2.169), i.e.

$$\Gamma^{\mathrm{NA}} = -\sum_{n=1}^{\infty} \frac{\pi m^2 c^2}{36 e^2} \underbrace{\frac{g_0}{(B_0^{\vartheta})^2}}_{=a} \underbrace{\left(\int_0^{2\pi} \frac{\mathrm{d}\vartheta}{B_0^2} |\nabla r_0| \right)^{-1}}_{=b} \underbrace{\int_0^{\infty} \mathrm{d}v \frac{f_M v^6}{\nu_d} \left(A_1 + \frac{m v^2}{2T} A_2 \right)}_{=c} \times \underbrace{\int_{1/B_0^{\max}}^{1/B_0^{\min}} \mathrm{d}\eta \frac{n^2 |H_n^2|}{\eta I}}_{=d}, \tag{3.1}$$

is compared to the result of Shaing given by Eq. (7) of Ref. [3]. Equation (3.1) is identically the same as the result of Ref. [10] (see this reference for the notation) if one retains in the result of [10] only the contribution of toroidally trapped particles, the only class of trapped particles remaining in a tokamak with perturbations which are small enough to avoid particle blocking by the perturbation field, see first condition in (2.89). A re-derivation of Shaing's formula is presented in Appendix A.2. In order to facilitate the comparison, the expression (3.1) is split into four factors which are inspected

independently. Factor a can be transferred to Shaing's notation as follows,

$$a = \left(\frac{\mathrm{d}\psi_{\mathrm{pol}}}{\mathrm{d}r}\right)^2 = \left(\frac{\mathrm{d}\hat{V}}{\mathrm{d}r}\chi'\right)^2 = \left(\frac{S\chi'}{4\pi^2}\right)^2, \tag{3.2}$$

where the prime denotes $\mathrm{d}/\mathrm{d}\hat{V}$, the flux surface label $\hat{V} = V/4\pi^2$ is the normalized volume enclosed by the flux surface, $\psi_{\mathrm{pol}} = \chi$ is the poloidal flux normalized by 2π and $S = \mathrm{d}V/\mathrm{d}r$ is the flux surface area (see, e.g., Eq. (28) of Ref. [10]). Using the definition of the effective radius, i.e. $\langle|\nabla r_0|\rangle = 1$, the large aspect ratio limit of factor b is given by

$$b = \left(\int_0^{2\pi} \frac{\mathrm{d}\vartheta}{B_0^2}|\nabla r_0|\right)^{-1} = \left(\int_0^{2\pi} \frac{\mathrm{d}\vartheta}{B_0^2}\right)^{-1} = \frac{\hat{B}_0^2}{2\pi}, \tag{3.3}$$

where $B_0 = \hat{B}_0(1 - \varepsilon_t \cos\vartheta)$ and ε_t is the inverse aspect ratio. The quantity c is transformed to

$$\begin{aligned} c &= \frac{N}{2\pi^{3/2}}\frac{v_T^4}{\nu_t}\int_0^\infty \mathrm{d}z e^{-z} z^{5/2}\frac{\nu_t}{\nu_d}\frac{S}{4\pi^2}\left[\left(\frac{p'}{p} + \frac{e\Phi'}{T}\right) + \left(z - \frac{5}{2}\right)\frac{T'}{T}\right] \\ &= \frac{2N}{\pi^{3/2}}\frac{v_T^4}{\nu_t}\frac{S}{4\pi^2}\left[\eta_1\left(\frac{p'}{p} + \frac{e\Phi'}{T}\right) + \eta_2\frac{T'}{T}\right], \end{aligned} \tag{3.4}$$

where $\eta_j = (1/2)\int_0^\infty \mathrm{d}z e^{-z} z^{5/2}(z - 5/2)^{j-1}(\nu_t/\nu_D)$.
For the transformation of factor d to the form used by Shaing, the adiabatic invariant η is replaced by the pitch-angle parameter κ^2 (see, e.g., Eq. (7.25) of Ref. [21]),

$$\kappa^2 = \frac{1 - \tilde{\eta}(1 - \varepsilon)}{2\varepsilon\tilde{\eta}}, \qquad \tilde{\eta} = \eta\hat{B}_0, \tag{3.5}$$

which can be used to rewrite the absolute value of the parallel velocity as

$$|v_\parallel| = v\sqrt{1 - \eta B_0} = v\sqrt{2\tilde{\eta}\varepsilon}\sqrt{\kappa^2 - \sin^2\frac{\vartheta}{2}}. \tag{3.6}$$

Using the integral substitution $\kappa\sin x = \sin(\vartheta/2)$ and the relation $\kappa_{\max} = \sin(\vartheta_{\max}/2)$, the quantities I and H_n are evaluated in the large aspect ratio

limit as,

$$I = \int_{\vartheta_{\min}}^{\vartheta_{\max}} \frac{\mathrm{d}\vartheta}{B_0^2}\sqrt{1-\eta B_0} \;=\; \frac{4\sqrt{2\varepsilon}}{\hat{B}_0^2}\left[E(\kappa)-(1-\kappa^2)K(\kappa)\right] \tag{3.7}$$

and

$$H_n = \int_{\vartheta_{\min}}^{\vartheta_{\max}} \frac{\mathrm{d}\vartheta}{B_0^3}\sqrt{1-\eta B_0}\,(4-\eta B_0)\,\tilde{B}_n(\vartheta) \;=\; \frac{3\sqrt{2\varepsilon}}{\hat{B}_0^3}\int_{\vartheta_{\min}}^{\vartheta_{\max}} \sqrt{\kappa^2-\sin^2\frac{\vartheta}{2}}\,\tilde{B}_n(\vartheta), \tag{3.8}$$

respectively, where $\tilde{B}_n(\vartheta) = -\hat{B}_0(A_n(\vartheta) - iB_n(\vartheta))$. The square of its absolute value $|H_n|^2 = H_n H_n^*$ is given by

$$\begin{aligned}
|H_n|^2 &= \frac{18\varepsilon}{\hat{B}_0^4}\int_{\vartheta_{\min}}^{\vartheta_{\max}}\mathrm{d}\vartheta\int_{\vartheta_{\min}}^{\vartheta_{\max}}\mathrm{d}\vartheta'\sqrt{\kappa^2-\sin^2\frac{\vartheta}{2}}\sqrt{\kappa^2-\sin^2\frac{\vartheta'}{2}}\,\times \\
&\quad\times \underbrace{\left(A_n(\vartheta)-iB_n(\vartheta)\right)\left(A_n(\vartheta')+iB_n(\vartheta')\right)}_{=A_n(\vartheta)A_n(\vartheta')+B_n(\vartheta)B_n(\vartheta')+iB_n(\vartheta')A_n(\vartheta)-iB_n(\vartheta)A_n(\vartheta')} \\
&= \frac{18\varepsilon}{\hat{B}_0^4}\left[\left(\int_{\vartheta_{\min}}^{\vartheta_{\max}}\mathrm{d}\vartheta A_n(\vartheta)\sqrt{\kappa^2-\sin^2\frac{\vartheta}{2}}\right)^2+\left(\int_{\vartheta_{\min}}^{\vartheta_{\max}}\mathrm{d}\vartheta B_n(\vartheta)\sqrt{\kappa^2-\sin^2\frac{\vartheta}{2}}\right)^2\right],
\end{aligned} \tag{3.9}$$

where the complex part cancels after the integration over ϑ, ϑ'. The quantity d is eventually given by

$$\begin{aligned}
d &= n^2\frac{9\varepsilon^{3/2}}{\sqrt{2}\hat{B}_0^2}\int_0^1 \mathrm{d}\kappa^2\left[E(\kappa)-(1-\kappa^2)K(\kappa)\right]^{-1}\times \\
&\quad\times\left[\left(\int_{\vartheta_{\min}}^{\vartheta_{\max}}\mathrm{d}\vartheta A_n(\vartheta)\sqrt{\kappa^2-\sin^2\frac{\vartheta}{2}}\right)^2+\left(\int_{\vartheta_{\min}}^{\vartheta_{\max}}\mathrm{d}\vartheta B_n(\vartheta)\sqrt{\kappa^2-\sin^2\frac{\vartheta}{2}}\right)^2\right].
\end{aligned} \tag{3.10}$$

The large aspect ratio limit of the particle flux in the $1/\nu$ regime is then

$$\Gamma^{\mathrm{NA}} = -N\frac{\varepsilon^{3/2}}{4\sqrt{2}\pi^{3/2}}\left(\frac{mc}{e\chi'}\right)^2\frac{4\pi^2}{S}\frac{v_T^4}{\nu_t}\int\limits_0^1\frac{\mathrm{d}\kappa^2}{[E(\kappa)-(1-\kappa^2)K(\kappa)]}\sum_{n=0}^{\infty}n^2\times$$
$$\times\left[\left(\int\limits_{\vartheta_{\min}}^{\vartheta_{\max}}\mathrm{d}\vartheta A_n(\vartheta)\sqrt{\kappa^2-\sin^2\frac{\vartheta}{2}}\right)^2+\left(\int\limits_{\vartheta_{\min}}^{\vartheta_{\max}}\mathrm{d}\vartheta B_n(\vartheta)\sqrt{\kappa^2-\sin^2\frac{\vartheta}{2}}\right)^2\right]\times$$
$$\times\left[\eta_1\left(\frac{p'}{p}+\frac{e\Phi'}{T}\right)+\eta_2\frac{T'}{T}\right]. \tag{3.11}$$

If one considers that the definition of Γ^{NA} differs from Γ^{Shaing} by

$$\Gamma^{\mathrm{Shaing}} = \langle n\mathbf{V}\cdot\nabla\hat{V}\rangle \;=\; \langle n\mathbf{V}\cdot\nabla r\rangle\frac{\mathrm{d}\hat{V}}{\mathrm{d}r} \;=\; \Gamma^{\mathrm{NA}}\frac{S}{4\pi^2}, \tag{3.12}$$

one finds that Eq. (3.11) agrees with Eq. (7) of Ref. [3].

3.2 Numerical benchmarking results

For benchmarking, a tokamak configuration with circular cross-section and aspect ratio $A = 3.8$ is used. The results for the full linearized collision model correspond here to the ion component if not otherwise stated. The perturbation field is taken in the form of a single harmonic,

$$\delta B = \varepsilon_M B_0(r,\vartheta)\cos(m\vartheta + n\varphi). \tag{3.13}$$

Since transport coefficients have a simple, quadratic dependence on ε_M, this quantity has been set to 1 in all plots below. In cases where non-linear models are involved such as NEO [10] and DKES [6], results are obtained for $\varepsilon_M = 10^{-3}$ and are then rescaled.

In Fig. 3.1 the dependence of the effective field ripple $\varepsilon_{\mathrm{eff}}^{3/2}$ on the normalized toroidal flux $s = \psi_{\mathrm{tor}}/\psi_{\mathrm{tor}}^a$ is shown, where ψ_{tor}^a is the toroidal flux at the outermost flux surface. The effective field ripple determines the particle

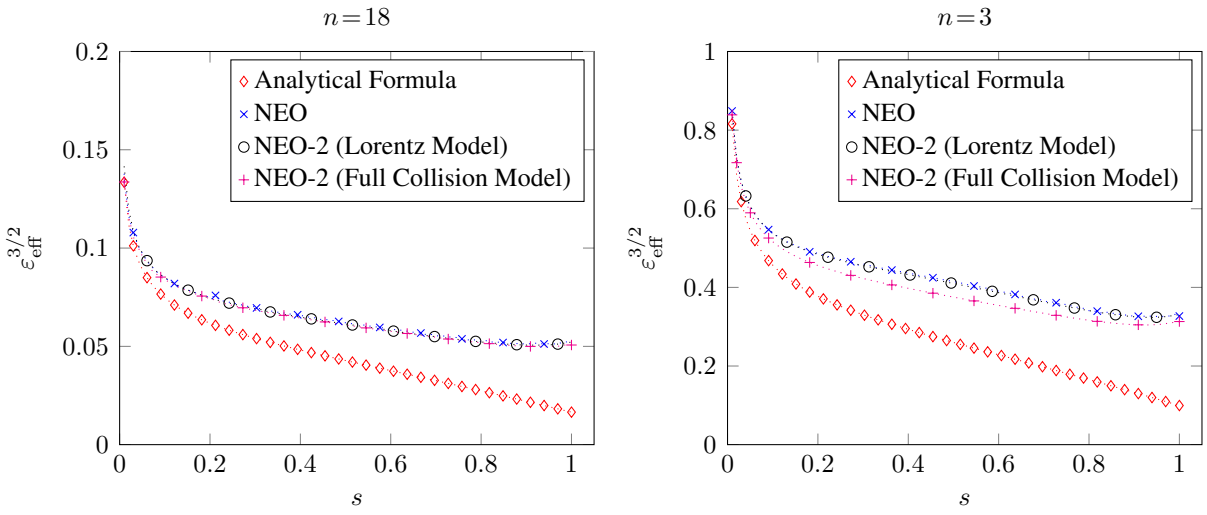

Figure 3.1: Effective ripple dependence on the normalized toroidal flux s for mode numbers $(m, n) = (0, 3)$ (left) and $(m, n) = (0, 18)$ (right) from the analytical par-axial approximation ($\Diamond$), NEO [10] ($\times$) and NEO-2 with Lorentz model ($\circ$) and full collision model ($+$).

flux density in the $1/\nu$ regime for the Lorentz collision model as follows [10],

$$\Gamma^{NA} = -\frac{\sqrt{8}}{9\pi^{3/2}} \frac{n_\alpha v_T^2 \rho_L^2}{R^2} \varepsilon_{\text{eff}}^{3/2} \int_0^\infty \frac{\mathrm{d}z \mathrm{e}^{-z} z^{5/2}}{\nu} \left(A_1 + A_2 z\right), \tag{3.14}$$

where $\nu = \nu_D/2$ and ν_D is the deflection frequency defined in (3.45) of Ref. [21]. The comparison of the quasilinear model (NEO-2) to the non-linear model (NEO [10]), which serves here as a benchmark, shows that even for large values of s, i.e., small aspect ratios (A=3.8 at the outer surface), the Lorentz model provides a good approximation for the transport. As one can expect, due to the assumption of small aspect ratio, the analytical results of Ref. [36] agree well with numerical results only in the par-axial region.

Results of benchmarking with the DKES code [6] are presented in Fig. 3.2. There scans over the collisionality parameter $\nu^* = 2\nu q R v_T^{-1}$ of the diffusion coefficient D_{11} normalized to the mono-energetic plateau diffusion coefficient,

$$D_p = \frac{\pi q v_T \rho_L^2}{16 R}, \tag{3.15}$$

are shown for various perturbation modes and for various radial electric fields given in terms of toroidal Mach numbers (normalized toroidal rotation velocity values) $M_t = \Omega_{tE} R v_T^{-1}$. For large scale perturbations ($n = 1$) and relatively slow toroidal rotation, the sequence of transport regimes realized with decreasing plasma collisionality ν^* consists of the Pfirsch-Schlüter, the plateau, the $1/\nu$ and the $\nu - \sqrt{\nu}$ regimes. The last two (long mean free path) regimes are well described by the bounce-averaged kinetic equation. This sequence is nearly the same as in stellarators [46] except for the absence of the retrapping-detrapping regime (ν-regime) which replaces the $\nu - \sqrt{\nu}$ regime at very low collisionality where the first one of conditions (2.90) is violated. Since the quasilinear approach assumes an infinitesimal perturbation amplitude ε_M, this transition is never realized here. In addition, those regimes, which are not described by the bounce-averaged theory (ripple-plateau and resonant diffusion), are clearly reproduced by both codes. The ripple-plateau regime is seen at intermediate collisionalities for the short scale perturbation field ($n = 18$) and the resonant diffusion limits the value of the transport coefficient from below at low collisionalities for fast enough rotation ($M_t = 2.8 \cdot 10^{-2}$) for all perturbations considered here. Finally, a significant increase in the non-ambipolar transport can be seen for the $(m, n) = (-3, 3)$ perturbation mode, which is nearly resonant for the actual safety factor value $q = 1.124$. The phase of such a perturbation stays almost unchanged along trapped particle orbits in contrast to non-resonant perturbations, which oscillate along these orbits and contribute to the bounce-averaged radial velocity of the trapped particles mainly near their banana tips. It should be noted that the discrepancies seen at high collisionality originate from the different treatment of the ambipolar transport in the two codes. Since DKES solves a general nonlinear problem, the contribution of the non-axisymmetric perturbation magnetic field to the transport coefficient D_{11} has been computed as a difference between these coefficients for the perturbed and for the unperturbed fields. This difference includes also the modification of the ambipolar transport, which would vanish if the collision model would conserve the momentum. In turn, such a modification is excluded from the NEO-2 result. Some minor discrepancies can also be seen for the lowest collisionality values

computed by DKES where the convergence of the code is at its limit (such low collisionalities are usually of no practical interest).

Results of the computation with the full linearized collision operator and the comparison to the universal formula of Shaing et al [3] are shown in Fig. 3.3. The collision frequency is from now on set to $\nu = 32\sqrt{\pi}ne^4\Lambda(3m^2v_T^3)^{-1}$. For this purpose a variant of the universal formula of Ref. [3] excluding the possibility of a collisionless retrapping-detrapping regime or a superbanana regime, as defined in Appendix B of Ref. [3], has been modified by using a more accurate expression for the kernel in the $\nu - \sqrt{\nu}$ regime. This kernel has been extracted analogously from the expression for the particle flux given by Eq. (29) of Ref. [54], which includes the complete pitch-angle dependence. Furthermore, the expression for the estimate of the collisional boundary layer width, Eq. (14) of Ref. [3], has been replaced everywhere by

$$\left(\Delta\kappa^2\right)_{\text{new}} = \left[\frac{\nu_{*d}/(1+\nu_{*d})}{\ln(16/\sqrt{\nu_{*d}/(1+\nu_{*d})})}\right]^{1/2}. \tag{3.16}$$

This guarantees that the universal formula of Ref. [3] is well defined over the whole collisionality range and has a smooth transition from the $1/\nu$ to the $\nu - \sqrt{\nu}$ regime. As shown in Fig. 3.3, the universal formula approximates the results from the full collision model unless the electric field or the collisionality exceeds a certain value. At relatively high collisionality NEO-2 results agree with the value of the ripple plateau coefficient [17],

$$D_{rp} = \frac{\sqrt{\pi}nq^2A^2v_T\rho_L^2\varepsilon_M^2}{4R}. \tag{3.17}$$

At low collisionality and high electric fields, the resonant diffusion regime [56] is seen. For $n = 18$ and the highest electric field few multiple bounce resonances contribute to the resonant diffusion simultaneously, and the result formally agrees with the stochastic diffusion coefficient [57] (it coincides with the ripple plateau coefficient). It can be seen that the "off-set" velocity coefficient k_{NA} tends to zero in the collisional case and has a rather peculiar behavior in the resonant diffusion regime. It should be noted that in the res-

onant diffusion regime not only trapped, but also passing particles contribute to the non-ambipolar transport (via "transit and drift" resonance [18]). The evaluation of this contribution requires the knowledge of the axisymmetric distribution function f_{10} (non-trivial in the passing region and the trapped-passing boundary layer) which enters Eq. (2.151) via the mirroring force.

Furthermore, the normalized ion and electron diffusion coefficients are shown for $E_r = 0$ in Fig. 3.4. The principal difference here is the absence of an approximate momentum conservation within a given species for electrons. The extension of the ripple plateau regime into the Pfirsch-Schlüter regime for ions (see also Ref. [18]) agrees with the MHD expression for the non-ambipolar diffusion coefficient due to TF ripples. For comparison, the flux surface averaged particle flux in the Pfirsch-Schlüter regime has been evaluated from the expression for the neoclassical toroidal plasma viscosity, Eq. (50) of Ref. [18], using the flux-force relation [37]. For this, the poloidal and toroidal components of the fluid velocity $\mathbf{V}$ and the heat flux $\mathbf{q}$ are rewritten in terms of thermodynamic forces. The fluid velocity and heat flux perpendicular to the magnetic flux surface are given by (2.15) and

$$\mathbf{q}_\perp = \frac{5p_i c}{2e_i B}\mathbf{h} \times \nabla T_i, \tag{3.18}$$

respectively. Furthermore, it is utilized that the first order (in Larmor radius expansion) fluid velocity and heat flux are divergence free, i.e., $\nabla \cdot \mathbf{V} = 0$ and $\nabla \cdot \mathbf{q} = 0$ (see, e.g., Ref. [21]). The resulting relation can be further simplified in case of ions in a pure plasma, where the flux surface averaged parallel heat flux $\langle q_{i\parallel} B\rangle$ is vanishingly small [21], and the diffusion coefficient corresponding to A_1 for the model magnetic field is obtained as follows,

$$D_{PS}^{NA} = \frac{3\mu_{i1}}{8}\frac{n^2 q^2 A^2 v_T^2 \rho_L^2 \tau_{ii}\varepsilon_M^2}{R^2} \sim \frac{n v_T \tau_i}{R} D_{rp}, \tag{3.19}$$

where $\mu_{i1} = 1.365$ (see Ref. [37]) and $\tau_{ii} = 3m_i^2 v_T^3 (16\sqrt{\pi} n_i e_i^2 \Lambda)^{-1}$ is the ion collision time. This result is identically the same as the result, which follows from the expression for the rotation slowing down rate in the generic

equation (85) of Ref. [58]. This expression becomes valid if the mean free path length, $v_T\tau_i$ is smaller than the toroidal ripple length Rn^{-1} what means higher collisionalities than needed for the onset of the axisymmetric Pfirsch-Schlüter transport regime. Note that in this plot, the normalizing mono-energetic plateau coefficient (3.15) for electrons is by square root of mass ratio smaller than for ions.

Finally, the comparison of NEO-2 results with the full collision operator in the superbanana plateau regime to the respective asymptotic formula of Shaing et al [59, 3] is shown in Fig. 3.5. At low collisionalities NEO-2 approaches the asymptotical value of the diffusion coefficient for the superbanana plateau for both signs of the radial electric field. The actual magnitude of the superbanana plateau coefficient is different for different signs of the radial electric field because the shape of the velocity space resonant curve (which is responsible for the formation of the superbanana plateau) depends on this sign [59].

3.3 Summary

The NEO-2 results shown in Section 3.2 are summarized in Figure 3.6 where the numerically evaluated non-axisymmetric ion transport coefficient D_{11}^{NA} is compared to asymptotical models for a tokamak with small amplitude magnetic perturbations. Non-ambipolar radial particle fluxes determined by D_{11}^{NA} and D_{12}^{NA} are responsible in tokamaks for the neoclassical toroidal viscous torque which is directly related to these fluxes via the flux-force relation [37, 3, 2]. This example corresponds again to a tokamak with circular concentric flux surfaces and perturbation in the form of a single toroidal harmonic, $B(\vartheta,\varphi) = B_0(\vartheta)(1+\varepsilon_M\cos(n\varphi))$ where $\varepsilon_M = 10^{-3}$. The diffusion coefficient is shown in the normalized form, $\hat{D}_{11}^{*} = D_{11}^{\mathrm{NA}}D_p^{-1}$ where $D_p = \pi q v_T \rho_L^2/(16R)$ is the plateau diffusion coefficient and $\rho_L = v_T/\omega_c$ is the Larmor radius for the reference magnetic field, as function of the plasma collisionality parameter $\nu_f^* = 2qR_0 l_c^{-1}$ for a few distinct values of the radial electric field specified via the toroidal Mach number $M_t = R_0\Omega_{tE}/v_T$ where Ω_{tE} is the toroidal $\mathbf{E}\times\mathbf{B}$ rotation frequency determined by the first term

in Eq. (2.147). Here, $l_c = v_T \tau_\alpha$ denotes the mean free path and τ_α is given by (2.201). Results correspond to a flux surface with aspect ratio $A = 10$ and toroidal harmonic number $n = 3$. The toroidal rotation due to the magnetic drift has been set to zero in (2.147) for all Mach numbers except $M_t = 10^{-5}$ while for $M_t = 10^{-5}$ this drift has been included for the ion temperature $T_i = 6.5 e_i \psi_{\mathrm{tor}} |\Omega_{tE}| / c$, where ψ_{tor} is the toroidal flux. Asymptotical models used for the comparison are indicated in the caption. It can be seen that NEO-2 accurately reproduces all asymptotical regimes in their validity domains. In particular, collisionless plateau diffusion, which corresponds at low collisionalities to the resonant diffusion regime at $M_t \geq 2.8 \cdot 10^{-2}$ and to the superbanana-plateau regime at $M_t = 10^{-5}$, is well resolved. The perturbed distribution in these regimes is highly localized around resonant curves in velocity space what presents a significant numerical difficulty in case of non-adaptive velocity space discretization.

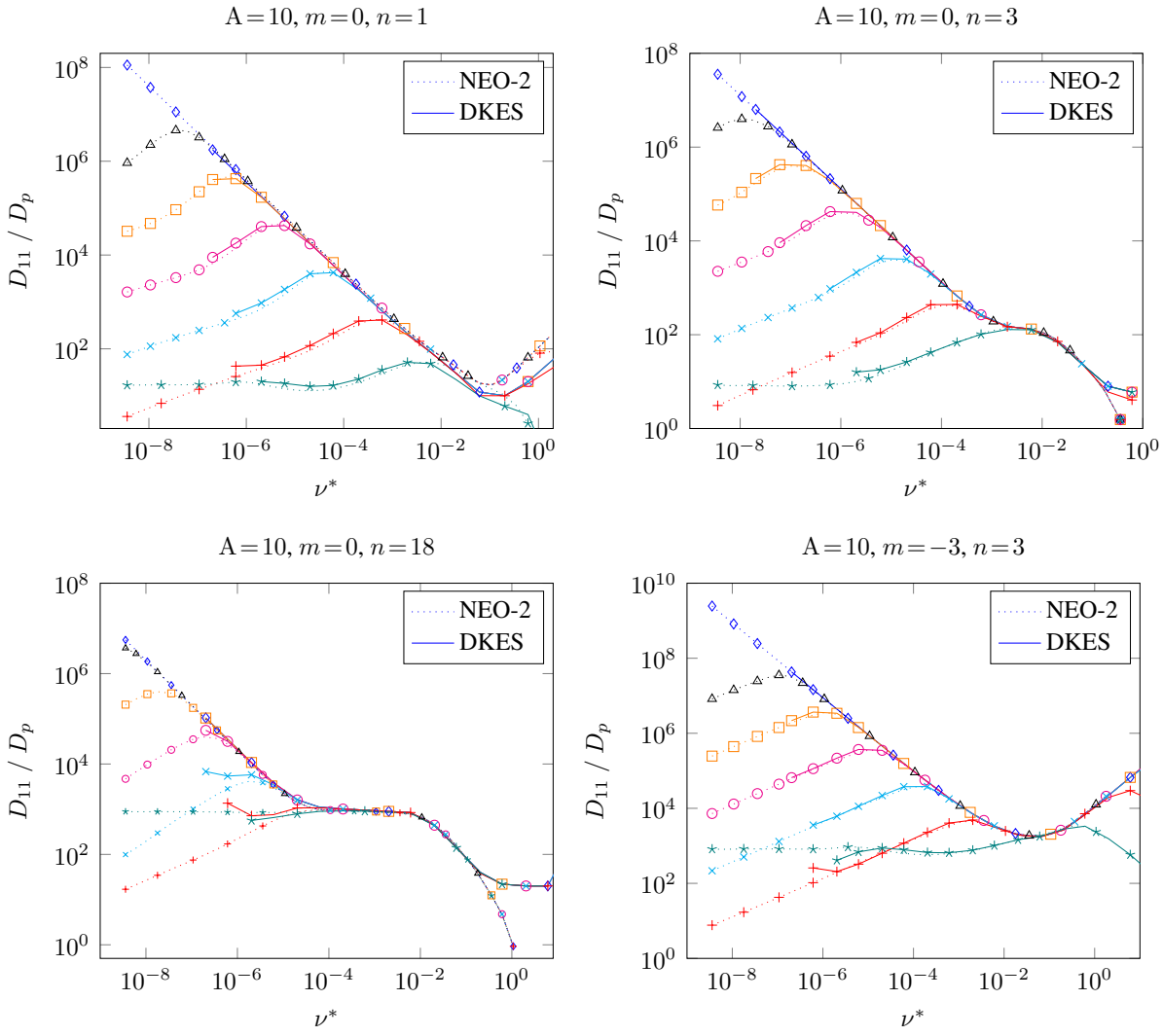

Figure 3.2: Normalized coefficient $D_{11}D_p^{-1}$ from NEO-2 (Lorentz collision model) and DKES [6] as a function of collisionality ν^* for various perturbation modes and toroidal Mach numbers $M_t = 0$ ($\Diamond$), $2.8 \cdot 10^{-7}$ ($\triangle$), $2.8 \cdot 10^{-6}$ ($\square$), $2.8 \cdot 10^{-5}$ ($\circ$), $2.8 \cdot 10^{-4}$ ($\times$), $2.8 \cdot 10^{-3}$ ($+$) and $2.8 \cdot 10^{-2}$ ($\star$). The toroidal rotation frequency due to magnetic drift is set to zero for the four cases shown above. Aspect ratio and mode numbers are indicated in the titles.

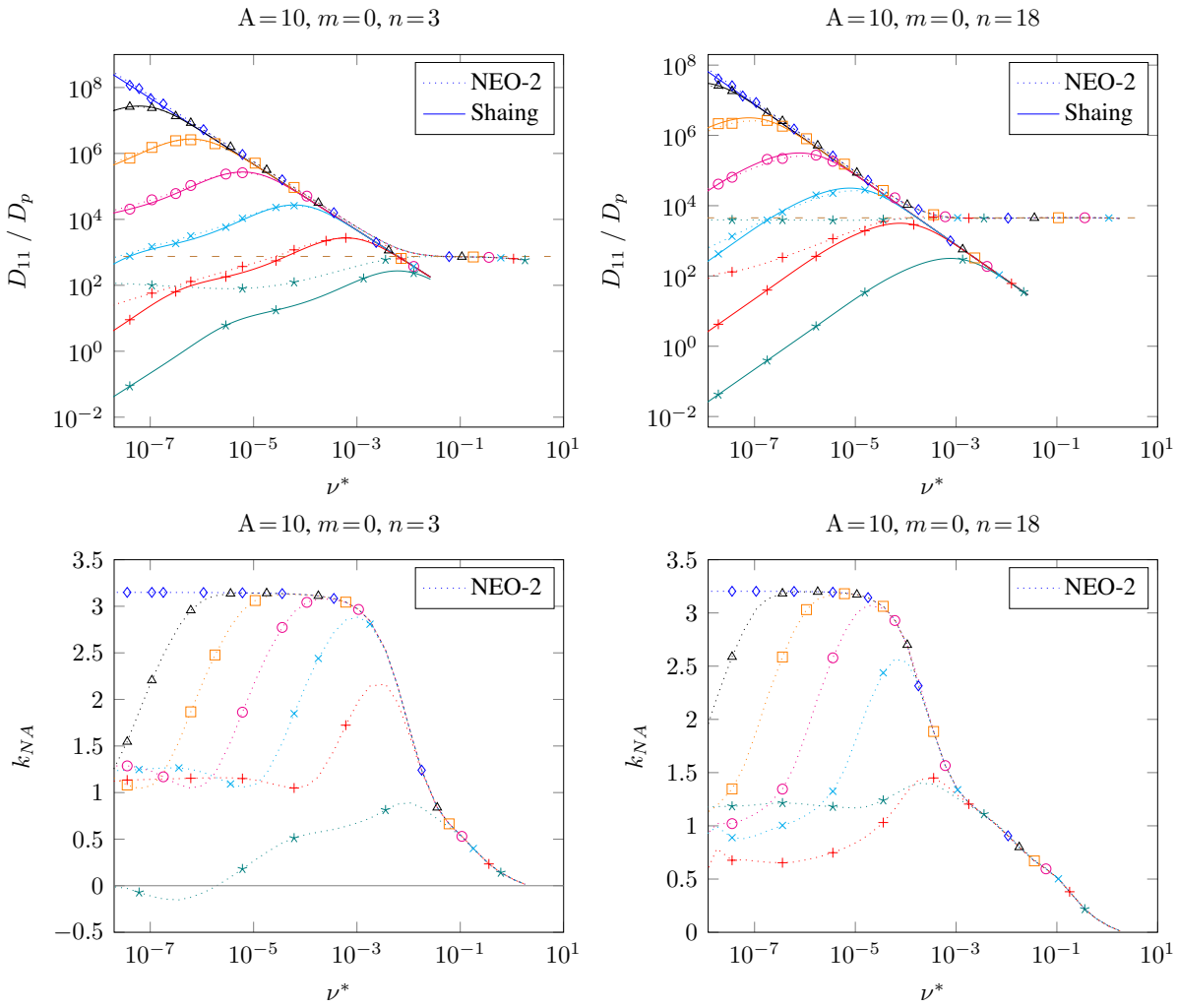

Figure 3.3: Normalized coefficient $D_{11}D_p^{-1}$ from NEO-2 (full collision model) and bounce-averaged model of Shaing [3] (upper panel) and "offset" rotation coefficient k_{NA} (2.88) from NEO-2 (lower panel) as functions of collisionality ν^* for various perturbation modes and toroidal Mach numbers $M_t = 0$ ($\Diamond$), $2.8 \cdot 10^{-7}$ ($\triangle$), $2.8 \cdot 10^{-6}$ ($\square$), $2.8 \cdot 10^{-5}$ ($\circ$), $2.8 \cdot 10^{-4}$ ($\times$), $2.8 \cdot 10^{-3}$ ($+$) and $2.8 \cdot 10^{-2}$ ($\star$). The toroidal rotation frequency due to magnetic drift is set to zero for the four cases shown above. Curves for the bounce-averaged model are shown up to the boundary with a usual plateau regime, $\nu^*_{TOK} = \nu^* A^{3/2} = 1$. Aspect ratio and mode numbers are indicated in the titles. The ripple-plateau diffusion coefficient (3.17) is shown with a dashed line at the upper panel.

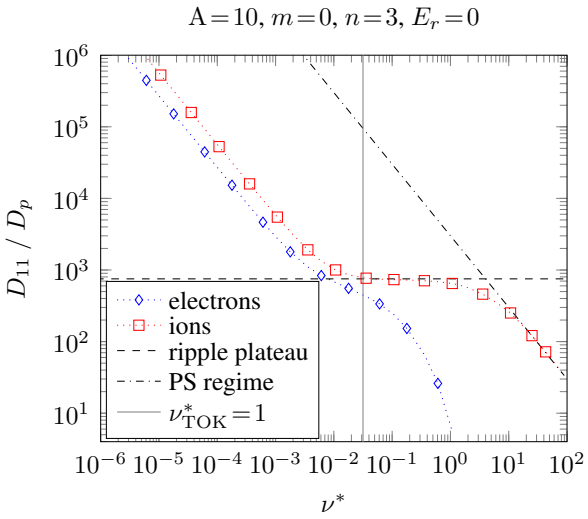

Figure 3.4: Normalized diffusion coefficients, $D_{11}D_p^{-1}$, for electrons ($\Diamond$) and ions ($\Box$). Dashed line shows the ripple plateau coefficient, dash-dotted line shows the asymptotical coefficient for the Pfirsch-Schlüter regime[58, 18] and solid line shows the axisymmetric plateau boundary.

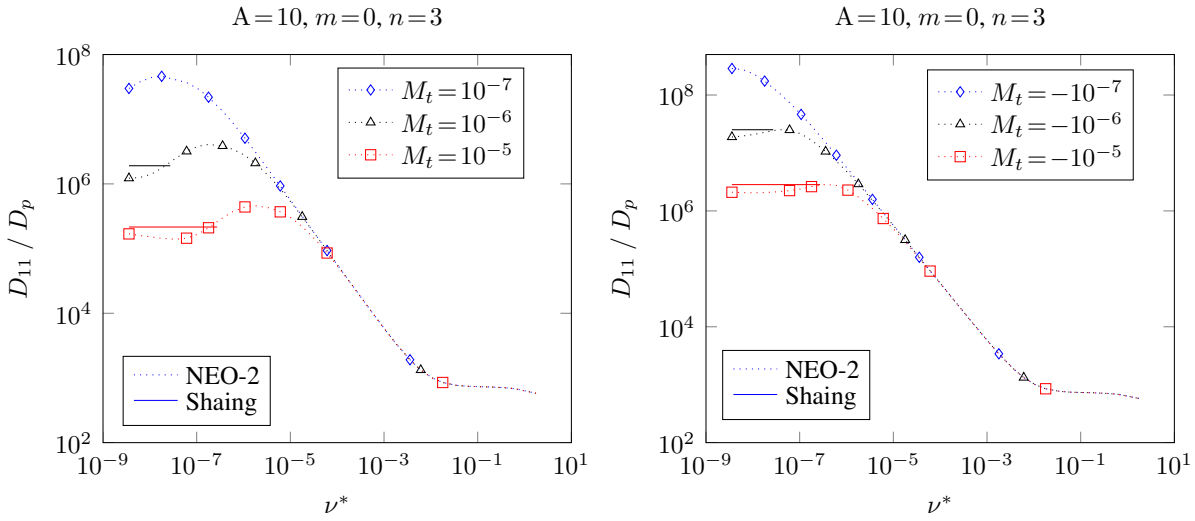

Figure 3.5: Normalized coefficient $D_{11}D_p^{-1}$ from NEO-2 (full collision model) and asymptotical formula of Shaing [3] as a function of collisionality ν^* for various toroidal Mach numbers. The reference toroidal rotation frequency due to magnetic drift, $\Omega_{tB}^{\mathrm{ref}} = cT_\alpha \left(e_\alpha \psi_{\mathrm{tor}}^a\right)^{-1}$, is set for all curves to $\Omega_{tB}^{\mathrm{ref}} = |\Omega_{tE}|$. Curves for the asymptotical formula are shown up to the boundary specified by the condition given in the paragraph before Eq. (28) of Ref. [3]. Aspect ratio and mode number are indicated in the title.

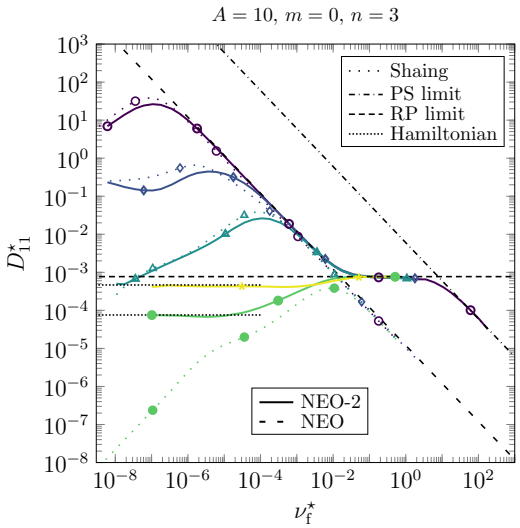

Figure 3.6: Normalized diffusion coefficient $\hat{D}_{11}^{\mathrm{NA}}$ from NEO-2 (solid line) and bounce-averaged model of Shaing [3] (loosely dotted line) as functions of collisionality ν^* for various toroidal Mach numbers $M_t = 2.8 \cdot 10^{-7}$ ($\circ$), 10^{-5} ($\Diamond$), $2.8 \cdot 10^{-4}$ ($\triangle$), $2.8 \cdot 10^{-2}$ ($\bullet$) and $6 \cdot 10^{-2}$ ($\star$). The collisionless limits for the $1/\nu$ regime (loosely dashed line) and the resonant diffusion regime (densely dotted line) are computed by NEO [10] and a semi-analytical model based on a Hamiltonian approach [19], respectively. The diffusion coefficients for the ripple-plateau regime [17] and the Pfirsch-Schlüter regime [58, 18] are shown with a densely dashed line and a dash-dotted line, respectively.

Chapter 4

Effect of 3D magnetic perturbations on the plasma rotation in ASDEX Upgrade

In this chapter the neoclassical toroidal viscous torque is evaluated numerically for an ASDEX Upgrade discharge using the codes NEO-2 [2] and SFINCS [13], as well as a discussion of the torque balance in this discharge is given. The results presented in this chapter have been published in the following journal article [60] and conference proceeding [61]:

- A. F. Martitsch, S. V. Kasilov, W. Kernbichler, G. Kapper, C. G. Albert, M. F. Heyn, H. M. Smith, E. Strumberger, S. Fietz, W. Suttrop, M. Landreman, the ASDEX Upgrade Team and the EUROfusion MST1 Team. Effect of 3D magnetic perturbations on the plasma rotation in ASDEX Upgrade. *Plasma Phys. Control. Fusion*, 58(7):074007, 2016.

- A. F. Martitsch, S. V. Kasilov, W. Kernbichler, M. F. Heyn, E. Strumberger, S. Fietz, W. Suttrop, A. Kirk, the ASDEX Upgrade Team and the EUROfusion MST1 Team. Evaluation of the neoclassical toroidal viscous torque in ASDEX Upgrade. In *42nd EPS Conference on Plasma Physics*, volume 39E, page P1.146, Lisbon, Portugal, 2015. European Physical Society.

4.1 Introduction

Stability and transport of tokamak plasmas are strongly influenced by toroidal plasma rotation. The knowledge of various mechanisms and corresponding torques driving the toroidal plasma rotation is therefore crucial for operation control of these fusion experiments. Dedicated experimental studies at NSTX [62], DIII-D [63] and JET [64, 65] have shown a strong dependence of the plasma rotation on non-axisymmetric magnetic perturbations (e.g., from coils for mitigation of edge localized modes (ELMs), from toroidal field (TF) coil ripple and from error fields). The observed changes in plasma rotation were in agreement with theoretical predictions for the torque produced by non-resonant non-axisymmetric magnetic perturbations, which are based on analytical and semi-analytical approaches [3, 4, 5]. The non-resonant torque produced by such perturbations is often expressed through a viscous force, terming the phenomenon also as neoclassical toroidal plasma viscosity (NTV). In this thesis the NTV torque is evaluated numerically for ASDEX Upgrade equilibria using the drift kinetic equation (DKE) solver NEO-2 [2, 1] and the results are compared to analytical models [3, 17] and a semi-analytical approach based on Hamiltonian theory [19], as well as to results from the DKE solver SFINCS [13].

Analytical and semi-analytical approaches presently used for the evaluation of the NTV torque [3, 4, 5] make simplifying assumptions concerning geometry and collision operators. A numerical approach without such simplifications is provided by the quasilinear version of the code NEO-2 [2]. In this code, the only assumption simplifying the general neoclassical ansatz for non-axisymmetric tori is that perturbations of the magnetic field are small enough such that the particle motion within perturbed flux surfaces is only weakly affected by the perturbation field. This reduces the "nonlinear" 4D problem, where all relevant toroidal Fourier modes of the perturbation field simultaneously affect the particle motion, to a set of uncoupled 3D problems. Those are solved for each toroidal Fourier mode separately and finally result in independent contributions to the torque. Such a quasilinear approach is well justified in many circumstances but might be only marginally justified for

high toroidal mode numbers of the perturbation. In a previous study [2], the quasilinear version of the code NEO-2 has been benchmarked for a simplified tokamak geometry against various analytical models [3, 36, 54, 59, 18, 17], as well as the nonlinear codes DKES [6] and NEO [10]. Here, also the DKE solver SFINCS [13] is used for benchmarking of the ion contribution to the torque. The code SFINCS is not limited to small values of the perturbation amplitude because it solves the nonlinear problem pertinent to neoclassical stellarator transport. Computationally, this is a much more demanding task than solving the quasilinear problem. In contrast to the DKES code, which solves the reduced monoenergetic problem, SFINCS as NEO-2 uses the full linearized Coulomb collision operator.

A set of perturbed ASDEX Upgrade equilibria studied here has been computed by the ideal MHD equilibrium solver NEMEC [11, 66]. These equilibria include both, perturbations from the TF ripple and from ELM mitigation coils with different distribution of current values resulting in different perturbation field spectra in the ASDEX Upgrade shot #30835. Due to the strong shielding of resonant magnetic perturbations (RMPs) by plasma response currents in AUG [12], magnetic fields computed within ideal MHD theory, where RMPs are shielded perfectly, provide a good approximation in a major part of the plasma volume except for narrow resonant layers around resonant rational flux surfaces.

Here, in order to identify various NTV regimes of importance for ASDEX Upgrade, comparisons of numerical results from NEO-2 and SFINCS with several analytical models and additional parameter scans have been undertaken. In addition, results for the integral torque are compared to the torque resulting from neutral beam injection (NBI) computed by the code NUBEAM [67] and the overall torque balance is discussed.

The structure of this chapter is as follows. In Section 4.2 the toroidal moment conservation equation and its simplified forms are introduced and basic definitions are given, e.g., expressions for the rotation velocity components and toroidal torque density in terms of plasma parameters and neoclassical transport coefficients. In Section 4.3 the NTV torque profiles computed by NEO-2 and SFINCS are shown for ASDEX Upgrade equilibria, as well

as a comparison to analytical and semi-analytical models is presented. In Section 4.4 additional momentum sources, which are not taken into account here, are discussed in order to stimulate further experiments and simulations, and finally in Section 4.5 the results are summarized.

4.2 Toroidal momentum conservation and neoclassical toroidal viscosity

In a tokamak plasma, charged particles and neutrals together with the electromagnetic field are represented by a coupled system, which can be characterized by the exact conservation law of the total toroidal momentum of particles and of the electromagnetic field. In a covariant notation this conservation law is given as (see, e.g., [2] for its toroidally averaged form),

$$\frac{\partial}{\partial t}P_\varphi + \left(\frac{\partial x^i}{\partial t}\right)_{\mathbf{r}} \frac{\partial}{\partial x^i}P_\varphi + \frac{1}{\sqrt{g}}\frac{\partial}{\partial x^i}\sqrt{g}\,\Pi^i_\varphi = 0, \tag{4.1}$$

where $\sqrt{g}$ is the metric determinant and x^i are some (generally time dependent) coordinates with rotational symmetry over the toroidal angle φ, such as cylindrical coordinates (R, φ, Z) or flux coordinates (r, ϑ, φ) associated with the unperturbed axisymmetric field, and $P_\varphi = \mathbf{P}\cdot\partial\mathbf{r}/\partial\varphi$ and $\Pi^i_\varphi = (\partial\mathbf{r}/\partial\varphi)\cdot\boldsymbol{\Pi}\cdot\nabla x^i$, are the toroidal co-variant components of the momentum density vector and the total stress tensor of particles and electromagnetic field respectively given by

$$\mathbf{P} = \sum_\alpha \mathbf{P}_{(\alpha)} + \frac{1}{c^2}\mathbf{S}, \qquad \boldsymbol{\Pi} = \sum_\alpha \boldsymbol{\Pi}_{(\alpha)} - \boldsymbol{\sigma}. \tag{4.2}$$

Here,

$$\mathbf{P}_{(\alpha)} = m_\alpha n_\alpha \mathbf{V}_\alpha, \;\; \boldsymbol{\Pi}_{(\alpha)} = m_\alpha n_\alpha \mathbf{V}_\alpha\mathbf{V}_\alpha + p_\alpha\mathbf{I} + \pi_\alpha \tag{4.3}$$

are the momentum density vector and the total stress tensor of particle species α, respectively, with pertinent mass m_α, density n_α, scalar pressure p_α, and viscous stress tensor π_α. Pointing flux $\mathbf{S}$ and Maxwell stress tensor

$\boldsymbol{\sigma}$ are respectively defined as

$$\mathbf{S} = \frac{c}{4\pi}\mathbf{E}\times\mathbf{B}, \qquad \boldsymbol{\sigma} = \frac{1}{4\pi}\left(\mathbf{E}\,\mathbf{E} - \frac{E^2}{2}\mathbf{I} + \mathbf{B}\,\mathbf{B} - \frac{B^2}{2}\mathbf{I}\right). \tag{4.4}$$

In the main plasma volume neoclassical "flux surface" averaging of (4.1) over unperturbed flux surfaces results in a one dimensional conservation law,

$$\frac{1}{S}\frac{\partial}{\partial t}S\left\langle P_\varphi\right\rangle + \frac{1}{S}\frac{\partial}{\partial r}S\left\langle \Pi^r_\varphi\right\rangle = 0, \tag{4.5}$$

where $\langle \ldots \rangle$ denotes the average, r is a flux surface label (effective radius) fixed by the condition $\langle|\nabla r|\rangle = 1$, and S is the (generally time dependent) flux surface area.

The exact equations (4.1) and (4.5) contain no volume source density. This means that the integral total momentum within the vacuum vessel can only be driven by sources located at the walls or outside the vessel. Since the Pointing flux is usually negligibly small, the toroidal momentum is approximately the same as the kinematic toroidal momentum of plasma particles and neutrals. However, the contribution of the electromagnetic field, $\boldsymbol{\sigma}$, to the total momentum flux density $\left\langle \Pi^r_\varphi\right\rangle$ is as important as the contributions by charged particles and neutrals, $\boldsymbol{\Pi}_{(\alpha)}$. In order to make equation (4.5) of practical use within a local 1D balance description, the nonlocal fluxes, which are not fully determined by local plasma parameters and a limited number of their derivatives, should be excluded from the total momentum flux $\left\langle \Pi^r_\varphi\right\rangle$ and turned into momentum sources (torque densities), which are described outside the closed set of balance equations. E.g., excluding the contribution of neutral particles, $\alpha = \mathrm{n}$, produced by NBI from the l.h.s. of (4.5), the pertinent torque density is obtained as

$$T^{\mathrm{NBI}}_\varphi = -\frac{1}{S}\frac{\partial}{\partial t}SP_{(\mathrm{n})\varphi} - \frac{1}{S}\frac{\partial}{\partial r}S\left\langle \Pi^r_{(\mathrm{n})\varphi}\right\rangle. \tag{4.6}$$

Formally the contributions from all external non-axisymmetric electromagnetic perturbations, including besides the static or slowly varying magnetic perturbations also the contribution from RF heating and current drive, can

be separated into the source term T_φ^{NA}. Generally, this separation is not so straightforward as (4.6), see, e.g., [2] for the case of non-resonant magnetic perturbations, and may even not always be meaningful in a general case (see discussion in Section 4.4). Thus, equation (4.5) turns into

$$\frac{1}{S}\frac{\partial}{\partial t}S\sum_\alpha m_\alpha \left\langle g_{\varphi\varphi} n_\alpha V_\alpha^\varphi \right\rangle + \frac{1}{S}\frac{\partial}{\partial r}S\left\langle \Pi^r_{[\mathrm{in}]\varphi}\right\rangle = T_\varphi^{\mathrm{NBI}} + T_\varphi^{\mathrm{NA}}, \tag{4.7}$$

where α denotes only plasma particles. The radial component of the total stress $\left\langle \Pi^r_{[\mathrm{in}]\varphi}\right\rangle$ (flux surface averaged radial flux density of the toroidal momentum) is the sum of the total stress from intrinsic turbulent modes (anomalous momentum flux density) and total axisymmetric stress including the contribution from the polarization current and a small contribution of axisymmetric neoclassical shear viscosity. In case of non-resonant external magnetic perturbations, T_φ^{NA} is directly linked through the flux-force relation to the non-ambipolar neoclassical particle flux densities $\Gamma_\alpha^{\mathrm{NA}}$ driven by these perturbations in a stationary radial electric field (see, e.g. [3, 2]),

$$T_\varphi^{\mathrm{NA}} = -\frac{1}{c}\sqrt{g}B^\vartheta \sum_\alpha e_\alpha \Gamma_\alpha^{\mathrm{NA}}. \tag{4.8}$$

Here, c is the speed of light, e_α is the charge of species α, and B^ϑ is the contra-variant magnetic field component linked to the poloidal flux ψ_{pol} by $\sqrt{g}B^\vartheta = \partial\psi_{\mathrm{pol}}/\partial r$. Torque produced by these thermal particle fluxes is called NTV torque. In presence of supra-thermal particle losses, the torque density (4.8) should include also the flux of these fast particles (see, e.g., [68, 69]). However, this type of flux cannot be described by the local neoclassical ansatz.

The non-ambipolar neoclassical particle flux densities are expressed through transport coefficients D_{ij}^{NA} and thermodynamic forces A_j,

$$\Gamma_\alpha^{\mathrm{NA}} = -n_\alpha \left(D_{11}^{\mathrm{NA}} A_1 + D_{12}^{\mathrm{NA}} A_2\right), \tag{4.9}$$

where the thermodynamic forces are specified by

$$\begin{aligned} A_1 &= \frac{1}{n_\alpha}\frac{\partial n_\alpha}{\partial r} - \frac{e_\alpha E_r}{T_\alpha} - \frac{3}{2T_\alpha}\frac{\partial T_\alpha}{\partial r}, \\ A_2 &= \frac{1}{T_\alpha}\frac{\partial T_\alpha}{\partial r}, \end{aligned} \tag{4.10}$$

with T_α and E_r being α species temperature and radial electric field, respectively. Thus, equations (4.8) and (4.9) reduce the problem to the evaluation of diffusion coefficients D_{ij}^{NA}, which are computed here numerically by NEO-2, SFINCS, and the Hamiltonian approach [19] using the perturbed equilibrium magnetic fields from the NEMEC code represented in Boozer coordinates (r, ϑ, φ). For the perturbed equilibria, these variables correspond to the perturbed magnetic field and are different from flux variables used in equations (4.1)-(4.7). In particular, φ is not an exact symmetry variable anymore. This difference, however, is small for weakly perturbed equilibria and can be ignored in (4.7) (see [2]). For evaluation of the analytical expressions of Shaing [3] magnetic fields have been converted from Boozer coordinates to Hamada coordinates. The radial electric field profile required for the forces (4.10) is calculated here from the toroidal rotation frequency of ions via the relation

$$\begin{aligned} V^\varphi &= \frac{c}{\sqrt{g}B^\vartheta}\left(E_r - \frac{1}{e_\mathrm{i} n_\mathrm{i}}\frac{\partial (n_\mathrm{i} T_\mathrm{i})}{\partial r}\right) + qV^\vartheta, \\ V^\vartheta &= \frac{c\,k\,B_\varphi}{e_\mathrm{i}\sqrt{g}\langle B^2\rangle}\frac{\partial T_\mathrm{i}}{\partial r}, \end{aligned} \tag{4.11}$$

where q is the safety factor. The coefficient $k = 5/2 - D_{32}/D_{31}$ is determined by the parallel ion flow obtained from the NEO-2 solution for the unperturbed, axisymmetric problem,

$$\begin{aligned} \langle V_{\parallel \mathrm{i}} B\rangle &= B_\varphi\left(V^\varphi - qV^\vartheta\right) + \frac{ckB_\varphi}{e_\mathrm{i}\sqrt{g}B^\vartheta}\frac{\partial T_\mathrm{i}}{\partial r} \\ &= -\left(D_{31}A_1 + D_{32}A_2\right). \end{aligned} \tag{4.12}$$

4.3 NTV torque in ASDEX-Upgrade

Evaluation of the NTV torque is performed here for a set of ASDEX Upgrade equilibria based on the shot #30835 ($B_t = -1.794$ T, $I_p = 0.8$ MA, $P_{\mathrm{heat}} = 9.753$ MW, $\nu^\star = 0.03$, $\kappa = 1.753$, $\delta_o = 0.151$, $\delta_u = 0.511$, H-mode). ASDEX Upgrade is equipped with 16 ELM mitigation coils, which form an upper and a lower ring each consisting of eight coils [70]. This setup allows for some control of the poloidal mode spectrum by varying the toroidal phase shift between the upper and lower coils $\Delta\phi_{\mathrm{ul}}$, which is also termed as varying the coil polarity. The NTV torque is computed here for the experimentally realized ELM mitigation coil polarity $\Delta\phi_{\mathrm{ul}} = 90°$ where good ELM mitigation has been achieved, as well as for a few simulated equilibria with other coil polarities. A simple (pure deuterium) plasma is assumed in this analysis. This assumption only weakly overestimates the ion density in case of high Z impurities and $Z_{\mathrm{eff}} \sim 1.7$. In Figure 4.1 the experimentally measured profiles of density n_{e}, temperatures T_{i} and T_{e}, toroidal ion rotation frequency V^φ, collisionality parameter $\nu^\star = 2\nu q R_0 v_T^{-1}$, and the resulting toroidal Mach number of the $\mathbf{E}\times\mathbf{B}$ rotation $M_t = cR_0E_r(v_T\sqrt{g}B^\vartheta)^{-1}$ as well as the safety factor for the corresponding shot are shown as functions of the normalized poloidal radius $\rho_{\mathrm{pol}} = (\psi_{\mathrm{pol}}/\psi^a_{\mathrm{pol}})^{1/2}$. The definition of the collisionality parameter differs from the standard definition $\nu^\star_{\mathrm{TOK}} = 2\nu q R_0 \epsilon_t^{-3/2} v_T^{-1}$ by a factor $2^{-1}\epsilon_t^{-3/2}$. Here, $\nu = 16\sqrt{\pi}n_\alpha e_\alpha^4 \Lambda (3m_\alpha^2 v_T^3)^{-1}$, Λ is the Coulomb logarithm, $v_T = (2T_\alpha/m_\alpha)^{1/2}$, ϵ_t is the inverse aspect ratio, R_0 is the mean major radius value at a given flux surface, $\psi_{\mathrm{pol}} = 0$ on the magnetic axis and ψ^a_{pol} is the poloidal flux value at the separatrix. The radial electric fields obtained from NEO-2 agree perfectly with those from SFINCS computations (not shown in this figure). Within this modeling effort of the NTV torque, magnetic perturbations due to both TF ripple (toroidal mode number $n = 16$) and ELM mitigation coils with various coil polarities in this shot ($n = 2$ with a minor contribution from $n = 6$), are studied (see Figure 4.2).

In Figure 4.3 radial profiles and scans over the normalized perpendicular adiabatic invariant $\eta = v_\perp^2 (v^2 B)^{-1}$ of the ion $\mathbf{E}\times\mathbf{B}$ drift frequency $\Omega_{tE} = M_t v_T R_0^{-1}$, bounce-averaged magnetic drift frequency $\langle\Omega_{tB}\rangle_{\mathrm{b}}$ (see def-

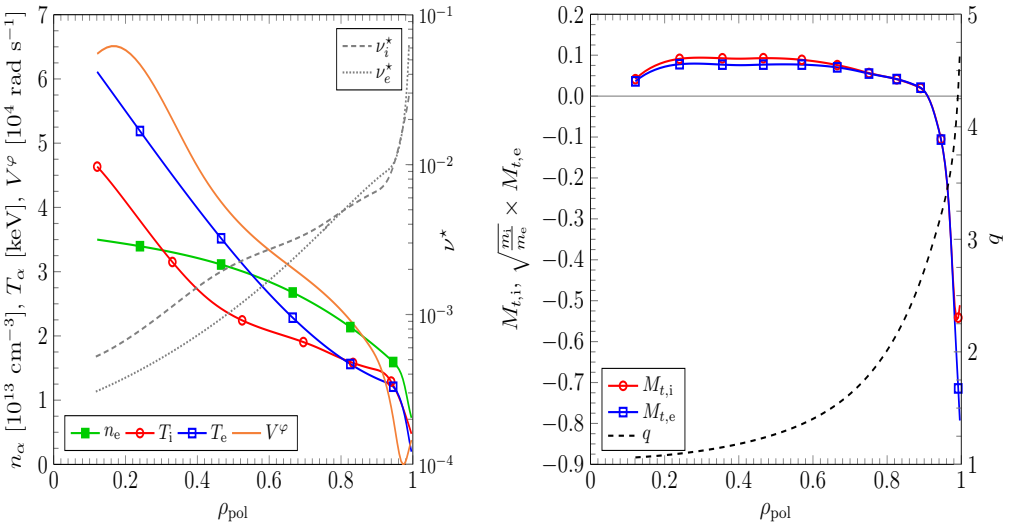

Figure 4.1: Radial profiles of density, temperatures, toroidal rotation frequency, collisionalities (left), toroidal Mach number and safety factor (right) for ASDEX Upgrade shot #30835 (with ELM mitigation coils switched on).

inition in (4.16)) and bounce frequency $\omega_{\rm b}$ are shown for various η-values and radial positions, respectively. Resonances between the different frequencies lead to the formation of resonant transport regimes, which are described by asymptotical formulas in the collisionless limit [17, 3, 18, 4]. The resonance condition for the superbanana-plateau (sb-p) regime [53, 19] is given by $\Omega_{tE} + \langle \Omega_{tB} \rangle_{\rm b} = 0$, whereas for drift-orbit resonances [17, 18, 4, 19] the condition $m_\vartheta \omega_{\rm b} + n(\Omega_{tE} + \langle \Omega_{tB} \rangle_{\rm b}) = 0$ must be fulfilled for trapped particles. Here, the bounce frequency mode number m_ϑ can take any positive or negative integer value. It can be seen that the sb-p resonance condition is fulfilled in the inner part of the plasma and in the vicinity of zero of the electric field where the contribution from the sb-p regime to the non-ambipolar particle fluxes is expected to be largest. Drift-orbit resonances can contribute to the non-ambipolar particle fluxes nearly over whole the radial domain, except for a certain region in the vicinity of the zero of the electric field. For sufficiently large values of m_ϑ drift-orbit resonances occur not only in the deeply trapped region but also in the vicinity of the trapped-passing boundary. This emphasizes the importance of a proper numerical discretization of the velocity

space in order to resolve the different resonant transport regimes.

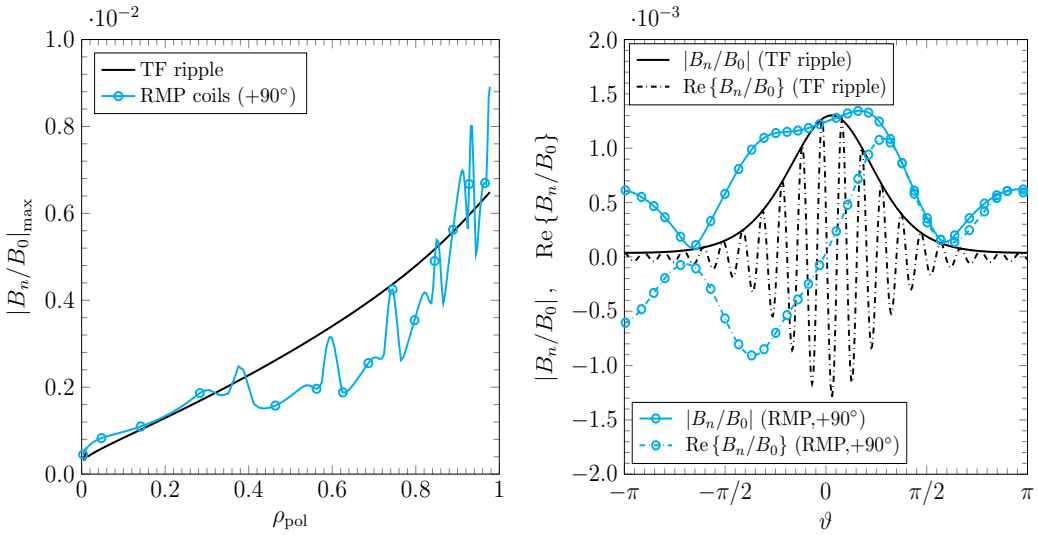

Figure 4.2: Left - radial profiles of the maximum value of the normalized perturbation field for the TF ripple and for RMP with 90° coil phase (see definition in Eq. (4.14)); right - Variation of the absolute value and real part of the normalized perturbation field along the field line for $\rho_{\mathrm{pol}} = 0.5$.

For the TF ripple a comparison of NEO-2 results with analytical estimates of the torque density and of the integral torque,

$$\left(T_\varphi^{\mathrm{NA}}\right)_{\mathrm{int}} = \int_{V(\rho_{\mathrm{pol}})} \mathrm{d}^3 r \; T_\varphi^{\mathrm{NA}}, \tag{4.13}$$

where $V(\rho_{\mathrm{pol}})$ is the volume limited by the flux surface with a given ρ_{pol}, is shown in Figure 4.4. In order to quantify the impact of nonlinear effects and to validate the quasilinear approach, the NTV torque density is also computed with the code SFINCS. It can be seen that the NTV torque acts in the direction opposite to the experimentally measured plasma rotation velocity and the integral torque computed by NEO-2 is about -0.6 Nm, whereas the SFINCS calculation predicts a value of -0.4 Nm. The NTV torque produced by TF ripples is mainly applied to ions and, in case of the quasilinear model, corresponds to the ripple-plateau regime [17] in a major part of the plasma volume. The difference between the NEO-2 result and the SFINCS result is about 30% for $\rho_{\mathrm{pol}} \leq 0.9$ and a rather large discrepancy is observed at

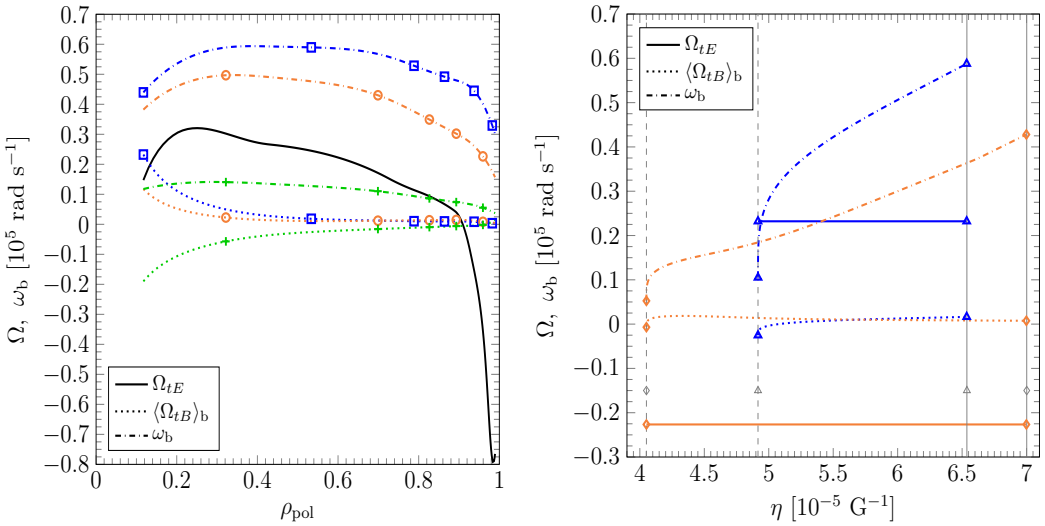

Figure 4.3: Left - radial profiles of the ion $\mathbf{E}\times\mathbf{B}$ drift frequency Ω_{tE}, bounce-averaged magnetic drift frequency $\langle\Omega_{tB}\rangle_b$ and bounce frequency ω_b in the deeply trapped ($\square$), trapped-passing boundary ($+$) and an intermediate ($\circ$) region. Right - drift and bounce frequencies as functions of the normalized perpendicular adiabatic invariant η at $\rho_{pol} = 0.57$ ($\triangle$) and $\rho_{pol} = 0.95$ ($\diamond$) for the trapped particle domain. The trapped-passing and deeply trapped boundaries are indicated by dashed and solid vertical lines, respectively.

outermost points with $\rho_{pol} > 0.9$. This correlates with the deviation from the quasilinear scaling of the NTV torque density, see Figure 4.5, and can be attributed to the onset of nonlinear transport due to locally trapped particles, which are blocked by the perturbation field. The respective quasilinear theory validity conditions (41) of Ref. [2] are clearly violated at outermost points and are marginally violated in the rest of the plasma volume. For the SFINCS calculation shown here, only the $\mathbf{E}\times\mathbf{B}$ drift of particles within flux surfaces has been taken into account. Therefore a strong increase of the torque is seen near the zero of radial electric field at $\rho_{pol} \approx 0.9$, where a contribution of $1/\nu$ transport appears. This increase is absent in the NEO-2 result where also the magnetic drift is taken into account (see a more detailed discussion of the RMP case below). Due to these differences, the value of the integral torque computed by NEO-2 is about 33% larger than the value predicted from SFINCS computations. The analytical estimate, used here for

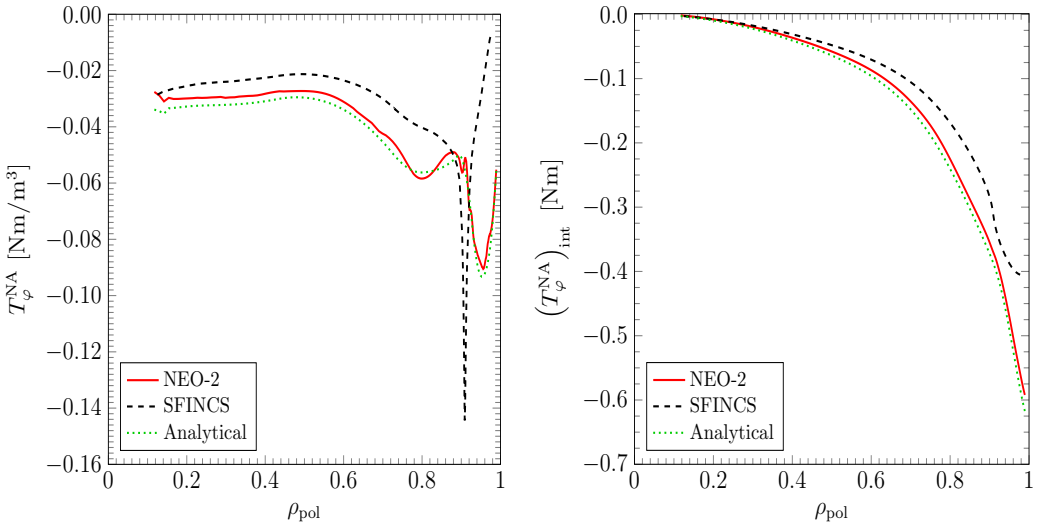

Figure 4.4: Radial profiles of the NTV torque density (left) and the integral torque (right) produced by the TF ripple.

comparison, is obtained from a general expression for the particle flux in the ripple-plateau regime (Eq. (45) of Ref. [17]) by replacing in this derivation the simplified magnetic field with the more general form,

$$B(r,\vartheta,\varphi) = B_0(r,\vartheta) + \mathrm{Re}\left\{B_n(r,\vartheta)\exp(in\varphi)\right\}, \tag{4.14}$$

where B_0 is the unperturbed magnetic field and B_n is a complex perturbation field amplitude. The non-ambipolar diffusion coefficients valid for a general tokamak geometry are then

$$\begin{aligned} D_{11}^{\mathrm{NA}} &= \frac{\sqrt{\pi}}{4}\frac{n m_i^2 c^2 v_T^3 B_0^2}{e_i^2 g (B_0^\vartheta)^2 B_0^\varphi}\left(\int_0^{2\pi}\frac{\mathrm{d}\vartheta}{B_0^2}\right)^{-1}\int_0^{2\pi}\frac{\mathrm{d}\vartheta}{B_0^3}\left|\frac{B_n}{B_0}\right|^2, \\ D_{12}^{\mathrm{NA}} &= 3D_{11}^{\mathrm{NA}}, \end{aligned} \tag{4.15}$$

where the notation is the same as in Ref. [2]. The difference in the integral torque between the NEO-2 result and the analytical estimate is less than 5%.

In Figure 4.6, the NEO-2 result for the ion NTV torque density produced by the ELM mitigation coils with $\Delta\phi_{\mathrm{ul}} = 90°$ is compared to the bounce-

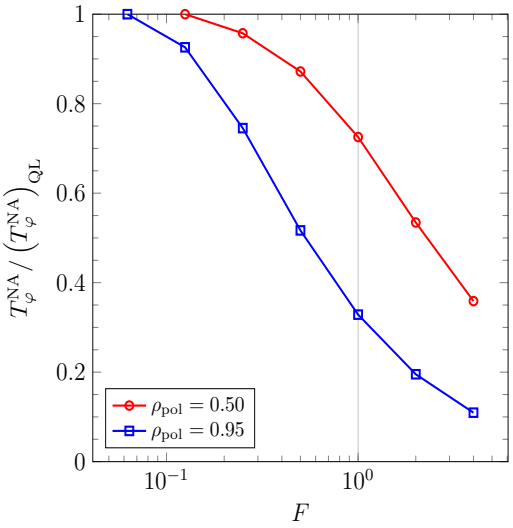

Figure 4.5: Ratio of the NTV torque density computed by SFINCS T_φ^{NA} to the quasilinear result $\left(T_\varphi^{NA}\right)_{\mathrm{QL}}$ as a function of the perturbation field scaled by a factor F for the TF ripple at different radial positions. $F = 1$ corresponds to the actual value of the perturbation field in the experiment.

averaged model of Shaing [3, 2] and, with the toroidal rotation due to the magnetic drift set to zero, also to a semi-analytical model based on a Hamiltonian approach [19] and to the code SFINCS. If only the $\mathbf{E} \times \mathbf{B}$ drift is considered, the agreement with SFINCS is nearly perfect (blocked particles are absent for medium scale perturbations), and there is a qualitatively good agreement between NEO-2 and the bounce-averaged model [3] in the vicinity of the zero of the electric field around $\rho_{\mathrm{pol}} = 0.9$. Apart from this radial domain NEO-2 results exceed the results of the bounce-averaged model [3] significantly. The discrepancies can be fixed by adding the NTV torque density from resonant (not bounce-averaged) transport regimes, which is computed by the semi-analytical model [19] in the collisionless limit, to the bounce-averaged model [3]. In radial domains with sufficiently large E_r, where the contribution from drift-orbit resonances to the NTV torque is dominating, a very good agreement between the NEO-2 result and the semi-analytical model is found. For the NEO-2 result including both, $\mathbf{E} \times \mathbf{B}$ drift and magnetic drift, a modification of the NTV torque density is observed in the core of the plasma and in the vicinity of the zero of the electric field. This em-

phasizes the necessity to include the magnetic drift into the computations. It should be noted that the contribution of the magnetic drift to the canonical toroidal banana precession frequency obtained within the Hamiltonian approach of Ref. [19] differs from the result of bounce averaging of the rotation frequency Ω_{tB} given by Eq. (67) of Ref. [2] by the presence of an additional term proportional to q', i.e. to the magnetic shear. This is the result of using the standard neoclassical ansatz as a starting point for the derivation of quasilinear equations in Ref. [2]. In the standard neoclassical ansatz orbits used for the computation of a linear perturbation of the distribution function are local, bounded to a particular flux surface (see also Refs. [13, 6]). The semi-analytical model [19] taking into account drift-orbit and sb-p resonances agrees very well with the local NEO-2 result over the whole radial domain, if the magnetic shear is neglected in that model. For $\rho_{\rm pol} > 0.7$ the sb-p resonance makes a dominant contribution to the NTV torque. A good agreement between the semi-analytical model considering only sb-p resonance and the bounce-averaged model [3] is found for $\rho_{\rm pol} < 0.2$. The discrepancies in the vicinity of the zero of the electric field are due to finite aspect ratio and deviations from the circular flux surface approximation.

The numerical approach implemented in the quasilinear version of the code NEO-2, which is based on a standard local neoclassical ansatz, can be extended to a non-local quasilinear NTV model. Here, the term 'non-local' is used to stress the difference to a standard approach where unperturbed orbits are truncated in order to stay within flux surfaces. This does not necessarily mean that the orbit width is comparable to the gradient length. However, even for large gradient lengths the effect of orbit displacement from the flux surface introduces a significant modification in the magnetic rotation frequency. Being rather different in derivation, the nonlocal quasilinear equation set and expressions for the non-ambipolar particle flux density are formally the same with results of Ref. [2]. Only the toroidal rotation frequency due to the magnetic drift Ω_{tB} is modified which, instead of local

Eq. (67) of Ref. [2], is now given by the following nonlocal expression,

$$\begin{aligned}\Omega_{tB} &= \frac{v^2\left(2-\eta B_0\right)}{2\sqrt{g_0}B_0\omega_{c0}}\left(\frac{B_r}{B_0}\frac{\partial B_0}{\partial\vartheta}-\frac{B_0}{B_0^{\vartheta}}\frac{\partial B_0}{\partial r}\right)+\\ &\quad+\frac{v^2\left(1-\eta B_0\right)}{\sqrt{g_0}B_0\omega_{c0}}\left(\frac{\partial}{\partial r}\left(B_\vartheta+qB_\varphi\right)-\frac{\partial B_r}{\partial\vartheta}\right),\end{aligned} \tag{4.16}$$

where the only difference from the local expression is the presence of the safety factor under radial derivative sign. The extended formalism pertinent to the non-local NEO-2 version will be presented in a separate publication. The additional magnetic shear term leads to a significant modification of the torque density profile, see Figure 4.7. Again a very good agreement between the non-local version of NEO-2 and the semi-analytical model [19] can be observed, which indicates the importance of contributions from various resonant transport regimes to the ion NTV torque density. In comparison to the results obtained by the local approach the sb-p regime covers only a narrow radial domain located at the zero of the electric field. Furthermore, a distinctive peak of the torque density is observed at $\rho_{\mathrm{pol}} = 0.4$. It should be noted that the expression for the NTV torque density in the sb-p regime derived from the Hamiltonian approach agrees analytically with Shaing's generalized formula [53] published recently.

As can be seen from Figure 4.8, not only ions but also electrons make a significant contribution to the NTV torque, which is in the direction of (positive) plasma rotation and which partly balances the negative ion torque. In the case where only the $\mathbf{E}\times\mathbf{B}$ drift is taken into account, the electron torque agrees up to a factor 3 with the result of the asymptotical model [3]. The observed discrepancies can be explained by uncertainties in the joining procedure of the different asymptotical regimes and by the rather small aspect ratio where the analytical model of Shaing [3] can significantly deviate from accurate computations with NEO-2 [2]. It can be observed that the agreement becomes better for larger aspect ratios closer to the center of the plasma and for small values of the radial electric field where the contribution from pure $1/\nu$ transport is dominant.

Including the magnetic drift term in the NEO-2 computation modifies

significantly the electron NTV torque density profile in the core of the plasma. In the inner part of the plasma only the trend seen from NEO-2 results is captured by the universal formula [3] connecting the $1/\nu$, $\nu - \sqrt{\nu}$ and sb-p transport regimes. The observed differences in the inner part of the plasma are due to the circular flux surface approximation used for the evaluation of the sb-p resonance condition, which can deviate significantly from accurate computations for a real tokamak geometry. It should also be noted that the torque density profile exhibits distinctive substructures in the vicinity of resonant surfaces, which are indicated by vertical lines. A rather peculiar point in this profile is the resonant surface $(m, n) = (6, 2)$ which almost coincides with the zero of the electric field. The increased electron torque density around this point is due to the fact that for small values of the electric field $1/\nu$ transport is dominant. The electron NTV torque density evaluated by the non-local version of NEO-2 differs considerably from local computations for $\rho_{\mathrm{pol}} > 0.3$. The additional magnetic shear term yields not only a modification of the sb-p transport at intermediate radii, but affects also the $1/\nu$ and $\nu - \sqrt{\nu}$ transport at the edge.

The NTV torque densities shown in Figure 4.7 and Figure 4.8 can be also expressed in terms of slowing down frequencies $\nu_{\mathrm{s}}^{\alpha}$ and offset rotation frequencies $V_{\mathrm{eq},\alpha}^{\varphi}$ via the generic form (see, e.g., (5) of Ref. [2]),

$$T_{\varphi}^{\mathrm{NA}} = -n_i m_i \sum_{\alpha} \nu_{\mathrm{s}}^{\alpha} \langle g_{\varphi\varphi}(V^{\varphi} - V_{\mathrm{eq},\alpha}^{\varphi}) \rangle = -n_i m_i \nu_{\mathrm{s}}^{i+e} \langle g_{\varphi\varphi}(V^{\varphi} - V_{\mathrm{eq},i+e}^{\varphi}) \rangle, \tag{4.17}$$

which provides a rather demonstrative representation. Here, $g_{\varphi\varphi} = R_0^2$ denotes the toroidal covariant metric tensor component. In Figure 4.9 the respective radial profiles of the species offset rotation frequencies evaluated by the non-local version of NEO-2 are shown. It can be seen that ions tend to rotate in the negative toroidal direction, whereas the offset rotation frequency of electrons is positive. The different sign of the offset rotation frequency of ions and electrons correlates with the sign of the torque density. The total offset rotation frequency exhibits a rather remarkable behavior at intermediate radial positions where it oscillates around the measured toroidal rotation frequency. At the edge the computed total offset rotation frequency deviates

significantly from the measured value.

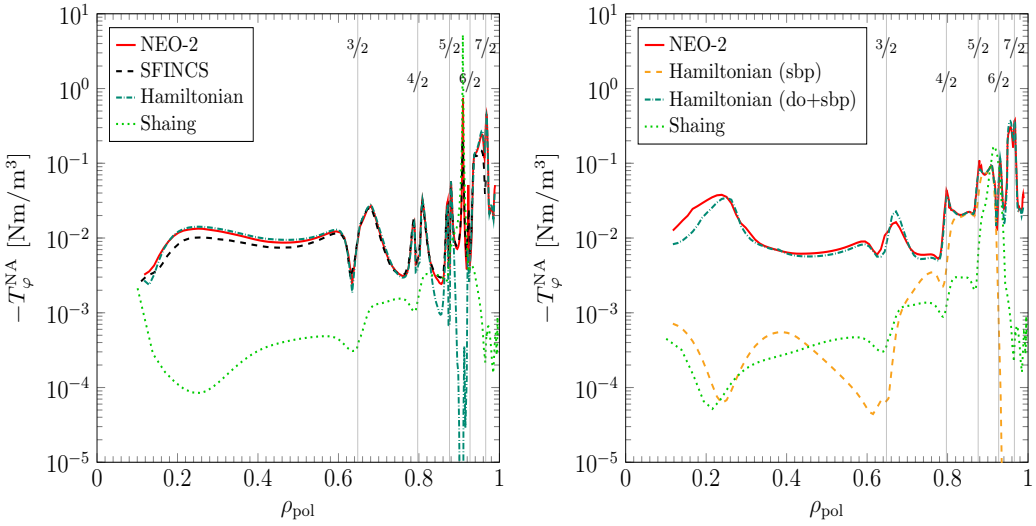

Figure 4.6: Ion contribution to the NTV torque density produced by the ELM mitigation coils with a phase of 90 degrees as a function of the normalized poloidal radius. Neglecting the effect of magnetic drift (left), the NEO-2 result (solid line) is compared to SFINCS (dashed line), to a semi-analytical Hamiltonian model [19] (dash-dotted line) and to the bounce-averaged model by Shaing [3, 2] (dotted line). The NEO-2 result including both, $\mathbf{E} \times \mathbf{B}$ drift and magnetic drift, is compared to the semi-analytical Hamiltonian model taking into account drift-orbit (do) and superbanana-plateau (sbp) resonances, as well as to the universal formula [3] connecting $1/\nu$, $\nu - \sqrt{\nu}$ and superbanana-plateau transport regimes (right). Vertical lines indicate the positions of resonant surfaces with $q(\rho_{\mathrm{pol}}) = m/n$, where m and n are the poloidal and toroidal mode numbers, respectively.

In order to determine relevant transport regimes, a scan of the diffusion coefficient D_{11}^{NA} normalized by the plateau diffusion coefficient D_p over collisionality parameter and otherwise the same parameters as in the experimental profile has been performed at different radial positions, see Figure 4.10. Here, $D_p = \pi q v_T \rho_L^2 (16 R_0)^{-1}$, $\rho_L = v_T/\omega_{c0}$, ω_{c0} is the mean cyclotron frequency value at a given flux surface, and only the dominant $n = 2$ perturbation toroidal mode has been taken into account. For electrons all quasilinear transport regimes described by the bounce-averaged drift kinetic equation can be seen. At $\rho_{\mathrm{pol}} = 0.30$ electrons are clearly in a transition regime be-

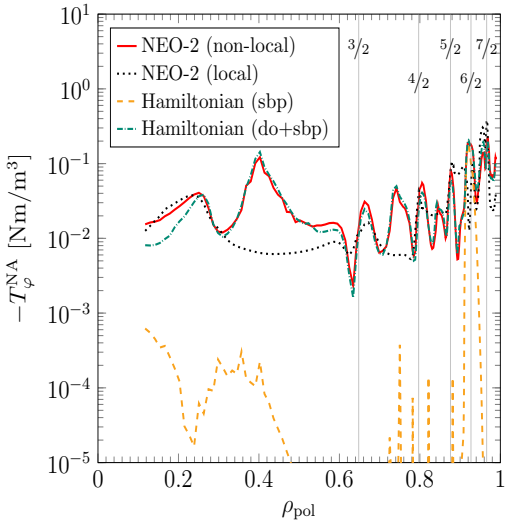

Figure 4.7: Ion contribution to the NTV torque density produced by the ELM mitigation coils with a phase of 90 degrees as a function of the normalized poloidal radius. The non-local NEO-2 result including both, $\mathbf{E}\times\mathbf{B}$ drift and magnetic drift, is compared to the NEO-2 result using a local approximation and to the semi-analytical Hamiltonian model taking into account drift-orbit (do) and superbanana-plateau (sbp) resonances. Vertical lines indicate the positions of resonant surfaces with $q(\rho_{\mathrm{pol}}) = m/n$, where m and n are the poloidal and toroidal mode numbers, respectively.

tween the $1/\nu$ and the superbanana-plateau regime. At $\rho_{\mathrm{pol}} = 0.50$ the onset of the $\nu - \sqrt{\nu}$ regime is observed, whereas at $\rho_{\mathrm{pol}} = 0.91$ electrons are still in the $1/\nu$ regime and only at lower collisionalities the transition to the superbanana plateau is observed. When the magnetic shear is taken into account in the non-local computations, the sb-p regime seen at $\rho_{\mathrm{pol}} = 0.91$ is replaced by a $\nu - \sqrt{\nu}$ regime. For other radii the computations with and without magnetic shear differ only slightly. It should be noted that the difference in the torque density seen in Figure 4.8 at $\rho_{\mathrm{pol}} = 0.50$ is due to the contribution from the $n = 6$ perturbation, which is not considered here. The plateau like behavior of the ion diffusion coefficient indicates resonant "collisionless" diffusion regimes because the ion collisionality for $n = 2$ perturbations stays outside the lower boundary of the ripple plateau regime [17], which requires $\nu^* > (nq)^{-2}A^{-3/2}$ with A being the aspect ratio. The non-local results qual-

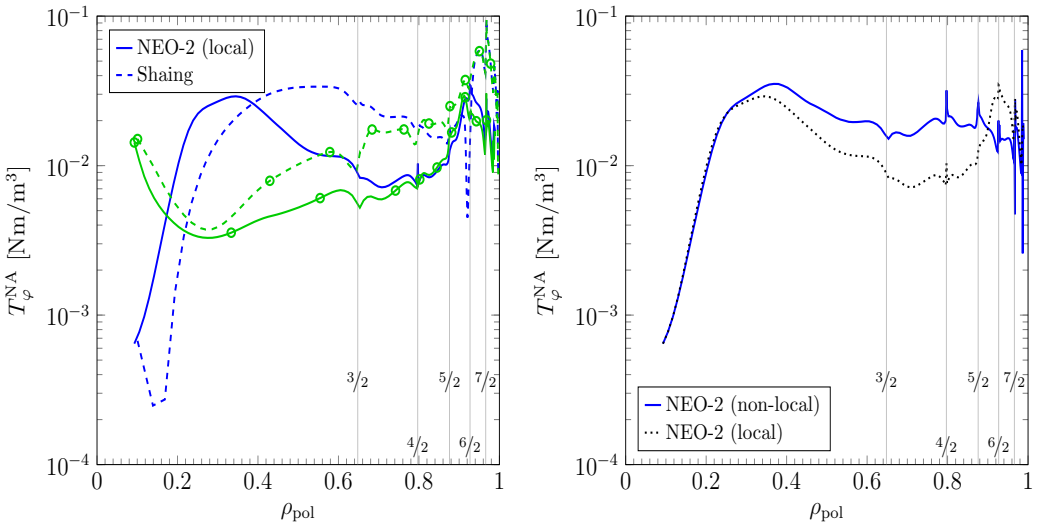

Figure 4.8: Electron contribution to the NTV torque density produced by the ELM mitigation coils with a phase of 90 degrees as a function of the normalized poloidal radius. Left - the NEO-2 results (solid lines) including magnetic drift (without markers) and neglecting magnetic drift (with markers) are compared to the bounce-averaged model by Shaing [3] (dashed lines) for the same cases. Right - the non-local NEO-2 result including both, $\mathbf{E}\times\mathbf{B}$ drift and magnetic drift, is compared to the NEO-2 result using a local approximation. Vertical lines indicate the positions of resonant surfaces with $q(\rho_{\mathrm{pol}}) = m/n$, where m and n are the poloidal and toroidal mode numbers, respectively.

itatively show the same dependence on collisionality, although the absolute value of the resonant regime can deviate significantly. These regimes are of different nature for different radii. For $\rho_{\mathrm{pol}} = 0.3$ and $\rho_{\mathrm{pol}} = 0.5$ where Mach numbers are rather large, the resonant regime corresponds to the regime of bounce resonances [56, 18]. It can be seen from Figure 4.6 that toroidal rotation due to the magnetic drift starts to be important for bounce resonances at smaller ρ_{pol}, in particular at $\rho_{\mathrm{pol}} = 0.3$, since the frequency of this rotation scales inversely with ρ_{pol}. In contrast to the two inner points in Figure 4.10, the ion diffusion coefficient at $\rho_{\mathrm{pol}} = 0.91$, which is close to $E_r = 0$ point, corresponds to the superbanana plateau regime. Its value there is much higher than the ripple plateau value, which is roughly the maximum value achievable in the regime of bounce resonances (see [19]). This can also be seen

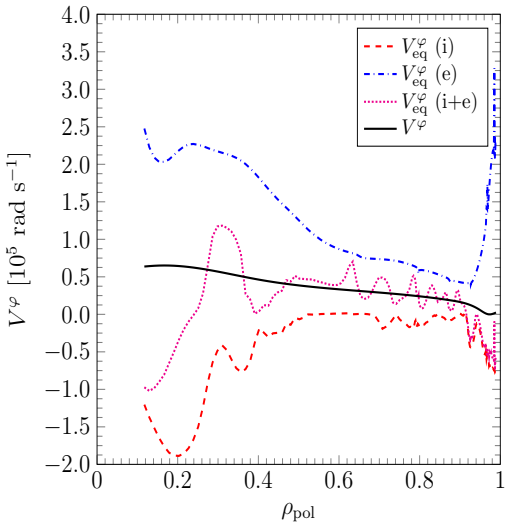

Figure 4.9: Non-local NEO-2 result for the offset rotation frequencies (4.17) produced by the ELM mitigation coils with a phase of 90 degrees as a function of the normalized poloidal radius for ions (dashed), electrons (dash-dotted) and sum over species (dotted). For comparison the radial profile of the measured toroidal rotation frequency (solid line) is shown.

from Figure 4.6, where at $E_r = 0$ a spike of the torque appears in case of a pure $\mathbf{E} \times \mathbf{B}$ rotation because of a strong $1/\nu$ contribution. This is changed to a saturated value when the complete rotation model is used.

As seen in Figure 4.11 the integral NTV torque $\left(T^{\rm NA}_{\varphi}\right)_{\rm int}$, Eq. (4.13), is dominated by the ion contribution and is produced mainly at the plasma edge. The maximum value of the total integral NTV torque as computed by NEO-2 is -1 Nm, which is less than the NBI torque value of +4.1 Nm. As can be seen from the gradients of the integral torque, the NTV torque density is larger than the one from NBI at $\rho_{\rm pol} > 0.9$ where NTV dominates above NBI in the formation of the toroidal rotation profile.

In the torque from RMP coils electrons play an equally important role as ions and may even dominate in the plasma core for some coil polarities making the torque in the core positive (see Figure 4.12). In turn, for $\rho_{\rm pol} > 0.8$ ions are always dominant, and finally the ions determine the sign of the total torque from RMP coils in all cases. The magnitude of NTV torque produced by the RMP coils depends strongly on the poloidal field spectrum.

The largest values of the integral NTV torque can be seen for $\Delta\phi_{\mathrm{ul}} = +90°$ and $\Delta\phi_{\mathrm{ul}} = -150°$. In case of $\Delta\phi_{\mathrm{ul}} = +30°$ and $\Delta\phi_{\mathrm{ul}} = +52°$ the smallest electron contribution to the NTV torque is observed, whereas for negative values of the phase shift the electron NTV torque is considerably increased. The effect of magnetic shear, which is taken into account by the non-local computations, is largest for negative coil polarities and for $\Delta\phi_{\mathrm{ul}} = +90°$, whereas $\Delta\phi_{\mathrm{ul}} = +30°$ and $\Delta\phi_{\mathrm{ul}} = +52°$ are unaffected to a large extent. Here, ions dominate the integral NTV torque for $\rho_{\mathrm{pol}} > 0.4$, which is due to the additional peak in the ion torque density seen in Figure 4.7. A positive value of the torque in the core is only observed for negative coil polarities.

As seen in Figure 4.13, the magnitude of the RMP torque for various coil polarities correlates with the maximum value of the normalized perturbation field and with the maximum corrugation of flux surfaces (see Figure 4 in Ref. [66]) for the respective phases (roughly $|B_n/B_0|_{\max} \sim |\delta_{\mathrm{N}}|_{\max} R_0^{-1}$). This means that the main reason for the non-axisymmetric perturbation of the magnetic field magnitude B on perturbed flux surfaces is the meandering of these surfaces caused by the perturbation field component normal to the unperturbed flux surfaces, but not the direct change of B by the component which is parallel to the unperturbed field [3, 5, 4].

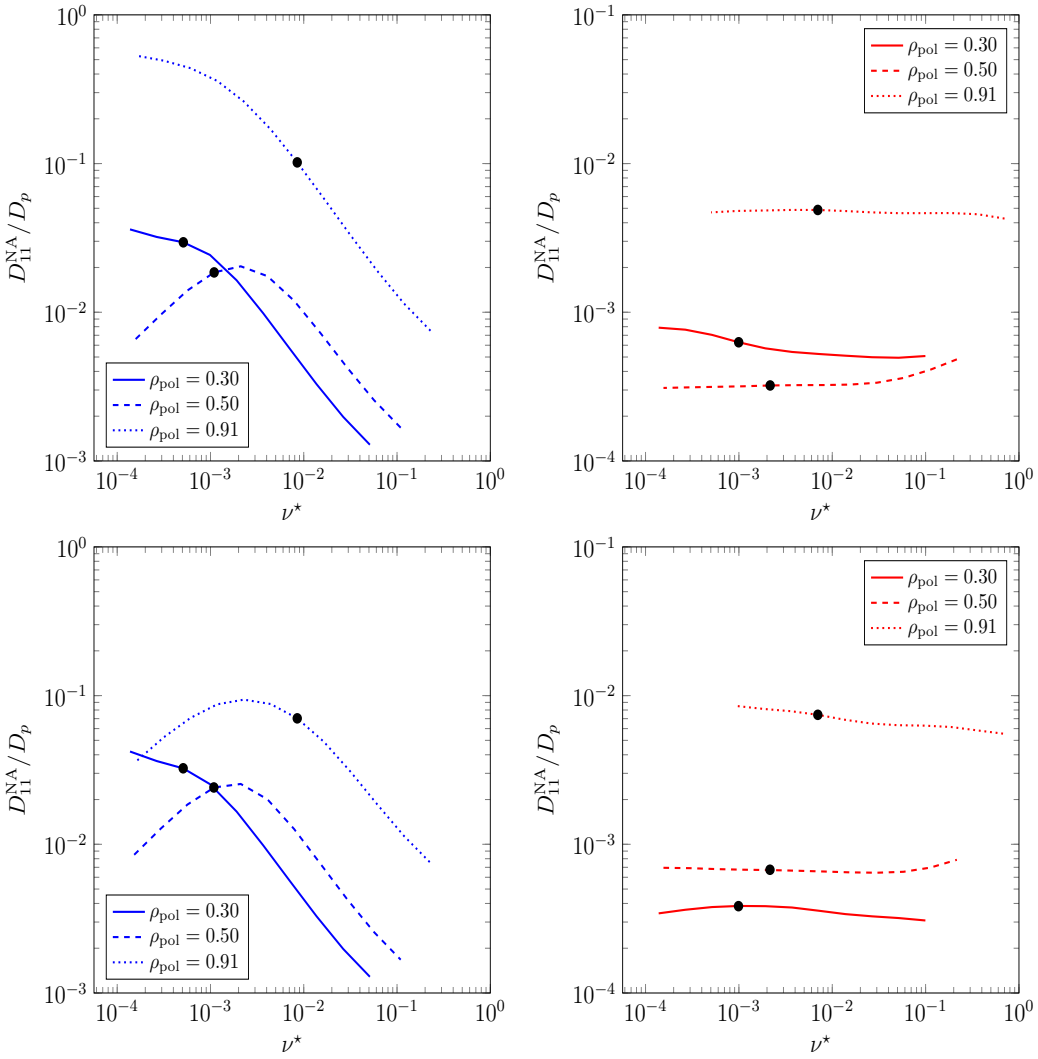

Figure 4.10: Normalized electron (left panel) and ion (right panel) diffusion coefficients D_{11}^{NA} computed with (lower panel) and without (upper panel) magnetic shear for various radii ρ_{pol} (see the legend) as functions of the collisionality parameter $\nu^\star$. Actual collisionalities in the experiment for the given poloidal radius are indicated by filled circles. Note that the normalizing plateau diffusion coefficient is by a a square-root of mass ratio smaller for electrons than for ions.

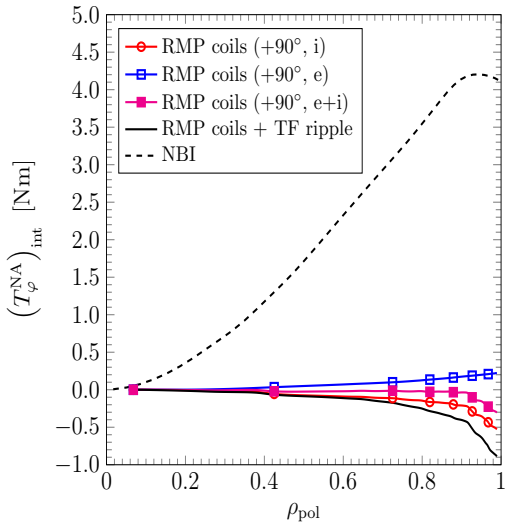

Figure 4.11: Profiles of various contributions to the integral NTV torque $\left(T_\varphi^{\mathrm{NA}}\right)_{\mathrm{int}}$ for 90° ELM mitigation coil polarity and of the integral NBI torque (see legend).

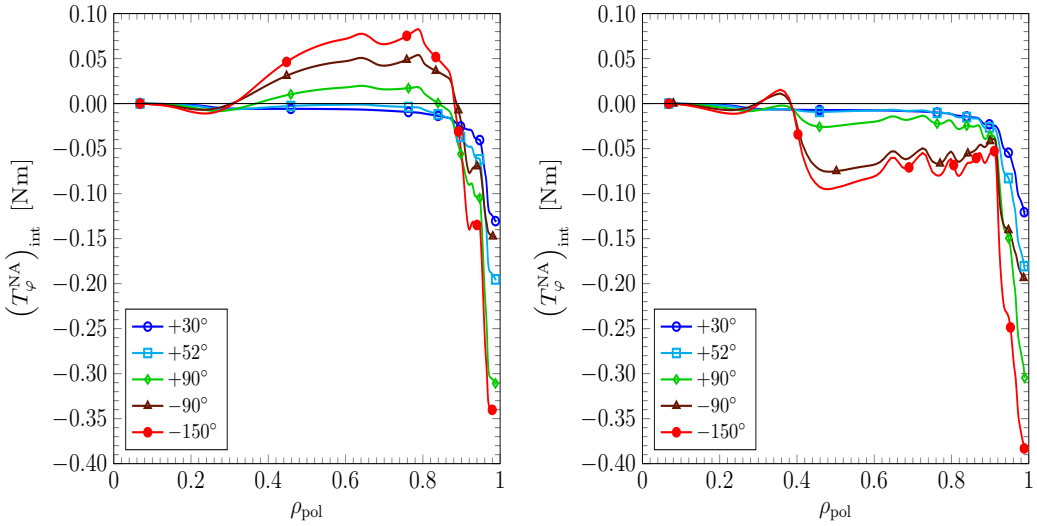

Figure 4.12: Profiles of total (i+e) integral NTV torque from ELM mitigation coils with various polarities (see legend) for local (left) and non-local (right) computations.

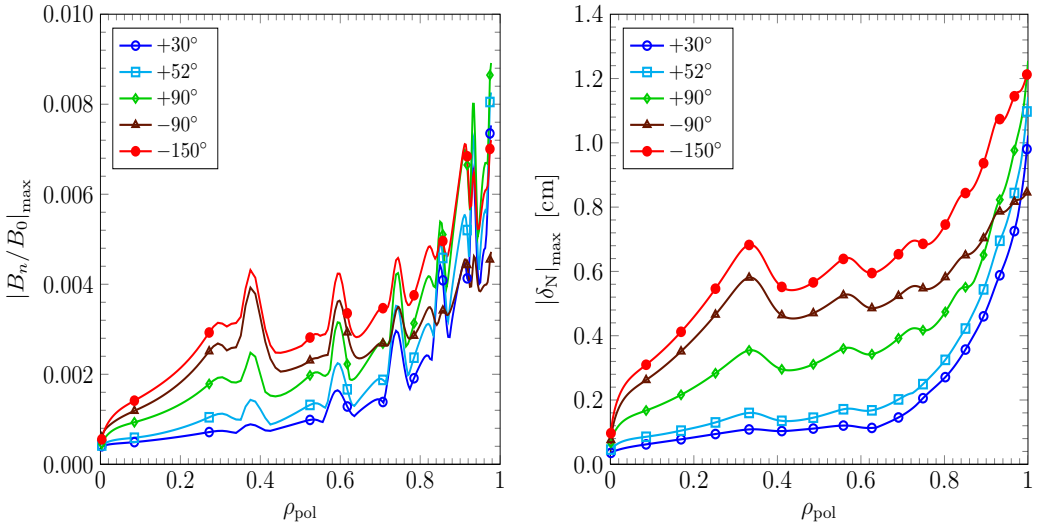

Figure 4.13: Profiles of the maximum value of the normalized perturbation field (left) and of the maximum corrugation of the 3D flux surface [66] (right) for ELM mitigation coils with various polarities (see legend).

4.4 Integral momentum balance and other momentum sources

It should be mentioned that plasma parameter profiles used in this modeling, in particular the toroidal rotation frequency, correspond to a (quasi-)steady state observed in shot #30835 at 3.2 s. In contrast to Ref. [62] where a modification of a steady state rotation profile by turning on perturbation coils has been shown to be in agreement with NTV induced by these coils, this can be hardly expected in the pertinent AUG shot. In this shot a significant density reduction and modification of temperature profiles has been observed after turning on the RMP coils, what leads also to a modification of turbulent transport. Therefore, a single steady state has been chosen for a study of the static torque balance. Since the integral rotational moment is a conserved quantity, the missing balance between the NTV torque and the NBI torque, which exceeds the NTV torque roughly by a factor four, clearly suggests the importance of other momentum sources. The complete integral torque balance follows from the integration of the steady state equation (4.7) over the main plasma volume,

$$\left(T_\varphi^{\mathrm{NBI}}\right)_{\mathrm{int}} + \left(T_\varphi^{\mathrm{NA}}\right)_{\mathrm{int}} + \left(T_\varphi^{\mathrm{tot}}\right)_{\mathrm{w}} = 0, \tag{4.18}$$

where $\left(T_\varphi^{\mathrm{tot}}\right)_{\mathrm{w}}$ is the momentum flux through the main plasma boundary (separatrix) via $\left\langle \Pi^r_{[\mathrm{in}]\varphi} \right\rangle$, the only momentum source where the anomalous and axisymmetric neoclassical transport provide a contribution. Note that at least formally, all three torques in this balance can be determined independently outside the main plasma volume [71]. Since each of the last two torques in (4.18) consists of a few contributions, they are discussed below in more detail.

The contributions entering $\left(T_\varphi^{\mathrm{NA}}\right)_{\mathrm{int}}$ besides the NTV torque are listed here roughly in the order of their importance. The first of these sources is related to losses of NBI generated fast particles [72, 73]. This torque would be negative (as the NTV torque of ions) and its value can be high enough to balance the NBI torque, as shown in Ref. [73] for JET. Estimations

of fast particle losses induced by violations of AUG axial symmetry using 3D Monte Carlo modeling in Boozer coordinates with help of the NEO-MC code [74] version for fast particles [75] have shown that the toroidal torque due to such losses cannot match the discrepancy because it is smaller than the NTV torque (about 5% of the NBI torque). Another important unaccounted momentum source is the resonant torque produced by RMPs in resonant layers around rational flux surfaces where the ideal MHD theory is not valid. Normally, RMPs are shielded by plasma response currents in the core, which results in a small torque. However, the situation might change at the plasma edge, where the RMP amplitudes can be large enough to modify the electron temperature profile in the resonant layer around some of the dominating resonances. This might significantly reduce the shielding by electrons [12]. An accurate quantitative description of this interaction is still missing. Besides the magnetic perturbations from the TF ripple and ELM mitigation coils there are two more possible magnetic perturbations, which can produce NTV and resonant torque and which are not taken into account here. These are the error fields and the fields from eddy currents induced in the wall and other external conductors by intrinsic MHD modes.

It should be noted that a description of the resonant torque in terms of a local torque density T_φ^{NA} is limited to cases where the non-axisymmetric part of gradients of plasma parameters is small everywhere including the islands produced by RMPs. This is the case where the quasilinear theory is valid (see, e.g., [12]). Otherwise, this description is only formally valid, but not useful, because plasma parameters become essentially 3D within and in some vicinity of islands, and only the integral torque is meaningful.

The last contributor to $\left(T_\varphi^{\mathrm{NA}}\right)_{\mathrm{int}}$, the torque due to ECRH/ECCD, consists of two parts. First, the direct toroidal momentum input by microwave radiation is related to the coupled ECRH power as $P_{\mathrm{ECRH}} R_0/c$, and for $P_{\mathrm{ECRH}} \sim 0.5$ MW is around 0.01 Nm. Second, losses of supra-thermal electrons, which are possible in presence of non-axisymmetric magnetic field perturbations, can produce only positive torque in the direction of the NBI torque. Therefore, the last contributor to $\left(T_\varphi^{\mathrm{NA}}\right)_{\mathrm{int}}$, the torque due to ECRH/ECCD, can be safely removed from the list.

Various contributions to the torque $\left(T_\varphi^{\mathrm{NA}}\right)_{\mathrm{int}}$ can be measured externally in a direct way because the integral torque due to electromagnetic perturbations is equal to the momentum flux carried by these perturbations through the plasma boundary in the form of Maxwell stress, essentially via its magnetic part. (Finally, this Maxwell stress is balanced by Lorentz forces onto the external currents that create the perturbations.) Therefore, it would be sufficient to determine the magnetic Maxwell stress by measuring the non-axisymmetric magnetic field outside the plasma [76, 71]. Alternatively, $\left(T_\varphi^{\mathrm{NA}}\right)_{\mathrm{int}}$ can be determined from the torque balance (4.18) using the measured $\left(T_\varphi^{\mathrm{NBI}}\right)_{\mathrm{int}}$ and $\left(T_\varphi^{\mathrm{tot}}\right)_{\mathrm{w}}$. In absence of significant NBI and non-axisymmetric torque outside the main plasma boundary, the momentum flux $\left(T_\varphi^{\mathrm{tot}}\right)_{\mathrm{w}}$ carried through the separatrix is finally recovered at the wall, as follows from the integration of equation (4.1) over the vacuum chamber volume. Flux $\left(T_\varphi^{\mathrm{tot}}\right)_{\mathrm{w}}$ consists of three contributions, which require different measurements. Presenting it as a sum of particle and electromagnetic field contributions, $\left(T_\varphi^{\mathrm{tot}}\right)_{\mathrm{w}} = \left(T_\varphi^{\mathrm{part}}\right)_{\mathrm{w}} + \left(T_\varphi^{\mathrm{EM}}\right)_{\mathrm{w}}$ and averaging this expression over the time scale of turbulent fluctuations, the toroidal reactive torque onto the main plasma due to charged and neutral particle fluxes to the wall is

$$\left(T_\varphi^{\mathrm{part}}\right)_{\mathrm{w}} = 2\pi \sum_\alpha m_\alpha \oint \mathrm{d}lR \int \mathrm{d}^3v \, f_\alpha \, \mathbf{v}\cdot\mathbf{n}\,\mathbf{v}\cdot\frac{\partial \mathbf{r}}{\partial\varphi}, \tag{4.19}$$

where f_α is the averaged distribution function, which is then axisymmetric. The poloidal integration contour here is along the wall surface, and the unit vector normal to the wall $\mathbf{n}$ points to the inside of the vessel. In contrast to the momentum flux of neutral particles ($\alpha = \mathrm{n}$), which appears due to charge exchange with the surrounding neutral gas, and which is spread over the wall, the momentum flux of charged particles (ions) is localized at the divertor target plates. Before the sheath this latter flux is determined mainly by parallel transport, $\mathbf{v}\cdot\mathbf{n}\,\mathbf{v}\cdot\partial\mathbf{r}/\partial\varphi \to (v_\parallel/B)^2\mathbf{B}\cdot\mathbf{n}\,\mathbf{B}\cdot\partial\mathbf{r}/\partial\varphi$. This means that the toroidal reactive torque on the plasma from the vicinity of a particular strike point scales with $\mathbf{B}\cdot\mathbf{n}$. Since $\mathbf{B}\cdot\mathbf{n}$ has opposite signs for inner and outer strike points, the integral torque onto the main plasma manifests itself as an imbalance between the toroidal momentum fluxes carried by particles

to the inner and outer divertor targets (see, e.g., Section 6.3 of Ref. [77] and Ref. [71]).

A simple expression for the intrinsic electromagnetic torque $\left(T_\varphi^{\mathrm{EM}}\right)_{\mathrm{w}}$, which has been omitted in Ref. [71], is obtained when the currents and charges induced by edge instabilities in the wall are negligible. In this case, only the axisymmetric part of the electromagnetic field resulting from averaging of this field over the fluctuation time scale contributes to the electromagnetic momentum flux, because only the axisymmetric field leads to a Lorentz force onto the axisymmetric currents in the wall. In a (quasi) steady state, the pertinent part of the Maxwell stress tensor $\boldsymbol{\sigma}$ is essentially determined by the magnetic field,

$$\frac{1}{\sqrt{g}}\frac{\partial}{\partial x^i}\sqrt{g}\sigma_\varphi^i = \frac{1}{4\pi}\nabla\cdot B_\varphi\mathbf{B} = \frac{1}{c}\nabla\cdot\psi_{\mathrm{pol}}\,\mathbf{j}. \tag{4.20}$$

The integral intrinsic electromagnetic torque is then

$$\begin{aligned}\left(T_\varphi^{\mathrm{EM}}\right)_{\mathrm{w}} &= \frac{2\pi}{c}\oint \mathrm{d}l\; R\left(\psi_{\mathrm{pol}}^a - \psi_{\mathrm{pol}}\right)\mathbf{j}\cdot\mathbf{n} \\ &\approx \frac{2\pi}{c}\sum_s R_s^2\left(\mathbf{n}\cdot\mathbf{B}\right)_s \int\limits_{l_s-\Delta l}^{l_s+\Delta l}\mathrm{d}l\,(l-l_s)\,\mathbf{j}\cdot\mathbf{n},\end{aligned} \tag{4.21}$$

where the final expression corresponds to the current localized around divertor strike points numbered here with subscript s. The term with ψ_{pol}^a in the first expression in (4.21) provides a zero contribution to the integral due to $\nabla\cdot\mathbf{j}=0$. It should be noted that due to (4.20) and $\nabla\cdot\mathbf{j}=0$, currents flowing along ψ_{pol} contours (in particular, parallel currents) produce no steady state toroidal torque since they produce no toroidal $\mathbf{j}\times\mathbf{B}$ force. Only currents which are closed across ψ_{pol} contours produce toroidal torque. This relates to both the currents in the plasma and to the poloidal currents in the wall, which close the plasma currents to the wall. The former produces the torque onto the plasma and the latter the torque onto the wall, thus balancing the force onto the plasma by third Newton's law. In the equilibria studied here, ψ_{pol} increases from the private flux region towards the scrape-off layer. Thus,

currents in the wall (target plates), which balance the positive NBI torque, flow in direction of increasing ψ_{pol}.

4.5 Summary

Computations of the NTV torque produced in ASDEX Upgrade by the TF ripple and magnetic perturbations from ELM mitigation coils show an agreement between different numerical (NEO-2, SFINCS) and semi-analytical models within their validity domains. Specific differences are also observed and discussed. It is clearly seen that ions as well as electrons contribute to the overall torque. It is remarkable that practically all quasilinear transport regimes except for the highly collisional Pfirsch-Schlüter regime are realized within the single discharge #30835, which is studied here. Various bounce averaged transport regimes as well as resonant regimes are important in specific radial positions. Those regimes have been identified by scans over collisionality and comparison with analytical and semi analytical computations. The quasilinear approach used in NEO-2 is well justified for computations of the torque driven by RMPs but slightly overestimates the torque from the TF ripple. The amplitude of the perturbations corresponding to the TF ripple is already marginally outside the validity range for the quasilinear approach, mainly because of the high toroidal mode number.

The NTV torque is produced mainly at the plasma edge where its density is comparable with the NBI torque density. However, the integral NTV torque balances only a quarter of the integral NBI torque. This emphasizes the importance of other momentum sources unaccounted here. Some of these sources (e.g. the torque due to fast particle losses) can be computed with present day models. An accurate description of the other sources connected with resonant interaction of magnetic perturbations at rational flux surfaces is still an open problem. Thus, measurements of discharges where the role of resonant interactions is minimized are of future interest.

The integral torque balance [71], which can be used to verify the modeling by measurements outside the plasma, is discussed here in some more detail. For this balance, in addition to measurements of the asymmetry of

the momentum flux carried by divertor fluxes [71], measurements of charge-exchange neutral spectra and of the currents between the plasma and the wall (divertor target plates) are shown to be of importance.

Besides the integral torque balance, an accurate description of the torque density profile resulting from non-axisymmetric magnetic field perturbations would be an important part of turbulent momentum transport studies, where the effect of turbulent momentum flux dominating in $\left\langle \Pi^r_{[\mathrm{in}]\varphi} \right\rangle$ in equation (4.7) on the rotation velocity profile is required in its pure form, i.e. the second term in l.h.s. of (4.7). The state of art of existing models discussed here does already allow for such a description for the NTV torque.

Chapter 5

Multi-species version of the code NEO-2

For the multi-species problem the collision integral $\mathrm{St}(f_\alpha, f_\beta)$, where f_α and f_β are test and field particle distribution functions, respectively, is linearized as follows,

$$\mathrm{St}(f_\alpha, f_\beta) \approx \hat{L}_C^{D(\alpha,\beta)} \delta f_\alpha + \hat{L}_C^{I(\alpha,\beta)} \delta f_\beta, \tag{5.1}$$

where $\delta f_\alpha = f_\alpha - f_{\alpha 0}$ is the perturbation of the α-species Maxwellian $-f_{\alpha 0}$, and $\hat{L}_C^{D(\alpha,\beta)}$ and $\hat{L}_C^{I(\alpha,\beta)}$ are linear differential and integral operators, respectively, defined as follows

$$\hat{L}_C^{D(\alpha,\beta)} \delta f_\alpha = \mathrm{St}(\delta f_\alpha, f_{\beta 0}), \qquad \hat{L}_C^{I(\alpha,\beta)} \delta f_\beta = \mathrm{St}(f_{\alpha 0}, \delta f_\beta). \tag{5.2}$$

The linearized drift kinetic equation for the multi-species problem is then presented in the discretized form (2.193) solved by NEO-2 [2],

$$\sigma \frac{\partial f^\sigma_{m,\alpha}}{\partial \varphi_s} - \frac{1}{h^\varphi} \sum_{m'=0}^{M} \sum_{\beta} \left(\hat{L}^{D(\alpha,\beta)}_{mm'} f^\sigma_{m',\alpha} + \hat{L}^{I(\alpha,\beta)}_{mm'} f^\sigma_{m',\beta} \right) + \sum_{m'=0}^{M} i\omega^{(\alpha)}_{mm'} f^\sigma_{m',\alpha} = Q_{m,\alpha}, \tag{5.3}$$

where the operators $\hat{L}^{D(\alpha,\beta)}_{m,m'}$ and $\hat{L}^{I(\alpha,\beta)}_{m,m'}$ denote the matrix elements of the differential and integral operator defined above, and otherwise the same notation as in Section 2.3.4 is used. It can be seen that the interaction with other species in (5.3) is solely contained in the integral part of the collision

integral $\hat{L}^{I(\alpha,\beta)}_{mm'} f^{\sigma}_{m',\beta}$. The integral part of the collision integral is taken into account by means of direct or pre-conditioned iterations in NEO-2,

$$\sum_{\beta} \hat{L}^{I,(\alpha,\beta)}_{m,m'} f^{\sigma}_{m,\beta} = \sum_{l=0}^{L} \sum_{\beta} P_l(\lambda) I^{\alpha\beta,(l)}_{mm'} \int_{-1}^{1} \mathrm{d}\lambda' P_l(\lambda') f^{\sigma}_{m,\beta}(\lambda'), \qquad (5.4)$$

where λ is the pitch angle parameter and $P_l(\lambda)$ are Legendre polynomials. The direct or pre-conditioned iterations are based on the solution of the differential part of the integro-differential equation (5.3), which contains no interaction with the perturbed distribution function of other species. For the numerical solution of the differential part of (5.3) a conservative finite difference (finite volume) scheme on an adaptive grid over the field line parameter φ_s and the normalized perpendicular adiabatic invariant η is used. The resulting linear system of equations is solved with help of a sparse solver based on direct L-U decomposition.

In NEO-2 the multi-species problem is thus cast in a form which is well-suited for parallelization with help of MPI [78]. A very efficient MPI interface [79] is already used for the computation of the generalized Spitzer function in stellarators [55] and has been adapted for the multi-species version of NEO-2. For each species the differential part of the drift kinetic equation can be computed on a separate processor since the different species interact only via the field particle part of the collision operator. Only within the iterations of the integral part of the collision operator, the processes corresponding to different species have to be synchronized. The communication between the processes is minimized because only the scalar product of the perturbed distribution function with Legendre polynomials is shared between the processors and not the perturbed distribution function itself. It should be also noted that the factorization of the differential part of (5.3) on different processors allows for a distribution of the memory to different computer nodes and, therefore, relieves the memory constraints.

Since (5.3) is linear, the solution can be looked in form of a superposition

of thermodynamic forces A_j^α,

$$f_{m,\alpha}^\sigma = \sum_\beta \left(f_{m,\alpha\beta}^{\sigma,(1)} A_1^\beta + f_{m,\alpha\beta}^{\sigma,(2)} A_2^\beta + f_{m,\alpha\beta}^{\sigma,(3)} A_3^\beta \right). \tag{5.5}$$

Analogously, the right hand side of (5.3) is presented as a superposition of thermodynamic forces,

$$Q_{m,\alpha} = Q_{m,\alpha}^{(1)} A_1^\alpha + Q_{m,\alpha}^{(2)} A_2^\alpha + Q_{m,\alpha}^{(3)} A_3^\alpha. \tag{5.6}$$

Upon inserting (5.5) and (5.6) into the drift kinetic equation (5.3), it becomes clear that the contribution of A_j^β to $f_{m,\alpha}^\sigma$ is only non-vanishing (for $\alpha \neq \beta$) if the integral part of the collision operator is considered. The expression for the particle flux in terms of diffusion coefficients $D_{ij}^{\alpha\beta}$ and thermodynamic forces is generalized according to (5.5),

$$\Gamma_\alpha = -n_\alpha \sum_\beta \left(D_{11}^{\alpha\beta} A_1^\beta + D_{12}^{\alpha\beta} A_2^\beta + D_{13}^{\alpha\beta} A_3^\beta \right). \tag{5.7}$$

Since this further upgrade of the quasilinear version of NEO-2 [2] affects only the field particle part of the collision operator responsible for momentum conservation, reliable benchmarks of the computed transport coefficients can be performed for axisymmetric tokamak equilibria, see Figure 5.1. In Figure 5.1 a scan of the normalized diffusion coefficient $D_{11}^{\alpha\alpha'}(D_p^{\alpha\alpha'})^{-1}$ over the collisionality parameter is shown for a two-species plasma consisting of deuterium d and carbon C with charge number $Z_C = 3$. Due to momentum conservation, the radial currents must balance in an axisymmetric tokamak equilibrium, i.e., $\sum_\alpha e_\alpha \Gamma_\alpha = 0$. Considering a two species plasma where only one of the thermodynamic forces is non-zero, this leads to a simple relation for the normalized transport coefficients,

$$\frac{D_{1j}^{\alpha\alpha}}{D_{1j}^{\alpha'\alpha}} \frac{D_p^{\alpha'\alpha}}{D_p^{\alpha\alpha}} = \frac{D_{1j}^{\alpha\alpha'}}{D_{1j}^{\alpha'\alpha'}} \frac{D_p^{\alpha'\alpha'}}{D_p^{\alpha\alpha'}} = -\frac{T_{\alpha'} n_{\alpha'}}{T_\alpha n_\alpha} = r_{\alpha,\alpha'}, \tag{5.8}$$

where

$$D_p^{\alpha\alpha'} = \frac{\pi q v_{T,\alpha} \rho_{L,\alpha} \rho_{L,\alpha'}}{16R}, \tag{5.9}$$

R, $v_{T,\alpha}$ and $\rho_{L,\alpha}$ are the plateau diffusion coefficient, major radius, α species thermal velocity and Larmor radius, respectively. Relations (5.8) and (5.9) for the case shown in Figure 5.1 are fulfilled with an accuracy of less than 1% what is in a good agreement with the exact result. Since the only part of the kinetic equation modified for the treatment of multiple species is the collision operator, which is the same for both, the axisymmetric (2.138) and the non-axisymmetric case (2.144), the test presented in Figure 5.1 is also sufficient for the non-axisymmetric multi-species problem.

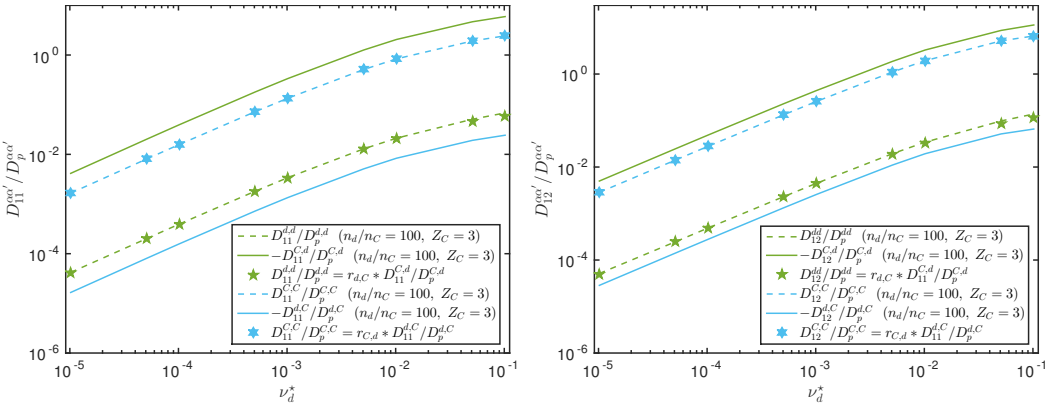

Figure 5.1: Normalized diffusion coefficient for a two-species plasma (deuterium d and carbon C with charge number $Z_C = 3$) as a function of the collisionality parameter $\nu^\star$ with respect to species deuterium (see definitions in Ref. [2]) at aspect ratio $A = 10$.

Chapter 6

Synopsis

Plasma rotation velocity in tokamaks is known to be an important quantity, which has an effect on plasma confinement and direct influence on measurements of plasma and turbulence parameters. Although anomalous effects play a role in radial transport of momentum, they do not provide a volume momentum source (toroidal torque density). Therefore, the computation of plasma rotation is done using the volume sources computed within the framework of neoclassical theory. In its standard form, neoclassical theory uses lowest order expansion in Larmor radius. Typically, plasma rotation in a tokamak is separated into two parts, namely poloidal and toroidal rotation. In contrast to the poloidal velocity, which is strictly determined by the gradient of the ion temperature (see, e.g., Ref [21]), the toroidal velocity is a quantity, which in standard neoclassical theory is linked through a linear relation to the radial electric field and to the ion pressure gradient. Thus, either the radial electric field or the toroidal velocity can be considered as a free parameter, while the other one is determined by a linear relation. Whenever the poloidal velocity differs from its equilibrium value, which is determined by the standard neoclassical theory, it is quickly returned to this value by relaxation processes within the flux surface. In the collisional Pfirsch-Schlüter regime this relaxation process is poloidal (parallel) viscosity. In the long mean free path regime relaxation of poloidal rotation is caused by collisional exchange between trapped and passing particles resulting in

a relaxation time of the order of the ion collision time. Relaxation of the toroidal velocity, however, is due to radial momentum transport, which has a time scale of the order of the profile relaxation time scale. Therefore, toroidal velocity relaxes on a much longer time scale than poloidal velocity. Thus, even a weak source of toroidal momentum can produce a significant change of toroidal velocity, whereas poloidal velocity can hardly be deviated from its equilibrium value.

The general equation governing the toroidal rotation in tokamaks has been analyzed in various papers (e.g., Refs. [35, 41, 3, 80, 71]). This equation includes momentum sources and transport terms, which are responsible for redistribution of toroidal angular momentum over the plasma radius. Although the momentum transport is believed to be dominated by anomalous effects [41], the most important momentum sources can be calculated using existing knowledge. Besides neutral beam injection (NBI), the violation of axial symmetry of the tokamak magnetic field by external magnetic field perturbations is causing an important source term. In particular, such perturbations result from the toroidal field ripple (TF ripple), which is caused by the discreteness of the toroidal field coils. Perturbations can also be produced either unintentionally by errors in the main magnetic field (error field) or deliberately by special coils for mitigation of edge localized modes (ELMs) [81, 82]. External magnetic perturbations can be non-resonant or resonant. Resonant are those perturbations, where the Fourier series expansion of the perturbation vector potential over poloidal ϑ and toroidal φ angles contains those harmonics, which satisfy the resonance condition $m + nq = 0$. Here, m and n are poloidal and toroidal wave numbers, respectively, and q is the safety factor. Resonant harmonics modify the magnetic field topology through creation of islands at resonant surfaces and produce a strongly localized toroidal torque around these surfaces. Non-resonant harmonics do not modify the magnetic field topology and produce a torque, which usually has a much lower radial density but is distributed over the whole plasma volume. In both cases, the generation of toroidal rotation by perturbation fields is due to creation of non-ambipolar particle fluxes, which lead to plasma polarization and, therefore, to changes in the radial electric field.

The torque resulting from non-resonant magnetic perturbations is usually described in terms of neoclassical toroidal viscosity (NTV) [36, 83, 54, 84, 59, 85, 3, 86, 4, 5]. This follows the terminology, which has been introduced for general non-axisymmetric magnetic field configurations in Ref. [37]. In this approach, the electromagnetic field of the perturbation is assumed to satisfy the condition of ideal MHD theory that the total electrostatic potential stays constant on perturbed magnetic flux surfaces. For such perturbed flux surfaces, an associated flux coordinate system with straight field lines is chosen and usually these are Hamada coordinates. With this, the problem of calculation of NTV in a tokamak is reduced to a particular application of neoclassical transport theory for general non-axisymmetric toroidal devices. This general theory has been developed earlier for transport studies in stellarators.

It should be noted that in contrast to stellarators, non-axisymmetric magnetic field perturbations in tokamaks are rather small. Therefore, there exists a variety of regimes where these perturbations can be treated within perturbation theory with respect to their amplitude. The resulting expressions for the NTV torque are then obtained as sums over contributions from separate harmonics of the toroidal perturbation field. Those contributions are quadratic in amplitudes of the harmonics [36, 83, 54, 59, 3, 4, 5]. Such regimes will be called below quasilinear regimes. These quasilinear regimes occur if the mechanism of particle decorrelation from the perturbation field is independent from the perturbation field itself. Namely, this is the case when the phase of the perturbation field is fully determined by parallel and perpendicular ($\mathbf{E} \times \mathbf{B}$ drift and magnetic drift) particle motion within the flux surface and when the perturbation field itself has only a negligible effect on this motion.

Note that for sufficiently small perturbation field amplitudes, besides the non-resonant torque, also the resonant torque can be described within quasilinear theory. In this case, however, the assumption that the perturbed equipotential surfaces coincide with the perturbed magnetic flux surfaces does not hold because ideal MHD theory is not valid in the resonant layer where the plasma response current to the perturbation field and, respec-

tively, the main contribution to the toroidal torque is localized (see, e.g. Refs [87, 88, 44, 89]).

It should be mentioned that the results discussed above basically cover the non-resonant NTV in the whole parameter range of interest. However, all these results have been obtained analytically. This has required certain simplifying assumptions pertinent to particular transport regimes, simplified device geometry, and Coulomb collision models. The overall purpose of the present thesis is to treat quasilinear regimes numerically within a general approach without using any simplifying assumptions on collisionality, geometry, and collision models.

As a result of this work a tool for the numerical evaluation of the NTV torque due to non-resonant magnetic perturbations in a real tokamak device has been developed. This numerical tool, an upgraded version of the code NEO-2 [1, 2], allows for an efficient evaluation of non-ambipolar particle fluxes due to non-axisymmetric electromagnetic field perturbations, which in turn produce a toroidal torque affecting the plasma rotation. This is accomplished without making simplifying assumptions for all quasilinear regimes. Well-established codes for the evaluation of particle fluxes in stellarators as the code DKES [6] make often also use of certain simplifications of the underlying drift kinetic equation. For example, DKES uses a Lorentz collision model and neglects the contribution from magnetic drifts to the poloidal and toroidal rotation velocity. With respect to Monte-Carlo methods [7, 8, 9], which provide also a universal approach for the evaluation of NTV, the numerical approach realized within the upgraded version of NEO-2 is more efficient and thus would allow for the use of NEO-2 within a 1D transport code. The upgraded version of NEO-2 has also been validated and benchmarked against various analytical and semi-analytical models, as well as against the nonlinear codes DKES and SFINCS (see below). The derivations of the theoretical framework for the upgraded code NEO-2 and the results of the extensive benchmarking phase are discussed in Chapter 2 and Chapter 3, respectively. In Chapter 2 aside from the developed theoretical formalism also a re-derivation of the exact toroidal momentum conservation equation and its approximate form including all leading order terms in Larmor radius

and perturbation amplitude is presented.

Furthermore, a procedure for the evaluation of the NTV torque for ASDEX Upgrade discharges has been developed. For the evaluation of the non-ambipolar particle fluxes and of the associated torque density the non-axisymmetric magnetic perturbations have to be known. At the present stage the magnetic field spectrum including the non-axisymmetric magnetic perturbations is computed by the code NEMEC [11] and then transformed to Boozer coordinates using the code COTRANS [66]. Within NEO-2 the magnetic field spectrum of the non-axisymmetric perturbations is transformed to the requested representation, which is given by (2.150). Since the contributions from different toroidal mode numbers to the non-ambipolar particle fluxes are independent of each other within quasilinear theory, the NEO-2 computations can be easily parallelized. For the final evaluation of the non-ambipolar particle fluxes only the individual contributions of the toroidal mode numbers have to be summed up.

Computations of the NTV torque produced in ASDEX Upgrade by the TF ripple and magnetic perturbations from ELM mitigation coils show an agreement between different numerical (NEO-2, SFINCS [13]) and semi-analytical models within their validity domains, see Chapter 4. Specific differences are also observed and discussed here. It is clearly seen that ions as well as electrons contribute to the overall torque. It is remarkable that practically all quasilinear transport regimes except for the highly collisional Pfirsch-Schlüter regime are realized within the single discharge #30835, which is studied here. Various bounce averaged transport regimes as well as resonant regimes are important in specific radial positions. Those regimes have been identified by scans over collisionality and comparison with analytical and semi-analytical computations. The quasilinear approach used in NEO-2 is well justified for computations of the torque driven by RMPs but slightly overestimates the torque from the TF ripple. The amplitude of the perturbations corresponding to the TF ripple is already marginally outside the validity range for the quasilinear approach, mainly because of the high toroidal mode number. The NTV torque is produced mainly at the plasma edge where its density is comparable with the NBI torque density. However,

the integral NTV torque balances only a quarter of the integral NBI torque. This emphasizes the importance of other momentum sources unaccounted here. Some of these sources (e.g. the torque due to fast particle losses) can be computed with present day models. An accurate description of the other sources connected with resonant interaction of magnetic perturbations at rational flux surfaces is still an open problem. Thus, measurements of discharges where the role of resonant interactions is minimized are of future interest. The integral torque balance [71], which can be used to verify the modeling by measurements outside the plasma, is discussed here in some more detail. For this balance, in addition to measurements of the asymmetry of the momentum flux carried by divertor fluxes [71], measurements of charge-exchange neutral spectra and of the currents between the plasma and the wall (divertor target plates) are shown to be of importance. Besides the integral torque balance, an accurate description of the torque density profile resulting from non-axisymmetric magnetic field perturbations would be an important part of turbulent momentum transport studies, where the effect of turbulent momentum flux dominating in $\left\langle \Pi^r_{[\mathrm{in}]\varphi} \right\rangle$ in equation (4.7) on the rotation velocity profile is required in its pure form, i.e. the second term in l.h.s. of (4.7). The state of art of existing models discussed here does already allow for such a description for the NTV torque.

The code NEO-2 has also been upgraded for the computation of the NTV torque in a multi-species plasma, i.e. a plasma with significant impurity content, see Chapter 5. For this further upgrade of the quasilinear version of NEO-2 [2], reliable benchmarks of the computed transport coefficients can be performed for axisymmetric tokamak equilibria because only the field particle part of the collision operator responsible for momentum conservation is affected. Relations (5.8) and (5.9), which result from the balance of radial currents in an axisymmetric tokamak equilibrium, are fulfilled with an accuracy of less than 1% what is in a good agreement with the exact result. Since the only part of the kinetic equation modified for the treatment of multiple species is the collision operator, which is the same for both, the axisymmetric (2.138) and the non-axisymmetric case (2.144), the test presented here is also sufficient for the non-axisymmetric multi-species problem.

The quasilinear version of the code NEO-2 is an evolving tool which has a large capacity for upgrades. An important upgrade would be to allow for the treatment of nonlinear effects (such as observed for the TF ripple in ASDEX Upgrade in comparison with the nonlinear code SFINCS). Since these effects are either small or of the order one, they can be taken into account iteratively using the pre-conditioned iteration procedure, which is already used in NEO-2 for the account of the integral part of the collision operator (this procedure does not generally require the perturbing part of the equation to be small). Another upgrade would be to generalize the approach for the case of Mach numbers of the order one (near-sonic rotations), which might be the case in some experiments. With these upgrades, a universal solution for the NTV problem in tokamaks will be achieved.

Appendices

Appendix A

Non-ambipolar fluxes in the $1/\nu$-regime

A.1 Quasilinear approach

In the $1/\nu$-regime the rotation frequency can be ignored in the kinetic equation (2.166). After inserting the Lorentz collision operator (2.168) into (2.166) and a subsequent multiplication of the result with the normalized bounce time (2.162), following equation is obtained

$$-4\nu_d \frac{\partial}{\partial \eta} \eta I \frac{\partial f_n}{\partial \eta} = in \frac{mcv^2}{3e\sqrt{g_0} B_0^{\vartheta}} \frac{\partial H_n}{\partial \eta} \frac{\partial f_M}{\partial r}, \tag{A.1}$$

where the notation is as follows

$$I = \int_{\vartheta_{\min}}^{\vartheta_{\max}} \frac{\mathrm{d}\vartheta}{B_0^2} \sqrt{1 - \eta B_0}, \tag{A.2}$$

$$H_n = \int_{\vartheta_{\min}}^{\vartheta_{\max}} \frac{\mathrm{d}\vartheta}{B_0^3} \sqrt{1 - \eta B_0}\,(4 - \eta B_0)\, B_n. \tag{A.3}$$

A boundary condition of (A.1) is that the collisional flux at the deeply trapped boundary $\eta = 1/B_0^{\max}$ becomes zero (finite derivative of f_n there).

Using this boundary condition, Eq. (A.1) can be integrated once,

$$\frac{\partial f_n}{\partial \eta} = -in\frac{mcv^2}{12e\sqrt{g_0}B_0^{\vartheta}}\frac{H_n}{\nu_d \eta I}\frac{\partial f_M}{\partial r}. \tag{A.4}$$

After integration over η by parts the flux (2.167) can be expressed through the derivative of the distribution function,

$$\Gamma^{NA} = \sum_{n=1}^{\infty}\frac{\pi mc}{3e\sqrt{g_0}B_0^{\vartheta}}\left(\int_0^{2\pi}\frac{\mathrm{d}\vartheta}{B_0^2}|\nabla r_0|\right)^{-1}\int_0^{\infty}\mathrm{d}v v^4\int_{1/B_0^{\max}}^{1/B_0^{\min}}\mathrm{d}\eta\; n\;\mathrm{Im}\frac{\partial f_n}{\partial \eta}H_n^*. \tag{A.5}$$

Substituting (A.4) and the derivative of the Maxwellian (2.92) into (A.5), the flux density becomes

$$\begin{aligned}\Gamma^{NA} = & -\sum_{n=1}^{\infty}\frac{\pi m^2c^2}{36e^2g_0\left(B_0^{\vartheta}\right)^2}\left(\int_0^{2\pi}\frac{\mathrm{d}\vartheta}{B_0^2}|\nabla r_0|\right)^{-1}\int_0^{\infty}\mathrm{d}v\frac{f_M v^6}{\nu_d}\left(A_1+\frac{mv^2}{2T}A_2\right)\times \\ & \times\int_{1/B_0^{\max}}^{1/B_0^{\min}}\mathrm{d}\eta\;\frac{n^2|H_n|^2}{\eta I}.\end{aligned} \tag{A.6}$$

The flux density (A.6) is transformed to the form (2.169) by changing the integration variable from v to the normalized kinetic energy (2.171), whereby the effective ripple is defined as

$$\epsilon_{\mathrm{eff}}^{3/2} = \frac{\pi}{16\sqrt{2}}\frac{R^2B_{\mathrm{ref}}^2}{g_0(B_0^{\vartheta})^2}\left(\int_0^{2\pi}\frac{\mathrm{d}\vartheta}{B_0^2}|\nabla r_0|\right)^{-1}\sum_{n=1}^{\infty}\int_{1/B_0^{\max}}^{1/B_0^{\min}}\mathrm{d}\eta\;\frac{n^2|H_n|^2}{\eta I}. \tag{A.7}$$

Note that in the version of Boozer coordinates used here the flux surface label r_0 is an arbitrary flux function. The definition of the effective ripple of Ref. [10] specifies it as an effective radius fixed by the condition (2.5), which

in Boozer coordinates is

$$\int_0^{2\pi} \frac{\mathrm{d}\vartheta}{B_0^2} |\nabla r_0| = \int_0^{2\pi} \frac{\mathrm{d}\vartheta}{B_0^2}. \tag{A.8}$$

Original Boozer coordinates use the normalized toroidal flux ψ as a flux surface label where

$$\psi(r) = \frac{1}{2\pi} \int_0^r \mathrm{d}r' \int_0^{2\pi} \mathrm{d}\vartheta \sqrt{g} B^\varphi = \int_0^r \mathrm{d}r' \sqrt{g} B^\varphi. \tag{A.9}$$

From this expression above it follows that

$$\frac{\mathrm{d}\psi}{\mathrm{d}r} = q\sqrt{g_0} B_0^\vartheta. \tag{A.10}$$

Using this relation and condition (A.8) in (A.7), one obtains the effective ripple in the form (2.172).

Next it is checked that the quasilinear limit (2.172) agrees with the general expression for the effective ripple, Eq. (43) of Ref. [10]. It should be noted that a change of the field line integration variable, from the toroidal angle ζ to the poloidal angle θ, reduces to the simultaneous replacement of the differential $\mathrm{d}\zeta$ with $\mathrm{d}\theta$ in Eqs. (43), (44) and (45) of Ref. [10] because the safety factor cancels out. The integration limits, of course, should also be changed. Due to the first condition in Eq. (2.89), which is required for the applicability of the quasilinear limit, blocked particles are absent while the amount of particles trapped in more than one toroidal well scales with the amplitude of the perturbation field, i.e. it is negligibly small compared to the amount of single trapped particles. Thus, various classes mean just single trapped particles in different toroidal field periods on the field line and the summation index j in Eq. (44) of Ref. [10] just enumerates these periods. Since one has to label now the field line with $\varphi_0 = \zeta - q\theta$, last parentheses

in Eq. (44) of Ref. [10] are rewritten as

$$I\frac{\partial B}{\partial \zeta} - J\frac{\partial B}{\partial \theta} = q(J + \iota I)\frac{\partial B}{\partial \varphi_0} - J\frac{\partial B}{\partial \theta}, \tag{A.11}$$

and the last term here does not contribute to the integral because it is a derivative along the field line. Since the axisymmetric field does not contribute to the first term, one can see that this term provides the leading order contribution. The perturbation field should be ignored elsewhere because it gives just a next order correction. Thus, Eq. (44) of Ref. [10] is simplified to

$$H_{fj} => H_{(j)} = \frac{q}{b'}\int \frac{\mathrm{d}\theta}{B_0^2}\sqrt{b' - \frac{B_0}{B_{\mathrm{ref}}}}\left(4\frac{B_{\mathrm{ref}}}{B_0} - \frac{1}{b'}\right)\frac{\partial}{\partial \varphi_0}\delta B(\theta, \varphi_0 + 2\pi q j), \tag{A.12}$$

where the periodicity has been used to transform the θ values to the first toroidal period on the field line. Note that B_0 in Ref. [10] is used for the reference magnetic field value, whereas the notation in (A.12) follows the notation of Ref. [2]. Since only leading order contributions of the perturbation field are considered, explicit field line integrals in Eq. (44) of Ref. [10] can be replaced by integrals over one poloidal period times the number of periods on the field line, $j_{\max}$. Quantity I_{fj}, Eq. (45) of Ref. [10], is then the same for all periods and, after the replacement of differentials, is the same with quantity I, Eq. (A.2), if one considers $B_{\mathrm{ref}}b' = 1/\eta$. Thus, Eq. (44) of Ref. [10] is transformed to

$$\epsilon_{\mathrm{eff}}^{3/2} = \frac{\pi R^2}{8\sqrt{2}}\int_0^{2\pi}\frac{\mathrm{d}\vartheta}{B_0^2}\left(\int_0^{2\pi}\frac{\mathrm{d}\vartheta}{B_0^2}|\nabla\psi|\right)^{-2}\int \mathrm{d}b'\frac{1}{I}\lim_{j_{\max}\to\infty}\frac{1}{j_{\max}}\sum_{j=1}^{j_{\max}} H_{(j)}^2, \tag{A.13}$$

where $|\nabla\psi| = \sqrt{g^{11}}$. In order to obtain equation (2.172), the integration variable is changed from b' to $\eta = 1/(B_{\mathrm{ref}}b')$, as well as the Fourier series representation of δB (2.150) and the following identity valid for a periodic

function $F(\varphi_0)$ and irrational q,

$$\lim_{j_{\max}\to\infty} \frac{1}{j_{\max}} \sum_{j=1}^{j_{\max}} F(\varphi_0 + 2\pi q j) = \overline{F}, \tag{A.14}$$

are used.

A.2 Shaing's approach

In this section the result for the non-ambipolar particle flux given by Eq. (16) of Ref. [36] is re-derived. The flux surface averaged particle flux across the flux surface is defined in Ref. [36] as

$$\Gamma^{\text{Shaing}} = \langle n_\alpha \mathbf{V} \cdot \nabla V \rangle \qquad \text{with} \qquad n_\alpha \mathbf{V} \;=\; \int \mathrm{d}^3 v \; \mathbf{v} f, \tag{A.15}$$

where f denotes the first order perturbed distribution function and the flux surface label V is here the volume enclosed by the flux surface divided by $4\pi^2$. Introducing the drift velocity $\mathbf{v}_d$ and Hamada coordinates $(V, \vartheta_{\mathrm{H}}, \varphi_{\mathrm{H}})$, one can express the particle flux through

$$\Gamma^{\text{Shaing}} = \left\langle \int \mathrm{d}^3 v \; f \left(\mathbf{v}_d \cdot \nabla V \right) \right\rangle \;= \frac{1}{4\pi^2} \int_0^{2\pi} \int_0^{2\pi} \mathrm{d}\vartheta_{\mathrm{H}} \mathrm{d}\varphi_{\mathrm{H}} \int \mathrm{d}^3 v \; f \left(\mathbf{v}_d \cdot \nabla V \right). \tag{A.16}$$

In order to evaluate the expression for the particle flux, the contra-variant radial component of the drift velocity $\mathbf{v}_d \cdot \nabla V$ is expressed in terms of $(\partial f_{10}/\partial \eta)^2$. Using the linearized drift kinetic equation

$$v_\parallel \mathbf{h} \cdot \nabla f + \mathbf{v}_d \cdot \nabla V \; \frac{\partial f_M}{\partial V} = C(f) \qquad \text{with} \qquad \mathbf{h} \;=\; \frac{\mathbf{B}}{B}, \tag{A.17}$$

the following relation for the drift velocity is obtained

$$\mathbf{v}_d \cdot \nabla V = \left(\frac{\partial f_M}{\partial V} \right)^{-1} \left[C(f) - v_\parallel \mathbf{h} \cdot \nabla f \right]. \tag{A.18}$$

Equation (A.18) can be simplified, if one makes use of the Clebsch form of the B-field by introducing a new set of Hamada coordinates $(V, \vartheta_{\mathrm{H}}, \varphi_{\mathrm{H},0})$,

$$\mathbf{B} = \psi' \, \nabla V \times \nabla \vartheta_{\mathrm{H}} - \chi' \, \nabla V \times \nabla \varphi_{\mathrm{H}} = \nabla \chi \times \nabla \varphi_{\mathrm{H},0}, \tag{A.19}$$

where $\varphi_{\mathrm{H},0} = q\vartheta_{\mathrm{H}} - \varphi_{\mathrm{H}}$ and $q = \psi'/\chi'$ has been used. From this B-field representation one can immediately see that $\mathbf{B} \cdot \nabla V = \mathbf{B} \cdot \nabla \varphi_{\mathrm{H},0} = 0$ and the only non-vanishing component is $\mathbf{B} \cdot \nabla \vartheta_{\mathrm{H}} = \chi'/(\sqrt{g})_{\mathrm{H}}$. Now, the second term in the square brackets of Eq. (A.18) is inspected,

$$v_{\parallel} \mathbf{h} \cdot \nabla f = \frac{v_{\parallel}}{B} \, \frac{\chi'}{(\sqrt{g})_{\mathrm{H}}} \, \frac{\partial f}{\partial \vartheta_{\mathrm{H}}} \; = \; 0. \tag{A.20}$$

Since the lowest order distribution function from bounce averaged theory is of main interest here, i.e. $f = f_{10}$, the last identity in Eq. (A.20) follows from Eq. (11) of Ref. [36]. Finally, one obtains for the drift velocity

$$\mathbf{v}_d \cdot \nabla V = \left(\frac{\partial f_M}{\partial V} \right)^{-1} \, C(f_{10}), \tag{A.21}$$

whereby the Lorentz collision operator $C(f)$ is given by

$$\begin{aligned} C(f) \;&=\; \nu_D \, \frac{\sigma v \sqrt{1 - \eta B_0}}{B_0} \, \frac{2}{mv^2} \, \frac{\partial}{\partial \eta} \, m \, \frac{mv^2 \eta}{2} \, \sigma v \sqrt{1 - \eta B_0} \, \frac{2}{mv^2} \, \frac{\partial f}{\partial \eta} \\ &=\; \frac{2\nu_D}{B_0} \, \sqrt{1 - \eta B_0} \, \frac{\partial}{\partial \eta} \, \eta \sqrt{1 - \eta B_0} \, \frac{\partial f}{\partial \eta}. \end{aligned} \tag{A.22}$$

The derivative of f_{10} over η appearing in Eq. (A.22) can be obtained by bounce-averaging the equation for the next order correction f_{11}, see Eq. (12) of Ref. [36], and a subsequent integration over the normalized perpendicular adiabatic invariant,

$$\frac{\partial f_{10}}{\partial \eta} = \frac{cmv^2}{2e\chi' \nu_D} \, \frac{\partial f_M}{\partial V} \, \frac{\oint \mathrm{d}\vartheta_{\mathrm{H}} \sqrt{1 - \eta B_0} \, \frac{\partial B}{\partial \varphi_{\mathrm{H},0}}}{\oint \mathrm{d}\vartheta_{\mathrm{H}} \sqrt{1 - \eta B_0}}. \tag{A.23}$$

In terms of the new angular coordinates $(\vartheta_{\rm H},\varphi_{\rm H,0})$,

$$\begin{pmatrix} \mathrm{d}\vartheta_{\rm H} \\ \mathrm{d}\varphi_{\rm H,0} \end{pmatrix} = \begin{pmatrix} 1 & 0 \\ q & -1 \end{pmatrix} \cdot \begin{pmatrix} \mathrm{d}\vartheta_{\rm H} \\ \mathrm{d}\varphi_{\rm H} \end{pmatrix} \qquad \text{and} \qquad (\sqrt{g})_{\rm H,0} \;=\; -(\sqrt{g})_{\rm H}, \quad \text{(A.24)}$$

the flux surface average becomes

$$\frac{1}{4\pi^2}\int\limits_0^{2\pi}\int\limits_0^{2\pi} \mathrm{d}\vartheta_{\rm H}\mathrm{d}\varphi_{\rm H} = -\frac{1}{4\pi^2}\int\limits_0^{2\pi} \mathrm{d}\vartheta_{\rm H} \int\limits_{q\vartheta_{\rm H}}^{q\vartheta_{\rm H}-2\pi} \mathrm{d}\varphi_{\rm H,0}. \qquad \text{(A.25)}$$

Using these intermediate steps and the expression for the velocity space jacobian, see Eq. (7.21) of Ref. [21], the particle flux becomes

$$\begin{aligned}
\Gamma^{\rm Shaing} \;=\; & -\frac{1}{4\pi^2}\int\limits_0^{2\pi} \mathrm{d}\vartheta_{\rm H} \int\limits_{q\vartheta_{\rm H}}^{q\vartheta_{\rm H}-2\pi} \mathrm{d}\varphi_{\rm H,0} \int\limits_0^{\infty} \mathrm{d}v \int\limits_0^{1/B_0(\vartheta_{\rm H})} \mathrm{d}\eta \sum_{\sigma=\pm 1} \frac{\pi v^2 B_0}{\sqrt{1-\eta B_0}}\, f_{10} \times \\
& \times \left(\frac{\partial f_M}{\partial V}\right)^{-1} \frac{2\nu_D}{B_0}\sqrt{1-\eta B_0}\,\frac{\partial}{\partial \eta}\,\eta\sqrt{1-\eta B_0}\,\frac{\partial f_{10}}{\partial \eta} \\
= \; & -\sum_{\sigma=\pm 1}\frac{1}{2\pi}\int\limits_0^{2\pi} \mathrm{d}\vartheta_{\rm H} \int\limits_{q\vartheta_{\rm H}}^{q\vartheta_{\rm H}-2\pi} \mathrm{d}\varphi_{\rm H,0} \int\limits_0^{\infty} \mathrm{d}v\, v^2\nu_D \left(\frac{\partial f_M}{\partial V}\right)^{-1} \int\limits_0^{1/B_0(\vartheta_{\rm H})} \mathrm{d}\eta \;\times \\
& \times f_{10}\,\frac{\partial}{\partial \eta}\,\eta\sqrt{1-\eta B_0}\,\frac{\partial f_{10}}{\partial \eta} \\
= \; & -\sum_{\sigma=\pm 1}\frac{1}{2\pi}\int\limits_0^{2\pi} \mathrm{d}\vartheta_{\rm H} \int\limits_{q\vartheta_{\rm H}}^{q\vartheta_{\rm H}-2\pi} \mathrm{d}\varphi_{\rm H,0} \int\limits_0^{\infty} \mathrm{d}v\; v^2\nu_D \left(\frac{\partial f_M}{\partial V}\right)^{-1} \int\limits_0^{1/B_0(\vartheta_{\rm H})} \mathrm{d}\eta \;\times \\
& \times \left\{\frac{\partial}{\partial \eta}\, f_{10}\,\eta\sqrt{1-\eta B_0}\,\frac{\partial f_{10}}{\partial \eta} - \eta\sqrt{1-\eta B_0}\,\frac{\partial f_{10}}{\partial \eta}\,\frac{\partial f_{10}}{\partial \eta}\right\}. \qquad \text{(A.26)}
\end{aligned}$$

The first term in the curly brackets of Eq. (A.26) vanishes upon integration over η at the upper and lower boundary. By substituting the result for the first order distribution function from bounce averaged theory (A.23) into

Eq. (A.26), following expression for the particle flux is obtained

$$\Gamma^{\text{Shaing}} = \sum_{\sigma=\pm 1} \frac{1}{2\pi} \int_0^{2\pi} \mathrm{d}\vartheta_\mathrm{H} \int_{q\vartheta_\mathrm{H}}^{q\vartheta_\mathrm{H}-2\pi} \mathrm{d}\varphi_{\mathrm{H},0} \int_0^\infty \mathrm{d}v v^2 \nu_D \left(\frac{\partial f_M}{\partial V}\right) \int_0^{1/B_0(\vartheta_\mathrm{H})} \mathrm{d}\eta\, \eta \times$$
$$\times \sqrt{1-\eta B_0(\vartheta_\mathrm{H})} \left(\frac{cmv^2}{2e\chi'\nu_D}\right)^2 \frac{\left(\oint \mathrm{d}\tilde{\vartheta}_\mathrm{H} \sqrt{1-\eta B_0(\tilde{\vartheta}_\mathrm{H})} \frac{\partial B(\tilde{\vartheta}_\mathrm{H},\varphi_{\mathrm{H},0})}{\partial \varphi_{\mathrm{H},0}}\right)^2}{\left(\oint \mathrm{d}\tilde{\vartheta}_\mathrm{H} \sqrt{1-\eta B_0(\tilde{\vartheta}_\mathrm{H})}\right)^2}. \tag{A.27}$$

In order to obtain the result in the desired form, one has to interchange the integration over η with ϑ_H and to evaluate the integral over $\varphi_{\mathrm{H},0}$.

Since there is zero collisional flux at the deeply trapped boundary, $\eta = 1/B_0^{\max}$, only the integral over the trapped particle domain remains,

$$\int_0^{2\pi} \mathrm{d}\vartheta_\mathrm{H} \int_0^{1/B_0(\vartheta_\mathrm{H})} \mathrm{d}\eta = \int_0^{2\pi} \mathrm{d}\vartheta_\mathrm{H} \int_{1/B_0^{\max}}^{1/B_0(\vartheta_\mathrm{H})} \mathrm{d}\eta\,. \tag{A.28}$$

The permutation of the integrals over ϑ_H and η involves a non-injective function and, therefore, one has to split the integral into two parts. Furthermore, the axisymmetric magnetic field is assumed to be circular, $B_0 \approx \hat{B}_0(1 - \epsilon\cos\vartheta_\mathrm{H})$, and the border of the integral given by $\eta_\mathrm{b}(\vartheta_\mathrm{H}) = 1/(\hat{B}_0(1-\epsilon\cos\vartheta_\mathrm{H})$ is expressed in terms of ϑ_H,

$$\vartheta_\mathrm{H} = \arccos\left(\frac{1}{\epsilon}\left(1 - \frac{1}{\eta\hat{B}_0}\right)\right). \tag{A.29}$$

Now one can permute the order of the integrals in Eq. (A.28),

$$\int_0^{2\pi} \mathrm{d}\vartheta_\mathrm{H} \int_0^{1/B_0(\vartheta_\mathrm{H})} \mathrm{d}\eta = \int_{1/B_0^{\max}}^{1/B_0^{\min}} \mathrm{d}\eta \left[\int_{-\arccos\frac{\eta\hat{B}_0-1}{\eta\hat{B}_0\epsilon}}^{0} \mathrm{d}\vartheta_\mathrm{H} + \int_0^{\arccos\frac{\eta\hat{B}_0-1}{\eta\hat{B}_0\epsilon}} \mathrm{d}\vartheta_\mathrm{H} \right]$$
$$= \int_{1/B_0^{\max}}^{1/B_0^{\min}} \mathrm{d}\eta \int_{-\arccos\frac{\eta\hat{B}_0-1}{\eta\hat{B}_0\epsilon}}^{\arccos\frac{\eta\hat{B}_0-1}{\eta\hat{B}_0\epsilon}} \mathrm{d}\vartheta_\mathrm{H} \,. \qquad \text{(A.30)}$$

It is convenient to write the boundaries of the integral over ϑ_H in terms of turning points of the banana motion, $\vartheta_\mathrm{H}^{\max} = -\vartheta_\mathrm{H}^{\min}$. The turning points are related to the trapping parameter κ by the relation $\kappa_\mathrm{b} = \sin\vartheta_\mathrm{H}^{\max}$ and, in turn, the trapping parameter is related to η via $\kappa^2 = (1-\eta\hat{B}_0(1-\epsilon))/(2\epsilon\eta\hat{B}_0)$. Using these relations, one obtains for the upper boundary,

$$\vartheta_\mathrm{H}^{\max} = \arccos\left(\frac{\eta\hat{B}_0 - 1}{\eta\hat{B}_0\epsilon}\right). \qquad \text{(A.31)}$$

Finally, the subsequent expression is obtained for the interchanged integrals,

$$\int_0^{2\pi} \mathrm{d}\vartheta_\mathrm{H} \int_0^{1/B_0(\vartheta_\mathrm{H})} \mathrm{d}\eta = \int_{1/B_0^{\max}}^{1/B_0^{\min}} \mathrm{d}\eta \int_{\vartheta_\mathrm{H}^{\min}}^{\vartheta_\mathrm{H}^{\max}} \mathrm{d}\vartheta_\mathrm{H} = \int_{1/B_0^{\max}}^{1/B_0^{\min}} \mathrm{d}\eta \oint \mathrm{d}\vartheta_\mathrm{H} \,. \qquad \text{(A.32)}$$

Next the integral over $\varphi_{\mathrm{H},0}$ is evaluated. Since the nominator of Eq. (A.27) is the only term that depends on $\varphi_{\mathrm{H},0}$, the integral over $\varphi_{\mathrm{H},0}$ reduces to

$$I_{\varphi_{\mathrm{H},0}} = \int_{q\vartheta_\mathrm{H}}^{q\vartheta_\mathrm{H}-2\pi} \mathrm{d}\varphi_{\mathrm{H},0} \left(\oint \mathrm{d}\tilde{\vartheta}_\mathrm{H} \sqrt{1-\eta B_0(\tilde{\vartheta}_\mathrm{H})} \, \frac{\partial B(\tilde{\vartheta}_\mathrm{H}, \varphi_{\mathrm{H},0})}{\partial \varphi_{\mathrm{H},0}} \right)^2 , \qquad \text{(A.33)}$$

where the derivative of the module of the magnetic field over $\varphi_{\mathrm{H},0}$ is expressed

in terms of a Fourier series,

$$\frac{\partial B(\tilde{\vartheta}_{\mathrm{H}},\varphi_{\mathrm{H},0})}{\partial\varphi_{\mathrm{H},0}} = \hat{B}_0 \sum_{n=1}^{\infty} n \left\{ A_n\left(\tilde{\vartheta}_{\mathrm{H}}\right)\sin\left(n\varphi_{\mathrm{H},0}\right) - B_n\left(\tilde{\vartheta}_{\mathrm{H}}\right)\cos\left(n\varphi_{\mathrm{H},0}\right)\right\} . \tag{A.34}$$

Then integrals over $\tilde{\vartheta}_{\mathrm{H}}$ and $\varphi_{\mathrm{H},0}$ are interchanged,

$$\begin{aligned} I_{\varphi_{\mathrm{H},0}} = \hat{B}_0^2 \sum_{n,n'=1}^{\infty} nn' \oint \mathrm{d}\tilde{\vartheta}_{\mathrm{H}} \sqrt{1-\eta B_0(\tilde{\vartheta}_{\mathrm{H}})} \oint \mathrm{d}\hat{\vartheta}_{\mathrm{H}} \sqrt{1-\eta B_0(\hat{\vartheta}_{\mathrm{H}})} \int_{q\vartheta_{\mathrm{H}}}^{q\vartheta_{\mathrm{H}}-2\pi} \mathrm{d}\varphi_{\mathrm{H},0} \times \\ \times \left\{ A_n\left(\tilde{\vartheta}_{\mathrm{H}}\right) A_{n'}\left(\hat{\vartheta}_{\mathrm{H}}\right) \sin\left(n\varphi_{\mathrm{H},0}\right)\sin\left(n'\varphi_{\mathrm{H},0}\right) + B_n\left(\tilde{\vartheta}_{\mathrm{H}}\right) B_{n'}\left(\hat{\vartheta}_{\mathrm{H}}\right) \right. \\ \cos\left(n\varphi_{\mathrm{H},0}\right)\cos\left(n'\varphi_{\mathrm{H},0}\right) - A_n\left(\tilde{\vartheta}_{\mathrm{H}}\right) B_{n'}\left(\hat{\vartheta}_{\mathrm{H}}\right) \sin\left(n\varphi_{\mathrm{H},0}\right)\cos\left(n'\varphi_{\mathrm{H},0}\right) - \\ \left. - B_n\left(\tilde{\vartheta}_{\mathrm{H}}\right) A_{n'}\left(\hat{\vartheta}_{\mathrm{H}}\right) \cos\left(n\varphi_{\mathrm{H},0}\right)\sin\left(n'\varphi_{\mathrm{H},0}\right)\right\} . \end{aligned} \tag{A.35}$$

Only the first two terms provide non-vanishing contributions to the integral $I_{\varphi_{\mathrm{H},0}}$ in case of $n = n'$, e.g., the first term in Eq. (A.35) evaluates to

$$\int_{q\vartheta_{\mathrm{H}}}^{q\vartheta_{\mathrm{H}}-2\pi} \mathrm{d}\varphi_{\mathrm{H},0} \sin\left(n\varphi_{\mathrm{H},0}\right)\sin\left(n'\varphi_{\mathrm{H},0}\right) \;=\; -\pi\delta_{n,n'}. \tag{A.36}$$

Thus, the integral over $\varphi_{\mathrm{H},0}$ is reduced to

$$\begin{aligned} I_{\varphi_{\mathrm{H},0}} \;=\; \left(-\pi\hat{B}_0^2\right) \sum_{n=1}^{\infty} n^2 \left\{ \left(\oint \mathrm{d}\tilde{\vartheta}_{\mathrm{H}} \sqrt{1-\eta B_0(\tilde{\vartheta}_{\mathrm{H}})} A_n\left(\tilde{\vartheta}_{\mathrm{H}}\right)\right)^2 + \right. \\ \left. + \left(\oint \mathrm{d}\tilde{\vartheta}_{\mathrm{H}} \sqrt{1-\eta B_0(\tilde{\vartheta}_{\mathrm{H}})} B_n\left(\tilde{\vartheta}_{\mathrm{H}}\right)\right)^2 \right\} . \end{aligned} \tag{A.37}$$

In order to get the particle flux given by Eq. (A.27) in its desired form, one has to express the derivative of the Maxwellian in terms of thermodynamic forces,

$$\frac{\partial f_M}{\partial V} = f_M \left[\left(\frac{p'}{p} + \frac{e\Phi'}{T} \right) + \left(\frac{mv^2}{2T} - \frac{5}{2} \right) \frac{T'}{T} \right] \quad \text{with} \quad f_M \;=\; \frac{n_\alpha}{\pi^{3/2} v_T^3}\, \mathrm{e}^{-v^2/v_T^2} , \tag{A.38}$$

and to exchange the integration variable v by $z = v^2/v_T^2$. Then, the integral over the velocity module v becomes

$$\int_0^\infty \frac{\mathrm{d}v v^6}{\nu_D}\frac{\partial f_M}{\partial V} = \frac{v_T^4\, n_\alpha}{\nu_t\, \pi^{3/2}}\left[\lambda_1\left(\frac{p'}{p}+\frac{e\Phi'}{T}\right)+\lambda_2\left(\frac{mv^2}{2T}-\frac{5}{2}\right)\frac{T'}{T}\right]$$

$$\text{with}\quad \lambda_j = \frac{1}{2}\int_0^\infty \mathrm{d}z\, \mathrm{e}^{-z}\, z^{5/2}\left(z-\frac{5}{2}\right)^{j-1}\frac{\nu_t}{\nu_D}\,. \tag{A.39}$$

Inserting Eq. (A.32), Eq. (A.37) and Eq. (A.39) into Eq. (A.27), one obtains for the particle flux the expression,

$$\Gamma^{\mathrm{Shaing}} = -\frac{n_\alpha}{4\pi^{3/2}}\left(\frac{cm}{e\chi'}\right)^2\left[\lambda_1\left(\frac{p'}{p}+\frac{e\Phi'}{T}\right)+\lambda_2\frac{T'}{T}\right]\int_{1/B_0^{\max}}^{1/B_0^{\min}}\mathrm{d}\eta\eta\hat{B}_0^2\times$$
$$\times\left(\oint \mathrm{d}\tilde{\vartheta}_{\mathrm{H}}\sqrt{1-\eta B_0}\right)^{-1}\sum_{n=1}^{\infty} n^2\left\{\left(\oint \mathrm{d}\tilde{\vartheta}_{\mathrm{H}}\sqrt{1-\eta B_0}\,A_n\left(\tilde{\vartheta}_{\mathrm{H}}\right)\right)^2+\right.$$
$$\left.+\left(\oint \mathrm{d}\tilde{\vartheta}_{\mathrm{H}}\sqrt{1-\eta B_0}\,B_n\left(\tilde{\vartheta}_{\mathrm{H}}\right)\right)^2\right\}, \tag{A.40}$$

which agrees with the results given by Eq. (16) of Ref. [36] and Eq. (7) of Ref. [3], respectively.

Appendix B

Relation between Boozer and Hamada coordinates

B.1 Coordinate Transformation

Let $(s,\vartheta_\mathrm{B},\varphi_\mathrm{B})$ denote the Boozer coordinates of a given point in space, where $s = \psi_\mathrm{tor}/\psi^a_\mathrm{tor}$ is the normalized toroidal flux, and let $(\hat{V},\vartheta_\mathrm{H},\varphi_\mathrm{H})$ denote the Hamada coordinates of the respective point in space, where $\hat{V} = V/(4\pi^2)$ is the normalized volume. Then, the Jacobians of Boozer coordinates and Hamada coordinates are

$$\sqrt{g_\mathrm{B}} = \psi^a_\mathrm{tor}\,\frac{\iota B_{\vartheta_\mathrm{B}} + B_{\varphi_\mathrm{B}}}{B^2} \quad \text{and} \quad \sqrt{g_\mathrm{H}} \;=\; 1, \tag{B.1}$$

respectively. The equations of transformations between the angles are given by the following relations

$$\begin{aligned} \vartheta_\mathrm{H} &= \vartheta_\mathrm{B} + \frac{\mathrm{d}\Psi_\mathrm{pol}}{\mathrm{d}s} G_\mathrm{H}(s,\vartheta_\mathrm{B},\varphi_\mathrm{B}) \quad \text{with} \quad \frac{\mathrm{d}\Psi_\mathrm{pol}}{\mathrm{d}s} = 2\pi\iota\psi^a_\mathrm{tor} \\ \varphi_\mathrm{H} &= \varphi_\mathrm{B} + \frac{\mathrm{d}\Psi_\mathrm{tor}}{\mathrm{d}s} G_\mathrm{H}(s,\vartheta_\mathrm{B},\varphi_\mathrm{B}) \quad \text{with} \quad \frac{\mathrm{d}\Psi_\mathrm{tor}}{\mathrm{d}s} = 2\pi\psi^a_\mathrm{tor}. \end{aligned} \tag{B.2}$$

Using this set of transformation equations, the Jacobian of Hamada coordinates can be expressed through Boozer coordinates,

$$\begin{aligned}\left(\sqrt{g_{\mathrm{H}}}\right)^{-1} &= \left(\sqrt{g_{\mathrm{B}}}\right)^{-1} \frac{\mathrm{d}\hat{V}}{\mathrm{d}s} \left[1 + 2\pi\psi^a_{\mathrm{tor}} \left(\iota \frac{\partial}{\partial \vartheta_{\mathrm{B}}} + \frac{\partial}{\partial \varphi_{\mathrm{B}}}\right) G_{\mathrm{H}}\right] \\ &= \frac{\mathrm{d}\hat{V}}{\mathrm{d}s} \left[\left(\sqrt{g_{\mathrm{B}}}\right)^{-1} + 2\pi \left(\mathbf{B}\cdot\nabla\right) G_{\mathrm{H}}\right]. \end{aligned} \tag{B.3}$$

Equation (B.3) is of the form of a magnetic differential equation,

$$\left(\mathbf{B}\cdot\nabla\right) G_{\mathrm{H}} = \frac{1}{2\pi} \left[\left(\frac{\mathrm{d}\hat{V}}{\mathrm{d}s}\right)^{-1} - \left(\sqrt{g_{\mathrm{B}}}\right)^{-1}\right] \equiv S, \tag{B.4}$$

which has to fulfill certain solubility conditions. A magnetic differential equation can be solved by expanding the transformation function G_{H} and the source term S in a Fourier series,

$$\begin{aligned}\sqrt{g_{\mathrm{B}}} S &= \Re\left\{\sum_{m,n} a^{(\mathrm{B})}_{mn}(s)\ e^{i(m\vartheta_{\mathrm{B}} + n\varphi_{\mathrm{B}})}\right\} \\ G_{\mathrm{H}} &= \Re\left\{\sum_{m,n} G^{(\mathrm{B})}_{\mathrm{H},mn}(s)\ e^{i(m\vartheta_{\mathrm{B}} + n\varphi_{\mathrm{B}})}\right\}, \end{aligned} \tag{B.5}$$

whereby the Fourier coefficients $a^{(\mathrm{B})}_{mn}$ are given by the relation

$$\begin{aligned} a^{(\mathrm{B})}_{mn}(s) &= \frac{1}{(2\pi)^2} \int_0^{2\pi} \mathrm{d}\vartheta_{\mathrm{B}} \int_0^{2\pi} \mathrm{d}\varphi_{\mathrm{B}} \left(\sqrt{g_{\mathrm{B}}} S\right) e^{-i(m\vartheta_{\mathrm{B}} + n\varphi_{\mathrm{B}})} \\ &= \frac{\psi^a_{\mathrm{tor}} \left(\iota B_{\vartheta_{\mathrm{B}}} + B_{\varphi_{\mathrm{B}}}\right)}{2\pi\left(\mathrm{d}V/\mathrm{d}s\right)} \left(\int_0^{2\pi} \mathrm{d}\vartheta_{\mathrm{B}} \int_0^{2\pi} \mathrm{d}\varphi_{\mathrm{B}} \frac{e^{-i(m\vartheta_{\mathrm{B}} + n\varphi_{\mathrm{B}})}}{B^2}\right) - \frac{\delta_{m,0}\delta_{n,0}}{2\pi}. \end{aligned} \tag{B.6}$$

Inserting Eq. (B.5) into Eq. (B.4) gives the relation for the unknown Fourier coefficients of the transformation function $G^{(\mathrm{B})}_{\mathrm{H},mn}$,

$$G^{(\mathrm{B})}_{\mathrm{H},mn} = -i\ \frac{a^{(\mathrm{B})}_{mn}}{\psi^a_{\mathrm{tor}}\,(\iota m + n)}. \tag{B.7}$$

Using the transformation function, the Fourier spectrum of the magnetic field in Hamada coordinates can be evaluated in terms of Boozer coordinates,

$$\begin{aligned} B^{(\mathrm{H})}_{mn} &= \frac{1}{(2\pi)^2}\int_0^{2\pi}\mathrm{d}\vartheta_{\mathrm{H}}\int_0^{2\pi}\mathrm{d}\varphi_{\mathrm{H}}\ B\ e^{-i(m\vartheta_{\mathrm{H}}+n\varphi_{\mathrm{H}})} \\ &= \frac{1}{(2\pi)^2}\int_0^{2\pi}\mathrm{d}\vartheta_{\mathrm{B}}\int_0^{2\pi}\mathrm{d}\varphi_{\mathrm{B}}\ \left|\frac{\partial\,(\vartheta_{\mathrm{H}},\varphi_{\mathrm{H}})}{\partial\,(\vartheta_{\mathrm{B}},\varphi_{\mathrm{B}})}\right|\ B\ e^{-i(m\vartheta_{\mathrm{H}}(\vartheta_{\mathrm{B}},\varphi_{\mathrm{B}})+n\varphi_{\mathrm{H}}(\vartheta_{\mathrm{B}},\varphi_{\mathrm{B}}))}, \end{aligned} \tag{B.8}$$

where the Jacobian $\left|\frac{\partial(\vartheta_{\mathrm{H}},\varphi_{\mathrm{H}})}{\partial(\vartheta_{\mathrm{B}},\varphi_{\mathrm{B}})}\right|$ is expressed through $\sqrt{g_{\mathrm{B}}}$ and $\sqrt{g_{\mathrm{H}}}$,

$$\left|\frac{\partial\,(\vartheta_{\mathrm{H}},\varphi_{\mathrm{H}})}{\partial\,(\vartheta_{\mathrm{B}},\varphi_{\mathrm{B}})}\right| \;=\; \left|\frac{\partial\big(\hat{V},\vartheta_{\mathrm{H}},\varphi_{\mathrm{H}}\big)}{\partial\big(s,\vartheta_{\mathrm{B}},\varphi_{\mathrm{B}}\big)}\right|\ \left|\frac{\mathrm{d}s}{\mathrm{d}\hat{V}}\right| \;=\; \left|\frac{\mathrm{d}s}{\mathrm{d}\hat{V}}\right|\ \frac{\sqrt{g_{\mathrm{B}}}}{\sqrt{g_{\mathrm{H}}}}. \tag{B.9}$$

For the numerical evaluation the expression for magnetic field spectrum in Hamada coordinates is rewritten so that only angle-dependent quantities appear inside the integral,

$$B^{(\mathrm{H})}_{mn} = \frac{\psi^a_{\mathrm{tor}}\,(\iota B_{\vartheta_{\mathrm{B}}} + B_{\varphi_{\mathrm{B}}})}{\mathrm{d}V/\mathrm{d}s}\int_0^{2\pi}\mathrm{d}\vartheta_{\mathrm{B}}\int_0^{2\pi}\mathrm{d}\varphi_{\mathrm{B}}\ \frac{e^{-i(m\vartheta_{\mathrm{H}}(\vartheta_{\mathrm{B}},\varphi_{\mathrm{B}})+n\varphi_{\mathrm{H}}(\vartheta_{\mathrm{B}},\varphi_{\mathrm{B}}))}}{B}. \tag{B.10}$$

B.2 Solubility conditions

Using the equation of a field line

$$\frac{\mathrm{d}\vartheta}{\mathrm{d}l} = \frac{B^{\vartheta}}{B} \quad \text{or} \quad \frac{\mathrm{d}l}{B} \;=\; \frac{\mathrm{d}\vartheta}{B^{\vartheta}}, \tag{B.11}$$

the integral along the field line parameter l can be expressed through an integration along the angle ϑ,

$$\oint \mathrm{d}l \frac{S}{B} = \frac{1}{\iota \psi^a_{\mathrm{tor}}} \oint \mathrm{d}\vartheta \sqrt{g_{\mathrm{B}}} S \;=\; 0. \tag{B.12}$$

On a rational flux surface, $\iota = N/M$, the field line is closed after $2\pi\iota M$ poloidal turns ($\Delta\vartheta = 2\pi\iota M$),

$$\begin{aligned} \varphi_{\mathrm{B}} = \varphi_0 + q\vartheta \;&\Rightarrow \Delta\varphi_{\mathrm{B}} = \varphi_0 + q\Delta\vartheta = \varphi_0 + 2\pi M, \\ \vartheta_{\mathrm{B}} = \vartheta \;&\Rightarrow \Delta\vartheta_{\mathrm{B}} = 2\pi N. \end{aligned} \tag{B.13}$$

Since $\sqrt{g_{\mathrm{B}}}S$ is expanded in double periodic Fourier series, the solubility condition given by Eq. (B.12) restricts the values of the coefficients $a^{(\mathrm{B})}_{mn}(s)$,

$$\begin{aligned} \oint \mathrm{d}l \frac{S}{B} \;&=\; \frac{q}{\psi^a_{\mathrm{tor}}} \Re \left\{ \sum_{m,n} a^{(\mathrm{B})}_{mn}(s)\; e^{in\varphi_0} \int_0^{2\pi\iota M} \mathrm{d}\vartheta\; e^{i(m+nq)\vartheta} \right\} \\ &=\; \frac{q}{\psi^a_{\mathrm{tor}}} \Re \left\{ \sum_{m,n} a^{(\mathrm{B})}_{mn}(s_{MN}) e^{in\varphi_0} 2\pi\iota M \sum_k \left(\delta_{m,-kM}\delta_{n,kN} + \delta_{m,kM}\delta_{n,-kN}\right) \right\} \\ &=\; \frac{2\pi M}{\psi^a_{\mathrm{tor}}} \Re \left\{ \sum_k \left(a^{(\mathrm{B})}_{-kM,kN}(s_{MN})\; e^{ikN\varphi_0} + c.c. \right) \right\} \stackrel{!}{=} 0, \end{aligned} \tag{B.14}$$

where k means that the resonances can occur at every integer multiple of M and N ($k = 1, 2, 3, ...$). Since Eq. (B.14) must hold for any φ_0, the coefficients $a^{(\mathrm{B})}_{mn}$ have to vanish at rational flux surfaces,

$$a^{(\mathrm{B})}_{-kM,kN}(s_{MN}) = 0. \tag{B.15}$$

The second solubility condition states that the volume integral over the source term has to vanish,

$$\int \mathrm{d}\tau S \stackrel{!}{=} 0, \tag{B.16}$$

where $\mathrm{d}\tau = \sqrt{g_{\mathrm{B}}}\,\mathrm{d}s\,\mathrm{d}\vartheta_{\mathrm{B}}\mathrm{d}\varphi_{\mathrm{B}}$ specifies an infinitesimal volume element. This

solubility condition implies another restriction on the Fourier coefficients,

$$\begin{aligned}\int \mathrm{d}\tau S &= \int_0^1 \mathrm{d}s \int_0^{2\pi} \mathrm{d}\vartheta_\mathrm{B} \int_0^{2\pi} \mathrm{d}\varphi_\mathrm{B} \sqrt{g_\mathrm{B}} S = \int_0^1 \mathrm{d}s \sum_{m,n} a_{mn}^{(\mathrm{B})}(s) \int_0^{2\pi} \mathrm{d}\vartheta_\mathrm{B} \int_0^{2\pi} \mathrm{d}\varphi_\mathrm{B}\, e^{i(m\vartheta_\mathrm{B}+n\varphi_\mathrm{B})} \\ &= (2\pi)^2 \int_0^1 \mathrm{d}s\; a_{00}^{(\mathrm{B})}(s) \stackrel{!}{=} 0. \end{aligned} \tag{B.17}$$

Appendix C

Derivation of the quasilinear approach

In this appendix details and intermediate steps related to the derivation of the quasilinear approach presented in Section 2.3.2 are discussed.

Equation (2.107)

The flux-force relation for the axisymmetric tokamak is obtained by multiplying Eq. (2.104) with $v_\perp v_\parallel B^{-3}$ and a subsequent integration over velocity space components and poloidal angle,

$$0 = \int_0^{2\pi} \mathrm{d}\vartheta \int_0^{\infty} \mathrm{d}v_\perp \int_{-\infty}^{\infty} \mathrm{d}v_\parallel \frac{v_\perp v_\parallel}{B^3} \Bigg\{ \underbrace{v_\parallel \frac{B^\vartheta}{B} \frac{\partial f_1}{\partial \vartheta}}_{=I_1} + \underbrace{\frac{v_\perp B^\vartheta}{2B^2} \frac{\partial B}{\partial \vartheta} \left(v_\parallel \frac{\partial f_1}{\partial v_\perp} - v_\perp \frac{\partial f_1}{\partial v_\parallel} \right)}_{=I_2} - \\ - \underbrace{\hat{L}_{cL} f_1}_{I_3} - \underbrace{\frac{v_\perp^2 + 2v_\parallel^2}{2C_g \omega_c} B_\varphi \frac{\partial B}{\partial \vartheta} \frac{\partial f_M}{\partial r}}_{=I_4} \Bigg\} . \tag{C.1}$$

In order to facilitate the further discussion, the expression is split into four terms which are inspected separately. With help of partial integration over

ϑ the first term in Eq. (C.1) is transformed to

$$I_1 = -\frac{B^\vartheta}{4B^2} \int_0^{2\pi} \mathrm{d}\vartheta \int_0^\infty \mathrm{d}v_\perp \int_{-\infty}^\infty \mathrm{d}v_\parallel 4 v_\perp v_\parallel^2 f_1 \frac{\partial B^{-2}}{\partial \vartheta}, \tag{C.2}$$

where $B^\vartheta B^{-2} = f(r)$ is constant on a flux surface. The derivatives of the distribution function with respect to $v_\perp$ and $v_\parallel$ in I_2 can be removed using partial integration,

$$\begin{aligned} I_2 = \int_0^{2\pi} \mathrm{d}\vartheta \int_0^\infty \mathrm{d}v_\perp \int_{-\infty}^\infty \mathrm{d}v_\parallel \frac{B^\vartheta}{2B^5} \frac{\partial B}{\partial \vartheta} \Bigg[\frac{\partial}{\partial v_\perp} \left(v_\perp^2 v_\parallel^2 f_1 \right) - 2 v_\perp v_\parallel^2 f_1 - \\ - \frac{\partial}{\partial v_\parallel} \left(v_\parallel v_\perp f_1 \right) + v_\perp^3 f_1 \Bigg], \end{aligned} \tag{C.3}$$

where the first and third term are zero since the distribution function decays sufficiently fast at the integral boundaries $v_\perp = \infty$ and $v_\parallel = \pm\infty$, respectively. Analogue to (C.2), the derivative of the magnetic field module over ϑ in (C.3) is expressed via $\partial B^{-2}/\partial\vartheta$,

$$I_2 = \int_0^{2\pi} \mathrm{d}\vartheta \int_0^\infty \mathrm{d}v_\perp \int_{-\infty}^\infty \mathrm{d}v_\parallel \frac{B^\vartheta}{4B^2} \frac{\partial B^{-2}}{\partial \vartheta} \left[2 v_\perp v_\parallel^2 f_1 - v_\perp^3 f_1 \right]. \tag{C.4}$$

The fourth term I_4 vanishes because it can be written in terms of a full derivative over ϑ. Equation (C.1) is thus transformed to

$$0 = \int_0^{2\pi} \mathrm{d}\vartheta \int_0^\infty \mathrm{d}v_\perp \int_{-\infty}^\infty \mathrm{d}v_\parallel \left\{ v_\perp \frac{B^\vartheta}{4B^2} \frac{\partial B^{-2}}{\partial \vartheta} f_1 \left[v_\perp^2 + 2 v_\parallel^2 \right] + \frac{v_\perp v_\parallel}{B^3} \hat{L}_{cL} f_1 \right\}. \tag{C.5}$$

Substituting the expression for the particle flux (2.105) in the first term within the curly brackets in (C.5), gives equation (2.107),

$$
\begin{aligned}
0 &= \Gamma \frac{C_g \omega_c B^\vartheta}{2\pi B^3 B_\varphi} \left(\int_0^{2\pi} \mathrm{d}\vartheta \frac{|\nabla r|}{B^2} \right) + \int_0^{2\pi} \mathrm{d}\vartheta \int_0^{\infty} \mathrm{d}v_\perp \int_{-\infty}^{\infty} \mathrm{d}v_\parallel \frac{v_\perp v_\parallel}{B^3} \hat{L}_{cL} f_1 \\
&= \Gamma \frac{e_\alpha \sqrt{g} B^\vartheta}{2\pi m_\alpha c B_\varphi} + \frac{\int_0^{2\pi} \mathrm{d}\vartheta B^{-2}}{\int_0^{2\pi} \mathrm{d}\vartheta |\nabla r| B^{-2}} \left\langle \frac{1}{2\pi B} \int \mathrm{d}^3 v v_\parallel \hat{L}_{cL} f_1 \right\rangle \\
&= \Gamma \frac{e_\alpha \sqrt{g} B^\vartheta}{c} + \frac{1}{\langle |\nabla r| \rangle} \left\langle \frac{B_\varphi}{B} \int \mathrm{d}^3 v m_\alpha v_\parallel \hat{L}_{cL} f_1 \right\rangle . \qquad \text{(C.6)}
\end{aligned}
$$

Similar operations are performed to extract the non-ambipolar contribution to the particle flux Γ_{12} (2.128).

Equation (2.131)

In order to determine the contribution from the first term within the round brackets in (2.130) to the non-ambipolar particle flux, equation (2.121) is multiplied with $v_\parallel$ and integrated over velocity space and both angles,

$$
\begin{aligned}
&\underbrace{\left\langle B^2 \int \mathrm{d}^3 v \, v_\parallel \overline{\hat{L}}_{QA} f_{11} \right\rangle}_{=a} \left(\int_0^{2\pi} \mathrm{d}\vartheta B^{-2} \right) = \int_0^{2\pi} \mathrm{d}\vartheta \int_0^{2\pi} \mathrm{d}\varphi \int \mathrm{d}^3 v \, v_\parallel \overline{\hat{L}}_{QA} f_{11} = \\
&= \int_0^{2\pi} \mathrm{d}\vartheta \int_0^{2\pi} \mathrm{d}\varphi \int \mathrm{d}^3 v \, v_\parallel \left(-\delta \left(\frac{v_{gd}^r}{B^3} \right) \frac{\partial f_M}{\partial r} - \delta \hat{L}_\parallel f_{10} \right) = \\
&= \left\langle -\delta \left(\frac{v_{gd}^r}{B^3} \right) \frac{\partial f_M}{\partial r} - \delta \hat{L}_\parallel f_{10} \right\rangle \left(\int_0^{2\pi} \mathrm{d}\vartheta B^{-2} \right) . \qquad \text{(C.7)}
\end{aligned}
$$

Using the definition of the operator $\overline{\hat{L}}_{QA}$ (2.111), the flux surface average on the left hand side of (C.7) evaluates to

$$a = \left\langle B^2 \int \mathrm{d}^3v\, v_\parallel \frac{B^\vartheta}{B^2} \left[v_\parallel \overline{\left(\frac{1}{B^2}\right)} \frac{\partial f_{11}}{\partial \vartheta} + \frac{v_\perp}{4} \overline{\left(\frac{\partial}{\partial \vartheta}\frac{1}{B^2}\right)} \left(v_\perp \frac{\partial f_{11}}{\partial v_\parallel} - v_\parallel \frac{\partial f_{11}}{\partial v_\perp} \right) \right] \right\rangle - \\ - \left\langle B^2 \int \mathrm{d}^3v\, v_\parallel \overline{\left(\frac{1}{B^3}\right)} \hat{L}_{cL} f_{11} \right\rangle + \left\langle B^2 \int \mathrm{d}^3v\, v_\parallel \overline{\left(\frac{v_g^{\varphi_0}}{B^3}\right)} \frac{\partial f_{11}}{\partial \varphi_0} \right\rangle . \quad \text{(C.8)}$$

Analogue to the previous section, the derivatives of the distribution function can be removed using partial integration with respect to ϑ and velocity space components,

$$a = -\frac{1}{4} \left\langle B^\vartheta \overline{\left(\frac{\partial}{\partial \vartheta}\frac{1}{B^2}\right)} \int \mathrm{d}^3v\, f_{11} \left(v_\perp^2 + 2v_\parallel^2 \right) \right\rangle - \left\langle B^2 \overline{\left(\frac{1}{B^3}\right)} \int \mathrm{d}^3v\, v_\parallel \hat{L}_{cL} f_{11} \right\rangle + \\ + \left\langle B^2 \int \mathrm{d}^3v\, v_\parallel \overline{\left(\frac{v_g^{\varphi_0}}{B^3}\right)} \frac{\partial f_{11}}{\partial \varphi_0} \right\rangle . \quad \text{(C.9)}$$

Substituting (C.9) into(C.7) gives equation (2.131),

$$\frac{1}{4} \left\langle B^\vartheta \overline{\left(\frac{\partial}{\partial \vartheta}\frac{1}{B^2}\right)} \int \mathrm{d}^3v \left(v_\perp^2 + 2v_\parallel^2 \right) f_{11} \right\rangle = \\ = \left\langle B^2 \int \mathrm{d}^3v v_\parallel \frac{\partial f_M}{\partial r} \delta \left(\frac{v_{gd}^r}{B^3} \right) \right\rangle + \left\langle B^2 \int \mathrm{d}^3v v_\parallel \delta \hat{L}_\parallel f_{10} \right\rangle - \\ - \left\langle B^2 \overline{\left(\frac{1}{B^3}\right)} \int \mathrm{d}^3v v_\parallel \hat{L}_{cL} f_{11} \right\rangle + \left\langle B^2 \int \mathrm{d}^3v v_\parallel \overline{\left(\frac{v_{gd}^{\varphi_0}}{B^3}\right)} \frac{\partial f_{11}}{\partial \varphi_0} \right\rangle . \quad \text{(C.10)}$$

Equation (2.137)

The perturbation operator $\delta \hat{L}_\parallel$ (2.114),

$$\delta \hat{L}_\parallel = \frac{B^\vartheta}{B^2} \left[v_\parallel \delta \left(\frac{1}{B^2}\right) \frac{\partial}{\partial \vartheta} + \frac{v_\perp}{4} \delta \left(\frac{\partial}{\partial \vartheta}\frac{1}{B^2}\right) \times \right. \\ \left. \times \left(v_\perp \frac{\partial}{\partial v_\parallel} - v_\parallel \frac{\partial}{\partial v_\perp} \right) \right] - \delta \left(\frac{1}{B^3}\right) \hat{L}_{cL}, \quad \text{(C.11)}$$

can be linearized with respect to the perturbation field δB using

$$\delta\left(B^{-2}\right) = B^{-2} - \overline{(B^{-2})} \approx B_0^{-2} - \frac{2}{B_0^3}\left(B - B_0\right) - B_0^{-2} = -\frac{2\delta B}{B_0^3}, \tag{C.12a}$$

$$\delta\left(B^{-3}\right) \approx -\frac{3\delta B}{B_0^4}, \tag{C.12b}$$

$$\delta\left(-\frac{2}{B_0^3}\frac{\partial B}{\partial \vartheta}\right) \approx -2\delta\left(B^{-3}\right)\frac{\partial B_0}{\partial \vartheta} - \frac{2}{B_0^3}\frac{\partial \delta B}{\partial \vartheta} \approx \frac{6\delta B}{B_0^4}\frac{\partial B_0}{\partial \vartheta} - \frac{2}{B_0^3}\frac{\partial \delta B}{\partial \vartheta}. \tag{C.12c}$$

Substituting (C.12a), (C.12b) and (C.12c) into (C.11) and multiplying the result with B_0^3, yields the simplified operator $\delta\hat{L}_A$ (2.137),

$$\begin{aligned}\delta\hat{L}_A = &\frac{B_0^\vartheta}{B_0}\left[-2v_\parallel\frac{\delta B}{B_0}\frac{\partial}{\partial\vartheta} + \frac{v_\perp}{2B_0}\left(\frac{\partial\delta B}{\partial\vartheta} - \frac{3\delta B}{B_0}\frac{\partial B_0}{\partial\vartheta}\right)\times\right.\\ &\left.\times\left(v_\parallel\frac{\partial}{\partial v_\perp} - v_\perp\frac{\partial}{\partial v_\parallel}\right)\right] + \frac{3\delta B}{B_0}\hat{L}_{cL}.\end{aligned} \tag{C.13}$$

References

[1] W. Kernbichler, S. V. Kasilov, G. O. Leitold, V. V. Nemov, and K. Allmaier. Recent progress in NEO-2 - A code for neoclassical transport computations based on field line tracing. *Plasma and Fusion Research*, 3:S1061–1–S1061–4, 2008.

[2] S. V. Kasilov, W. Kernbichler, A. F. Martitsch, H. Maassberg, and M. F. Heyn. Evaluation of the toroidal torque driven by external non-resonant non-axisymmetric magnetic field perturbations in a tokamak. *Phys. Plasmas*, 21(9):092506, 2014.

[3] K. C. Shaing, S. A. Sabbagh, and M. S. Chu. An approximate analytic expression for neoclassical toroidal plasma viscosity in tokamaks. *Nuclear Fusion*, 50(2):025022, 2010.

[4] J. Park, A. H. Boozer, and J. E. Menard. Nonambipolar transport by trapped particles in tokamaks. *Phys. Rev. Letters*, 102(6):065002, 2009.

[5] Y. Sun, Y. Liang, K. C. Shaing, H. R. Koslowski, C. Wiegmann, and T. Zhang. Neoclassical toroidal plasma viscosity torque in collisionless regimes in tokamaks. *Phys. Rev. Letters*, 105(14):145002, 2010.

[6] S. P. Hirshman, K. C. Shaing, W. I. van Rij, C. O. Beasley, Jr., and E. C. Crume, Jr. Plasma transport coefficients for nonsymmetric toroidal confinement systems. *Phys. Fluids*, 29(9):2951–2959, 1986.

[7] J. D. Williams and A. H. Boozer. δf method to calculate plasma transport and rotation damping. *Phys. Plasmas*, 10(1):103–111, 2003.

[8] S. Satake, J.-K. Park, H. Sugama, and R. Kanno. Neoclassical toroidal viscosity calculations in tokamaks using a journalf monte carlo simulation and their verifications. *Phys. Rev. Letters*, 107(5):055001, 2011.

[9] K. Kim, J.-K. Park, and A. H. Boozer. Numerical verification of bounce-harmonic resonances in neoclassical toroidal viscosity for tokamaks. *Phys. Rev. Letters*, 110(18):185004, 2013.

[10] V. V. Nemov, S. V. Kasilov, W. Kernbichler, and M. F. Heyn. Evaluation of $1/\nu$ neoclassical transport in stellarators. *Phys. Plasmas*, 6(12):4622–4632, 1999.

[11] S. P. Hirshman, W. I. van RIJ, and P. Merkel. Three-dimensional free boundary calculations using a spectral green's function method. *Computer Physics Communications*, 43(1):143 – 155, 1986.

[12] M. F. Heyn, I. B. Ivanov, S. V. Kasilov, W. Kernbichler, P. Leitner, V. V. Nemov, W. Suttrop, and ASDEX Upgrade Team. Quasilinear Modelling of RMP Interaction with a Tokamak Plasma: Application to ASDEX Upgrade ELM Mitigation Experiments. *Nuclear Fusion*, 54(6):064005, 2014.

[13] M. Landreman, H. M. Smith, A. Mollén, and P. Helander. Comparison of particle trajectories and collision operators for collisional transport in nonaxisymmetric plasmas. *Phys. Plasmas*, 21(4):042503, 2014.

[14] A. H. Boozer. Plasma equilibrium with rational magnetic surfaces. *Physics of Fluids*, 24(11):1999–2003, 1981.

[15] S. Hamada. Hydromagnetic equilibria and their proper coordinates. *Nuclear Fusion*, 2(1-2):23, 1962.

[16] A. F. Martitsch, S. V. Kasilov, W. Kernbichler, and H. Maassberg. Evaluation of non-ambipolar particle fluxes driven by external non-resonant magnetic perturbations in a tokamak. In *41st EPS Conference on Plasma Physics*, volume 38F, page P1.049, Berlin, Deutschland, 2014. European Physical Society.

[17] A. H. Boozer. Enhanced transport in tokamaks due to toroidal ripple. *Phys. Fluids*, 23(11):2283–2290, 1980.

[18] K. C. Shaing, M. S. Chu, and S. A. Sabbagh. Eulerian approach to bounce-transit and drift resonance and neoclassical toroidal plasma viscosity in tokamaks. *Plasma Phys. Control. Fusion*, 51(5):075015, 2009.

[19] C. G. Albert, M. F. Heyn, S. V. Kasilov, W. Kernbichler, and A. F. Martitsch. Toroidal rotation in resonant regimes of tokamak plasmas due to non-axisymmetric perturbations in the action-angle formalism. In *42nd EPS Conference on Plasma Physics*, volume 39E, page P1.183, Lisbon, Portugal, 2015. European Physical Society.

[20] W. D. D'haeseleer, W. N. G. Hitchon, J. D. Callen, and J. L. Shohet. *Flux Coordinates and Magnetic Field Structure*. Springer-Verlag, Berlin, 1991.

[21] P. Helander and D. J. Sigmar. *Collisional transport in magnetized plasmas*. Cambridge University Press, Cambridge, 2002.

[22] R. D. Hazeltine. Rotation of toroidally confined, collisional plasma. *Phys. Fluids*, 17(5):961–968, 1974.

[23] F. L. Hinton and R. D. Hazeltine. Theory of plasma transport in toroidal confinement systems. *Rev. Mod. Phys.*, 48:239–308, 1976.

[24] S. P. Hirshman and D. J. Sigmar. Neoclassical transport of impurities in tokamak plasmas. *Nuclear Fusion*, 21(9):1079–1201, 1981.

[25] P. Helander, T. Fülöp, and Peter J. Catto. Controlling edge plasma rotation through poloidally localized refueling. *Phys. Plasmas*, 10(11):4396–4404, 2003.

[26] A. I. Morozov and L. S. Solov'ev. Motion of charged particles in electromagnetic fields. In *Reviews of Plasma Physics*, volume 2, pages 201–297. Consultants Bureau, New York, 1966.

[27] R. J. Littlejohn. Variational principles of guiding centre motion. *Journ. Plasma Phys.*, 29(1):111–125, 1983.

[28] P. Leitner. *Impact of Energy and Momentum Conservation on Fluid Resonances in the Kinetic Modelling of the Interaction of Resonant Magnetic Perturbations with a Tokamak Plasma*. PhD thesis, Institut für Theoretische Physik - Computational Physics, TU Graz, 2015.

[29] L. D. Landau. Die kinetische Gleichung für den Fall Coulombscher Wechselwirkung. *Phys. Z. Sowjetunion*, 10:154–164, 1936.

[30] B. A. Trubnikov. Particle interactions in a fully ionized plasma. In *Reviews of Plasma Physics*, volume 1, pages 105–204. Consultants Bureau, New York, 1965.

[31] L. D. Landau and E. M. Lifschitz. *Klassische Feldtheorie*. Akademie-Verlag, Berlin, 1981.

[32] J. D. Jackson. *Classical Electrodynamics*. John Wiley & Sons, Inc., New York - London - Sydney - Toronto, 1975.

[33] S. I. Braginskii. Transport processes in plasma. In *Reviews of Plasma Physics*, volume 1, pages 205–311. Consultants Bureau, New York, 1965.

[34] H. Sugama, T. H. Watanabe, and M. Nunami. Conservation of energy and momentum in nonrelativistic plasmas. *Phys. Plasmas*, 20(2):024503, 2013.

[35] J. D. Callen, A. J. Cole, and C. C. Hegna. Toroidal flow and radial particle flux in tokamak plasmas. *Phys. Plasmas*, 16(8):082504, 2009.

[36] K. C. Shaing. Magnetohydrodynamic-activity-induced toroidal momentum dissipation in collisionless regimes in tokamaks. *Phys. Plasmas*, 10(5):1443–1448, 2003.

[37] K. C. Shaing and J. D. Callen. Neoclassical flows and transport in non-axisymmetric toroidal plasmas. *Phys. Fluids*, 28(11):3315–3326, 1983.

[38] K. C. Shaing, M. S. Chu, and S. A. Sabbagh. Flux-force relation for non-axisymmetric tori in general flux coordinates and neoclassical toroidal plasma viscosity. *Nuclear Fusion*, 50(12):125012, 2010.

[39] K. T. Tsang and E. A. Frieman. Toroidal plasma rotation in axisymmetric and slightly nonaxisymmetric systems. *Phys. Fluids*, 19(5):747–756, 1976.

[40] S. P. Hirshman. The ambipolarity paradox in toroidal diffusion revisited. *Nuclear Fusion*, 18(7):917–927, 1978.

[41] J. D. Callen, A. J. Cole, and C. C. Hegna. Toroidal rotation in tokamak plasmas. *Nuclear Fusion*, 49(8):085021, 2009.

[42] K. C. Shaing. Theory for toroidal momentum pitch and flow reversal in tokamaks. *Phys. Rev. Letters*, 86(4):640–643, 2001.

[43] R. E. Waltz, G. M. Staebler, J. Candy, and F. L. Hinton. Gyrokinetic theory and simulation of angular momentum transport. *Phys. Plasmas*, 14(12):122507, 2007.

[44] M. F. Heyn, I. B. Ivanov, S. V. Kasilov, W. Kernbichler, I. Joseph, R. A. Moyer, and A. M. Runov. Kinetic estimate of the shielding of resonant magnetic field perturbations by the plasma in DIII-D. *Nuclear Fusion*, 48:024005, 2008.

[45] Y. Sun, K. C. Shaing, Y. Liang, T. Casper, A. Loarte, B. Shen, and B. Wan. Intrinsic plasma rotation determined by neoclassical toroidal plasma viscosity in tokamaks. *Nuclear Fusion*, 53(9):093010, 2013.

[46] C. D. Beidler, K. Allmaier, M. Yu. Isaev, S. V. Kasilov, W. Kernbichler, G. O. Leitold, H. Maaßberg, D. R. Mikkelsen, S. Murakami, M. Schmidt, D. A. Spong, V. Tribaldos, and A. Wakasa. Benchmarking of the monoenergetic transport coefficients - results from the international collaboration on neoclassical transport in stellarators (icnts). *Nucl. Fusion*, 51(7):076001, 2011.

[47] S. Nishimura, H. Sugama, H. Maaßberg, C. D. Beidler, S. Murakami, Y. Nakamura, and S. Hirooka. A convergence study for the laguerre expansion in the moment equation method for neoclassical transport in general toroidal plasmas. *Phys. Plasmas*, 17(8):082510, 2010.

[48] Y. N. Dnestrovskii and D. P. Kostomarov. *Numerical Simulation of Plasmas*. Springer Series in Computational Physics, Springer-Verlag, Berlin Heidelberg, 1986.

[49] W. Kernbichler, S. V. Kasilov, G. O. Leitold, V. V. Nemov, and N. B. Marushchenko. Generalized Spitzer function with finite collisionality in toroidal plasmas. *Contrib. Plasma Phys.*, 50(8):761–765, 2010.

[50] G. O. Leitold. *Computation of neoclassical transport coefficients and generalized Spitzer function in toroidal fusion plasmas*. PhD thesis, Institut für Theoretische Physik - Computational Physics, TU Graz, 2010.

[51] P. N. Yushmanov. Diffusive transport processes caused by ripple in tokamaks. In *Reviews of Plasma Physics*, volume 16, pages 117–242. Consultants Bureau, New York, 1990.

[52] K. C. Shaing. Transport theory in the collisional boundary layer regime for finite aspect ratio tokamaks with broken symmetry. *Physics of Plasmas*, 22(10), 2015.

[53] K. C. Shaing. Superbanana and superbanana plateau transport in finite aspect ratio tokamaks with broken symmetry. *J. Plasma Physics*, 81:905810203, 2015.

[54] K. C. Shaing, P. Cahyna, M. Becoulet, J.-K. Park, S. A. Sabbagh, and M. S. Chu. Collisional boundary layer analysis for neoclassical toroidal plasma viscosity in tokamaks. *Phys. Plasmas*, 15(8):082506, 2008.

[55] W. Kernbichler, S. V. Kasilov, G. Kapper, A. F. Martitsch, V .V. Nemov, C. G. Albert, and M. F. Heyn. Solution of drift kinetic equation in stellarators and tokamaks with broken symmetry using the code neo-2. *Plasma Phys. Control. Fusion*, page submitted, 2016.

[56] P. N. Yushmanov. *Dokl. Akad. Nauk SSSR*, 266:1123–1127, 1982.

[57] R. J. Goldston, R. B. White, and A. H. Boozer. Confinement of high-energy trapped particles in tokamaks. *Phys. Rev. Lett.*, 47(9):647–649, 1981.

[58] V. S. Tsypin, A. B. Mikhailovskii, R. M. O. Galvao, I. C. Nascimento, M. Tendler, C. A. de Azevedo, and A. S. de Assis. Plasma rotation in toroidal devices with circular cross-sections. *Phys. Plasmas*, 5(9):3358–3365, 1998.

[59] K. C. Shaing, S. A. Sabbagh, and M. S. Chu. Neoclassical toroidal plasma viscosity in the superbanana plateau regime for tokamaks. *Plasma Phys. Control. Fusion*, 51(3):035009, 2009.

[60] A. F. Martitsch, S. V. Kasilov, W. Kernbichler, G. Kapper, C. G. Albert, M. F. Heyn, H. M. Smith, E. Strumberger, S. Fietz, W. Suttrop, M. Landreman, the ASDEX Upgrade Team, and the EUROfusion MST1 Team. Effect of 3d magnetic perturbations on the plasma rotation in asdex upgrade. *Plasma Phys. Control. Fusion*, 58(7):074007, 2016.

[61] A. F. Martitsch, S. V. Kasilov, W. Kernbichler, M. F. Heyn, E. Strumberger, S. Fietz, W. Suttrop, A. Kirk, the ASDEX Upgrade Team, and the EUROfusion MST1 Team. Evaluation of the neoclassical toroidal viscous torque in asdex upgrade. In *42nd EPS Conference on Plasma Physics*, volume 39E, page P1.146, Lisbon, Portugal, 2015. European Physical Society.

[62] W. Zhu, S. A. Sabbagh, R. E. Bell, J. M. Bialek, M. G. Bell, B. P. LeBlanc, S. M. Kaye, F. M. Levinton, J. E. Menard, K. C. Shaing, A. C. Sontag, and H. Yuh. Observation of plasma toroidal-momentum dissipation by neoclassical toroidal viscosity. *Phys. Rev. Lett.*, 96:225002, Jun 2006.

[63] A. M. Garofalo, W. M. Solomon, M. Lanctot, K. H. Burrell, J. C. DeBoo, J. S. deGrassie, G. L. Jackson, J.-K. Park, H. Reimerdes, M. J. Schaffer, and E. J. Strait. Plasma rotation driven by static nonresonant magnetic fields. *Phys. Plasmas*, 16(5):056119, 2009.

[64] Y. Sun, Y. Liang, K. C. Shaing, Y. Q. Liu, H. R. Koslowski, S. Jachmich, B. Alper, A. Alfier, O. Asunta, P. Buratti, G. Corrigan, E. Delabie, C. Giroud, M. P. Gryaznevich, D. Harting, T. Hender, E. Nardon, V. Naulin, V. Parail, T. Tala, C. Wiegmann, S. Wiesen, T. Zhang, and JET-EFDA contributors. Non-resonant magnetic braking on JET and TEXTOR. *Nuclear Fusion*, 52(8):083007, 2012.

[65] E. Lazzaro, R. J. Buttery, T. C. Hender, P. Zanca, R. Fitzpatrick, M. Bigi, T. Bolzonella, R. Coelho, M. DeBenedetti, S. Nowak, O. Sauter, M. Stamp, and Contributors to the EFDA-JET work programme. Error field locked modes thresholds in rotating plasmas, anomalous braking and spin-up. *Phys. Plasmas*, 9(9):3906–3918, 2002.

[66] E. Strumberger, S. Günter, and C. Tichmann. MHD instabilities in 3D tokamaks. *Nuclear Fusion*, 54(6):064019, 2014.

[67] A. Pankin, D. McCune, R. Andre, G. Bateman, and A. Kritz. The tokamak monte carlo fast ion module NUBEAM in the national transport code collaboration library. *Computer Physics Communications*, 159(3):157 – 184, 2004.

[68] M. Honda, T. Takizuka, K. Tobita, G. Matsunaga, and A. Fukuyama. Alpha particle-driven toroidal rotation in burning plasmas. *Nuclear Fusion*, 51(7):073018, 2011.

[69] Ya. I. Kolesnichenko and Yu. V. Yakovenko. Alpha-particle-induced toroidal flows in tokamak reactor plasma. *Fusion Technology*, 18(12):597–605, 1990.

[70] W. Suttrop, O. Gruber, S. Günter, D. Hahn, A. Herrmann, M. Rott, T. Vierle, U. Seidel, M. Sempf, B. Streibl, E. Strumberger, D. Yadikin, O. Neubauer, B. Unterberg, E. Gaio, V. Toigo, and P. Brunsell. In-vessel saddle coils for MHD control in ASDEX upgrade. *Fusion Engineering and Design*, 84(2–6):290–294, 2009. Proceeding of the 25th Symposium on Fusion Technology(SOFT-25).

[71] V. D. Pustovitov. Integral torque balance in tokamaks. *Nuclear Fusion*, 51(1):013006, 2011.

[72] T. Kurki-Suonio, S. K. Sipilä, and J. A. Heikkinen. Active diagnostic of edge Er using neutral-particle analysers. *Plasma Physics and Controlled Fusion*, 42(5A):A277 – A282, 2000.

[73] T. Koskela, A. Snicker, S. Sipilä, A. Salmi, T. Johnson, C. Marchetto, M. Schneider, M. Romanelli, H. Weisen, and JET contributors. Improvement of neutron yield predictions in JET with ASCOT. In *42nd EPS Conference on Plasma Physics*, volume 39E, page P2.106, Lisbon, Portugal, 2015. European Physical Society.

[74] K. Allmaier, S. V. Kasilov, W. Kernbichler, and G. O. Leitold. Variance reduction in computations of neoclassical transport in stellarators using a δf method. *Physics of Plasmas*, 15(7), 2008.

[75] V. V. Nemov, S. V. Kasilov, and W. Kernbichler. Collisionless high energy particle losses in optimized stellarators calculated in real-space coordinates. *Physics of Plasmas*, 21(6), 2014.

[76] N. C. Logan, E. J. Strait, and H. Reimerdes. Measurement of the electromagnetic torque in rotating DIII-D plasmas. *Plasma Phys. Control. Fusion*, 52(4):045013, 2010.

[77] R. Schneider, X. , Bonnin, K. Borrass, D. P. Coster, H. Kastelewicz, D. Reiter, V. A. Rozhansky, and B. J. Braams. Plasma Edge Physics with B2-Eirene. *Contrib. Plasma Phys.*, 46(1-2):3–191, 2006.

[78] Message Passing Interface Forum. MPI: A Message-Passing Interface Standard. Technical Report Version 2.2, September 2009.

[79] G. Kapper. Development of a library for parallel computation of physical problems and its application to plasma physics. Master's thesis, Institut für Theoretische Physik - Computational Physics, TU Graz, 2013.

[80] J. D. Callen, C. C. Hegna, and A. J. Cole. Transport equations in tokamak plasmas. *Phys. Plasmas*, 17(5):056113, 2010.

[81] T. E. Evans, R. A. Moyer, K. H. Burrell, M. E. Fenstermacher, I. Joseph, A. W. Leonard, T. H. Osborne, and G. Porter. Edge stability and transport control with resonant magnetic perturbations in collisionless tokamak plasmas. *Nature Phys.*, 2(6):419–423, 2006.

[82] Y. Liang, H. R. Koslowski, P. R. Thomas, E. Nardon, B. Alper, P. Andrew, Y. Andrew, G. Arnoux, Y. Baranov, M. Bécoulet, M. Beurskens, T. Biewer, M. Bigi, K. Crombe, E. De La Luna, P. de Vries, W. Fundamenski, S. Gerasimov, C. Giroud, M. P. Gryaznevich, N. Hawkes, S. Hotchin, D. Howell, S. Jachmich, V. Kiptily, L. Moreira, and V. Parail. Active control of type-i edge-localized modes with $n = 1$

perturbation fields in the jet tokamak. *Phys. Rev. Lett.*, 98(26):265004, Jun 2007.

[83] K. C. Shaing, S. A. Sabbagh, and M. Peng. Neoclassical toroidal viscosity for an axisymmetric toroidal equilibrium with multiple trapping of particles. *Phys. Plasmas*, 14(2):024501, 2007.

[84] K. C. Shaing, S. A. Sabbagh, and M. S. Chu. Neoclassical toroidal plasma viscosity in the low collisionality regime for tokamaks. *Plasma Phys. Control. Fusion*, 51(3):035004, 2009.

[85] K. C. Shaing, S. A. Sabbagh, and M. S. Chu. Neoclassical toroidal plasma viscosity in the superbanana regime in tokamaks. *Plasma Phys. Control. Fusion*, 51(5):055003, 2009.

[86] K. C. Shaing, JaeChun Seo, Y. W. Sun, M. S. Chu, and S. A. Sabbagh. Effects of finite gradient b drift on collisional boundary layer analysis for neoclassical toroidal plasma viscosity in tokamaks. *Nuclear Fusion*, 50(12):125008, 2010.

[87] R. Fitzpatrick. Bifurcated states of a rotating tokamak plasma in the presence of a static error-field. *Phys. Plasmas*, 5(9):3325–3341, 1998.

[88] M. F. Heyn, I. B. Ivanov, S. V. Kasilov, and W. Kernbichler. Kinetic modeling of the interaction of rotating magnetic fields with a radially inhomogeneous plasma. *Nuclear Fusion*, 46(3):S159–S169, 2006.

[89] E. Nardon, P. Tamain, M. Becoulet, G. Huysmans, and F. L. Waelbroeck. Quasi-linear MHD modelling of H-mode plasma response to resonant magnetic perturbations. *Nuclear Fusion*, 50(3):034002, 2010.